SERI/TR-35-078
Volume I

August 1979

Fred R. 11/14/79
Doug -
Sunny -

Conversion System Overview Assessment

Volume I Solar Thermoelectrics

T. S. Jayadev
J. Henderson
J. Finegold
D. Benson

SERI

Solar Energy Research Institute
A Division of Midwest Research Institute

1536 Cole Boulevard
Golden, Colorado 80401

Operated for the
U.S. Department of Energy
under Contract No. EG-77-C-01-4042

Printed in the United States of America
Available from:
National Technical Information Service
U.S. Department of Commerce
5285 Port Royal Road
Springfield, VA 22161
Price:
Microfiche $3.00
Printed Copy $9.25

SERI/TR-35-078
VOLUME I OF III
UC CATEGORY: UC 59B,62,62E,64

CONVERSION SYSTEM OVERVIEW ASSESSMENT
VOLUME I SOLAR THERMOELECTRICS

AUGUST 1979

PARTICIPANTS:

T.S. JAYADEV, TASK LEADER
J. HENDERSON
J. FINEGOLD
D. BENSON

PREPARED UNDER TASK NO. 3503

Solar Energy Research Institute

1536 Cole Boulevard
Golden, Colorado 80401

A Division of Midwest Research Institute

Prepared for the
U.S. Department of Energy
Contract No. EG-77-C-01-4042

FOREWORD

This report documents work done on Task 3503, "Conversion System Overview Assessment," contained in SERI's FY78 Annual Operating Plan, on the following technologies:

- solar thermoelectrics,
- solar-wind hybrid systems,
- ocean thermal energy conversion, and
- synthetic fuels derived with solar energy.

SERI Task 3503 is divided into the following subtasks: Wind (3503.01); OTEC (3503.02); Solar-Wind Hybrid (3503.03); Solar Thermoelectrics (3503.04); and Synthetic Fuels (3503.05). This report documents work done on all of these subtasks except 3503.02 on Ocean Thermal Energy Conversion, which will be covered in a separate report.

This report is divided into three parts. Part I deals with solar thermoelectrics and Part II with solar-wind hybrid systems. Part III covers the production of synthetic fuels utilizing solar thermal heat. Two appendices document reports by General Atomics of LaJolla, California, and Syncal Corporation of Sunnyvale, California, on costing of thermoelectric generators. Each candidate technology was surveyed by reviewing the literature, by contacting individuals and companies active in the field, and by attending conferences.

Two of the technologies--solar thermoelectrics and solar-wind hybrid systems--are new. Presented here is a preliminary study to determine the viability of these new technologies and examples of typical applications.

Neil H. Woodley by W.A.Z.

Neil Woodley, Branch Chief
Systems Analysis

Approved for:

SOLAR ENERGY RESEARCH INSTITUTE

Kenneth J. Touryan

Dr. J. C. Grosskreutz
for Director for Technology Development

SUMMARY

The three volumes of this report cover three distinct areas of solar energy research: solar thermoelectrics, solar-wind hybrid systems, and synthetic fuels derived with solar thermal energy. Volume I represents the assessment, done at SERI, of thermoelectrics for solar energy conversion. It is concluded that there is significant potential for solar thermoelectrics in solar technologies where collector costs are low; e.g., Ocean Thermal Energy Conversion (OTEC) and solar ponds. It is expected that thermoelectrics also may have potential in other renewable energy source applications such as geothermal energy and waste heat utilization. Reports of two studies by manufacturers assessing the cost of thermoelectric generators in large scale production are included in the appendix, and several new concepts of solar thermoelectric systems are presented. Volume II discusses solar-wind hybrid systems. It is shown that there are large areas in the United States where solar and wind resources are comparable in magnitude, and there are diurnal and seasonal complementarities which offer the potential for cost-effective hybrid systems. There are also distinct engineering features of the two conversion technologies. Electric power generation from wind is straightforward and cost-effective, whereas solar thermal conversion to generate heat is more cost-effective than to generate electricity. Examples of hybrid systems utilizing these features in total energy applications are presented. Volume III deals with the conversion of synthetic fuels with solar thermal heat. The method is a hybrid combination of solar energy with either coal or biomass. A preliminary assessment of this technology is made by calculating the cost of fuel produced as a function of the cost of coal and biomass. It is shown that within the projected ranges of coal, biomass, and solar thermal costs, there are conditions when solar synthetic fuels with solar thermal heat will become cost-competitive.

CONVERSION SYSTEM OVERVIEW ASSESSMENT

TABLE OF CONTENTS

VOLUME I: SOLAR THERMOELECTRICS

TABLE OF CONTENTS

LIST OF FIGURES

LIST OF TABLES

SECTION 1.0

INTRODUCTION

Thermoelectric power generation is a solid state energy conversion process in which a temperature difference across suitable materials produces a voltage. In recent years important developments have been made in materials for thermoelectric generators; these have been used mainly in space power applications. However, virtually no modern research has been done on solar thermoelectric generators (STEG). Several features of STEG are particularly attractive:

- STEG are inherently maintenance-free with no moving parts;
- STEG are well suited for total energy (both electric and thermal) applications;
- the materials used are simple and potentially cheap because:
  - single crystal materials are not required,
  - semiconductor junctions are not required,
  - high purity is not required,
  - mass production techniques similar to processing ceramicware can be used,
- present capital costs of existing high-technology devices are already reasonably low -- $8 to $10/W, and it is highly probable that costs can be reduced to $0.10/W or less.

This report discusses in detail the potential of solar thermoelectric generators. The information is supported by available data and reports by two subcontractors who estimated independently the cost reduction potential of STEG produced on a large scale. Also presented are novel concepts for applications of thermoelectrics which show strong potential to be economically viable in the near future.

SECTION 2.0

HISTORICAL REVIEW

The first experiment in Solar Thermoelectric Generators (STEG) dates to 1913, when Coblentz obtained a patent for a generator using copper constantin thermocouples [1]. His generator had very low efficiency because of the unavailability of good thermoelectric materials at that time. Little work was done on STEG until the advent of semiconductors. In the early 1950s, Maria Telkes devoted considerable effort to a reassessment of the use of STEG [2]. Because most of the currently available thermoelectric materials had not been developed at that time, Telkes concluded in 1953 that conversion efficiencies of only about 3% were possible with flat plate solar collectors. Such low values of conversion efficiency from costly collectors did not justify the exploitation of this form of energy conversion, and the use of STEG remained dormant until the 1960s. By that time many new thermoelectric materials and associated technologies had been developed, justifying a new look at the field. The evaluation showed improved efficiency, but economic considerations continued to favor conventional power generation systems.

Toward the end of the 1960s and early 1970s, specialized fabrication techniques were developed for large-scale manufacture of thermoelectric devices. Most of these devices were intended for use with sources of heat from fossil or nuclear fuels. Studies focused on the use of solar thermoelectric generation in near-sun missions in space. The Navy developed a family of radioisotope-fueled thermoelectric generators well suited for remote applications because of reliability, ruggedness, and low maintenance [3].

Some past studies of thermoelectric power generation addressed the economics of this form of energy conversion. However, in all cases it was assumed that fairly small quantities of electrical power were to be generated. Such studies were aimed at determining the cost of specific STEG in a fairly low power output range. Katz, in 1961, described the details of construction of an STEG and estimated the cost of a 125-W generator in terms of the electricity produced by the generator [4]. He estimated that the cost of electricity produced by the generator was about 7¢ to 10¢/kWh in 1961. Today the thermoelectric field has available a broad spectrum of state-of-the-art thermoelectric materials and considerable experience in fabrication, testing, and operation of thermoelectric generators in terrestrial and space applications. This study on the effect of large-scale utilization on cost of electricity produced, presents, perhaps for the first time, the potential of solar thermoelectric generation deployed on a large scale.

Design and fabrication considerations are discussed, but no analysis of material availability is given. However, the current materials used for thermoelectric semiconductors (i.e., lead, bismuth, tellurium, and antimony) are plentiful either directly or as byproducts of copper and other metal mining.

SECTION 3.0

THERMOELECTRIC MATERIALS

3.1 STATE OF THE ART

The most widely used thermoelectric power generation materials are bismuth telluride, lead telluride, the selenides, and silicon-germanium alloys. Each material has a characteristic range of useful operating temperatures and figure-of-merit, a measure of conversion efficiency. Bismuth telluride is used in thermoelectric cooling as well as in power generation. In power generation, its useful range of operating temperature extends from room temperature to about 250 to 300°C. Lead telluride is commonly used in power generators at temperatures between room temperature and 600°C. The selenides are commonly used between 150 and 850°C; a phase transformation in the p-type material at 150°C renders its use at lower temperatures impractical. The useful range of operating temperatures of silicon-germanium alloys lies between room temperature and about 1000°C.

The relative values and temperature dependencies of the figures-of-merit of the four materials are shown in Figure 3-1 [5]. It is noted from Figure 3-1 that bismuth telluride possesses the highest figure-of-merit of any of the four materials. The selenides, lead telluride and silicon-germanium alloys have lower values of figure-of-merit, but their range of useful operating temperatures is higher.

ZT_{avg} is a factor proportional to the efficiency of conversion from heat to electricity, where Z is the figure-of-merit and T_{avg} is the average of hot and cold side temperatures. Figure 3-2 shows ZT values of low and medium temperature thermoelectric materials [6]. Bismuth telluride alloys have quite high ZT values from room temperature to 100°C. In fact, the alloys could be tailored to allow ZT to peak at the desired temperature in this range. Silicon-germanium alloys are the best materials in the high temperature range. They also have good mechanical properties: high mechanical strength, low coefficient of expansion, and light weight. Figure 3-3 shows ZT values for some high temperature thermoelectric materials [6].

In evaluating the potential of thermoelectric generators, it is necessary to select an appropriate material and its associated technology for a specific solar application. In this study it is necessary to consider the ability of materials to operate in an air environment. Although it may be possible to fabricate STEG in which the material is hermetically sealed under an inert gas atmosphere or in vacuum, if it is possible to eliminate the need for sealing, considerable cost savings result.

Of the four state-of-the-art thermoelectric materials, all except the selenides are capable of operation in air. For bismuth telluride and lead telluride, the maximum temperature of air operation is limited to about 200°C. At higher temperatures both materials are susceptible to oxygen poisoning resulting in degradation of thermoelectric properties. Only the alloys of

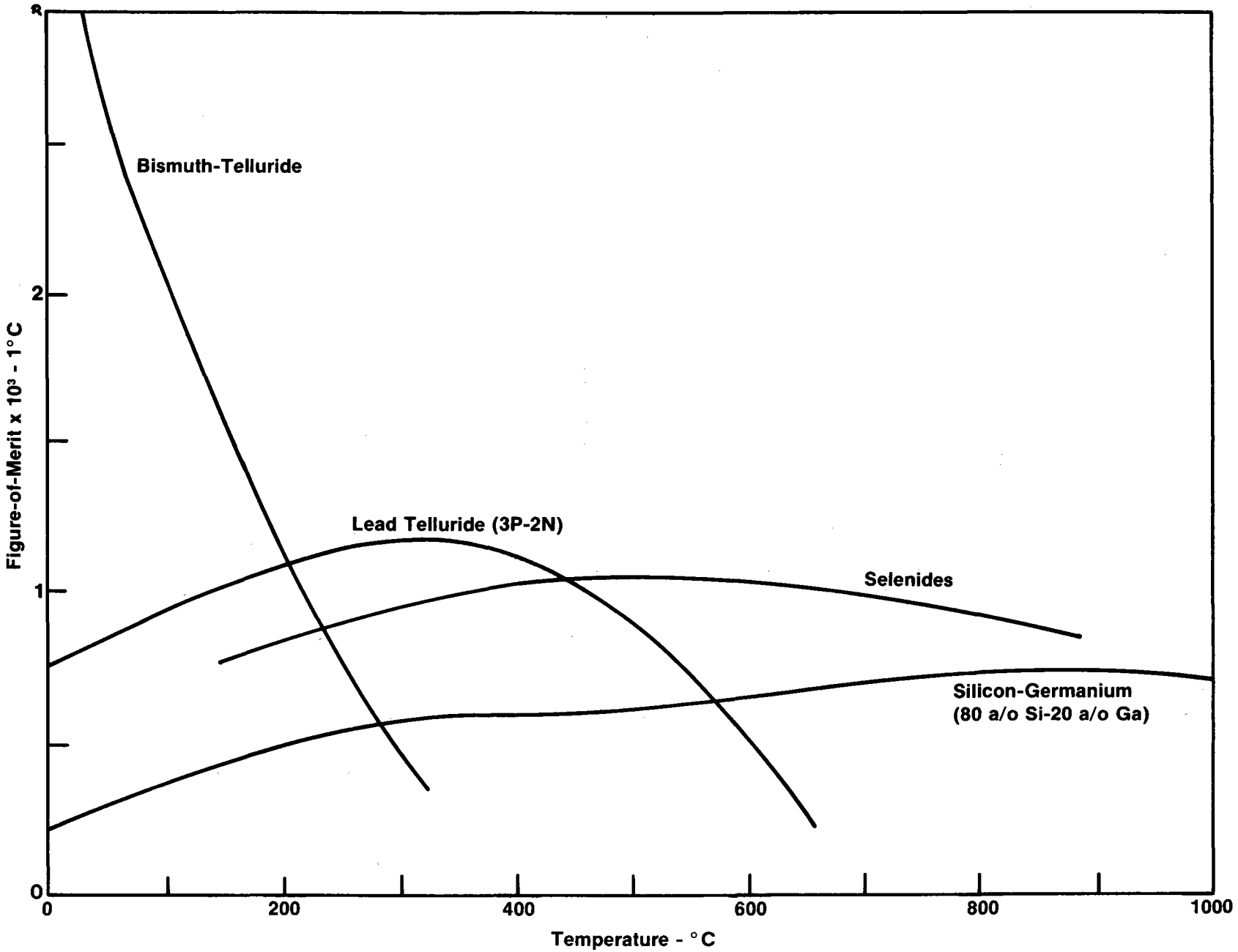

Figure 3-1. FIGURES-OF-MERIT FOR SEVERAL THERMOELECTRIC SEMICONDUCTORS

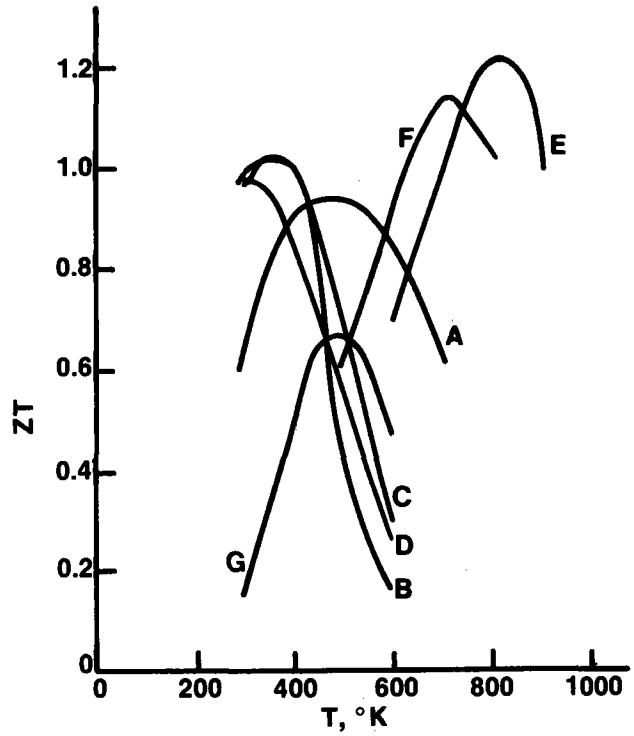

Figure 3-2. FIGURES-OF-MERIT OF SOME LOW AND MEDIUM TEMPERATURE THERMOELECTRIC MATERIALS

Curve A: n-type, 0.75 Bi_2Te_3, 0.25 Bi_2Se_3
Curve B: p-type, 0.30 Bi_2Te_3, 0.70 Sb_2Te_3(Te)
Curve C: p-type, 0.25 Bi_2Te_3, 0.75 Sb_2Te_3(Te)
Curve D: p-type, 0.25 Bi_2Te_3, 0.75 Sb_2Te_3(Se)
Curve E: p-type, 0.95 GeTe, 0.05 Bi_2Te_3
Curve F: p-type, 0.90 GeTe, 0.10 AgSbTe
Curve G: ZnSb

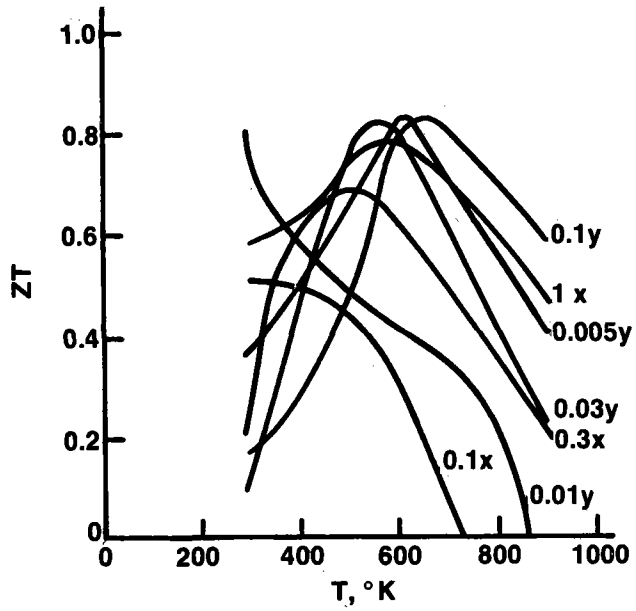

Figure 3-3. FIGURES OF MERIT OF SEVERAL LEAD TELLURIDE MATERIALS

p-type semiconductor with percentage of sodium as parameter (%X)

n-type semiconductor with percentage of lead diiodide as parameter (%Y)

silicon and germanium can operate in air at all temperatures for practical power conversion applications. Therefore, if the less expensive air environment is used in STEG applications, bismuth telluride (below 200°C) and silicon-germanium alloys (500 to 1000°C) are preferred.

3.2 THE COST OF THERMOELECTRIC MATERIALS

The most promising material for solar thermoelectric applications is bismuth telluride. The present commodity prices for bismuth and tellurium are about $8 per pound and $15 per pound respectively, but these prices are expected to decline if large orders are contracted.

Both bismuth and tellurium are byproducts. Bismuth is a byproduct of lead and gold refining; tellurium is a byproduct of copper refining. Both are abundant, but the present market is limited. Consequently, small-scale production facilities (with their attendant inefficiency) are used. Since the mining and most of the processing costs are borne by the primary products (copper, gold, and lead), the byproduct cost is determined by the cost of capital equipment, operation, and maintenance of the byproduct separation and purification operation. At present, these costs must be recovered by the sale of a relatively small volume of byproduct. As larger quantities are demanded, production equipment can be scaled up, its efficiency improved, and its costs spread over a much larger volume of byproduct. The result of this peculiar situation is an inverted supply-demand curve. The greater the demand, the lower the costs.

Information obtained by a subcontractor (General Atomics Company) from a major producer of bismuth and tellurium (ASARCO) indicates a very substantial reduction in material costs as demand increases. The following trend is predicted by General Atomics for the price of bismuth telluride.

10^3-lb order	$2.60/lb
10^4-lb order	$2.08/lb
10^5-lb order	$1.56/lb
10^6-lb order	$1.04/lb

SERI

SECTION 4.0

WHY SOLAR THERMOELECTRICS NOW?

It is generally believed that because thermoelectrics have poor efficiency, they are not competitive with other energy conversion technologies. Although this is true for fossil fuel powered generators, where fuel is the predominant cost, it is not necessarily true in solar applications. Cost of energy, which is the ultimate criterion for comparison, is a function of many factors, of which efficiency is but one. The cost of energy is calculated by:

$$\text{Cost of Energy} = \frac{[\text{Capital Investment}] \times [\text{FCR}] + \text{O\&M}}{(\eta \times I_{avg} \times A_c) \times 8760} \qquad (4.1)$$

Where: FCR = fixed charge rate,

η = solar to electric conversion efficiency,

I_{avg} = average solar insolation (kW/m^2),

A_c = collector area (m^2), and

O&M = levelized annual operation and maintenance cost ($).

The capital investment cost is determined from:

$$\text{Capital Investment} - C_A \times A_c + C_{con} + C_{storage} + C_{Other} \qquad (4.2)$$

With: C_A = cost of the collectors ($/m^2$),

C_{con} = cost of the conversion equipment ($),

$C_{Storage}$ = cost of the storage equipment ($), and

C_{Other} = other costs such as land and installation ($).

FCR, the fixed charge rate, is a very sensitive function of the life of the plant, because it includes mainly interest and depreciation on capital. Depreciation, in turn, depends on life of equipment. The fixed charge rate can be calculated by:

$$\text{FCR} = \frac{i(1+i)^n}{(1+i)^n - 1} + \text{other charges (insurance, taxes, etc.)} \qquad (4.3)$$

where i = cost of money (e.g., interest rate)

For i = 10%, the term $\frac{i(1+i)^n}{(1+i)^n-1}$

= 40.2% if equipment life is 3 years

= 11.7% if equipment life is 20 years

= 10.6% if equipment life is 30 years

Assuming 5% for "other charges,"

FCR for 3-year equipment life = 45.2%;
for 20-year equipment life = 16.7%; and
for 30-year equipment life = 15.6%.

The economic life of equipment has tremendous impact on the cost of energy produced. The cost equation shows that operation and maintenance costs are also important in determining the cost of energy.

From this analysis, it can be concluded that poor efficiency alone is not sufficient grounds for dismissing a technology like thermoelectrics. Low O&M costs, low capital costs, high reliability, and simplicity of installation and maintenance of thermoelectrics may more than offset the disadvantage of low efficiency. Further, from the point of view of a total system, the overall efficiency of thermoelectrics may not be much lower than that of other systems.

Early potential applications of thermoelectrics are in solar energy conversion systems with very low-cost collectors. In this report, two such applications are discussed:

- ocean thermal energy conversion where collector cost is zero, and
- solar ponds, where the cost of the collector can be as low as $\$3.5/m^2$ if the salt is free [7].

The economics of STEG in each application are compared with competing technologies. There is tremendous potential for reducing the cost of thermoelectric generators (e.g., to $100/kW or so) in large production quantities, as was determined by the costing group at General Atomics Company under subcontract to SERI. These cost projections are shown in Table 4-1.

Table 4-1. CAPACITY VS THERMOELECTRIC MATERIAL COST IN LARGE-SCALE PRODUCTION

Capacity (kW)	Cost ($/kW)
100	60
1000	45
10,000	32
100,000	19

With such promising cost estimates, there is very high probability that the cost of solar thermoelectrics may decrease to values at which many solar applications become viable. To illustrate the potential of solar thermoelectrics, two applications--OTEC and the solar pond--are presented in detail in Sections 5.0 and 6.0.

SECTION 5.0

STEG - OTEC

5.1 OCEAN THERMAL ENERGY CONVERSION SYSTEM DESCRIPTION

Ocean Thermal Energy Conversion (OTEC) uses the temperature differential between warm surface water and cold, deep ocean water to produce electric power. Conversion technology presently being investigated is called "closed cycle OTEC." In this scheme (Figure 5-1A), the warm water is pumped through an evaporator/heat exchanger containing a working fluid. The vaporized working fluid drives a Rankine-engine turbine which provides the plant's power. After the turbine, the vapor enters a condenser/heat exchanger cooled by colder water drawn from deep in the ocean. The condensed working fluid is then pumped back into the evaporator for recycle.

5.2 PROPOSED CONCEPT -- OTEC-TE [9]

A proposed concept that combines thermoelectrics (TE) with OTEC is shown schematically in Figure 5-1B. Warm water heats the hot side and cold water cools the cold side of the thermoelectric elements. The thermoelectric elements are connected in a series-parallel arrangement to obtain the desired voltage/current ratio. The simplicity of such a system is obvious: no working fluid is required, eliminating the problems of leaks, pressurized containers, etc. The advantages of such a system are summarized in Table 5-1.

Table 5-1. SUMMARY OF DESIGN ADVANTAGES OF THERMOELECTRIC OTEC OVER CLOSED CYCLE RANKINE OTEC

No working fluid required
no pressurized container or ducting needed
no shutdown due to leaks
no hazard to workers or environment from leaking ammonia, propane, etc.
no working fluid pump required
less capital cost
No turbine-generator required
less rotating equipment to maintain
less capital cost
Solid state power generation
higher reliability
modularity -- ease of repair and replacement
-- low cost, mass-production
-- design flexibility
-- sizing flexibility
redundancy -- high capacity factor
rugged design -- long lifetime
graceful failure of components

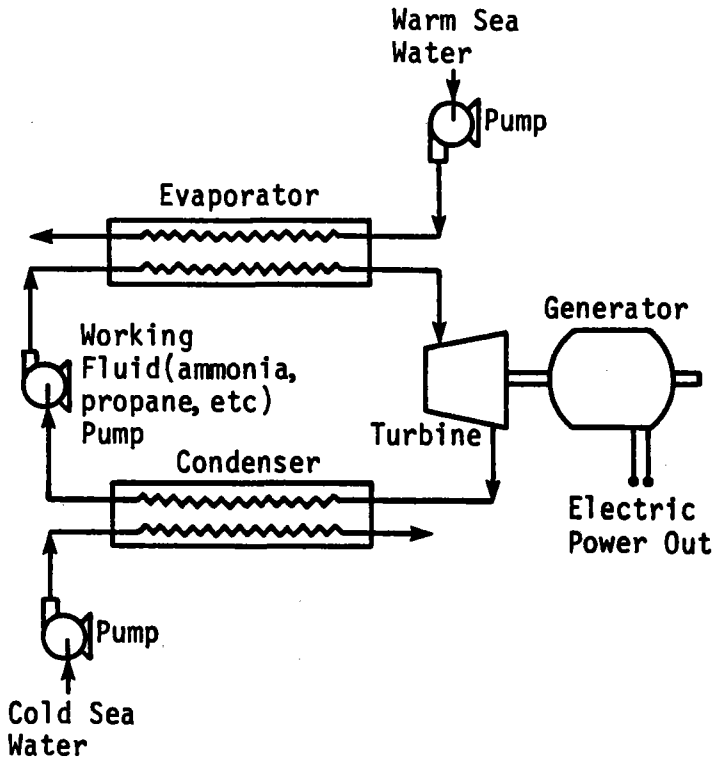

A. Schematic Closed Cycle OTEC

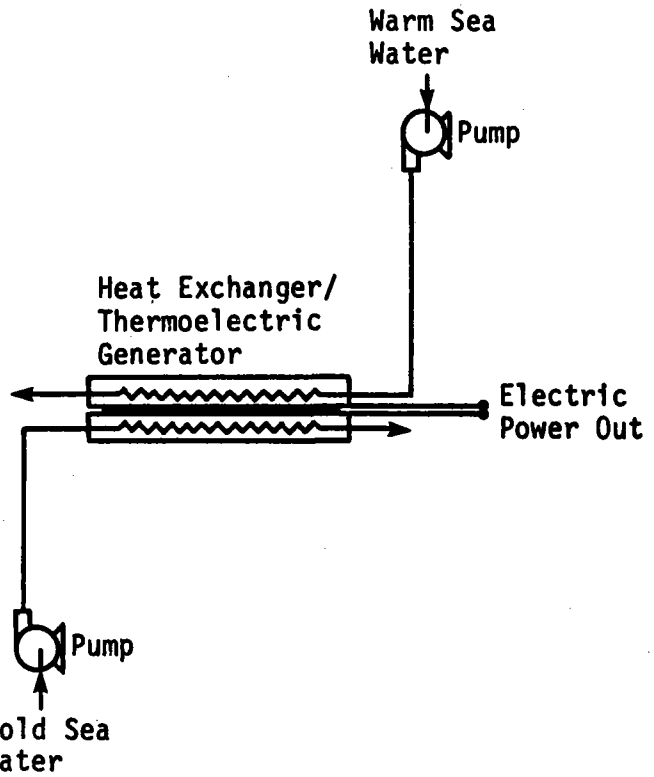

B. Schematic Thermoelectric OTEC

Figure 5-1. SCHEMATICS OF CLOSED CYCLE AND THERMOELECTRIC OTEC

5.3 PERFORMANCE ANALYSIS

A thermoelectric generator for OTEC and similar applications has been investigated to determine its electrical power production potential. A preliminary parametric study also has been completed. The analysis considers the standard thermoelectric generator illustrated in Figure 5-2.

The electric voltage/current ratio is determined by the connection scheme used between the elements. Numerous combinations are possible, and system power output is unaffected by any reasonable arrangement. This analysis investigates maximum power output potential for a unit area of the thermoelectric generator in an OTEC application. Thus, the connection scheme is immaterial. For convenience, all the thermoelectric p-n pairs are assumed to be connected in parallel. In the system configurations that have been considered, the generator is sandwiched between the plates of a plate-fin or parallel plane heat exchanger. Numerous plates would be stacked together to generate the desired electrical power output.

5.3.1 Nomenclature

The OTEC thermoelectric generator has been analyzed for a unit area (m^2) of heat exchanger plate. The variables and subscripts listed below are used in the analysis.

Variables:

- A: the fraction of heat exchanger plate covered with thermoelectric material
- CR: the contact resistance coefficient between the thermoelectric surface and the conducting plate (Ω-m^2)
- I: current (A)
- K: thermal conductivity (W/m°K)
- L: thickness of the semiconductor material (m)
- H: thermal conduction coefficient (W/m^2°K)
- R: electrical resistance (Ω)
- P: output power per unit area (W/m^2)
- Q: heat flux (W/m^2)
- T: temperature (°K or °C)
- V: voltage (V)
- α: Seebeck coefficient (V/°K)
- ρ: electrical resistivity (Ω-m)

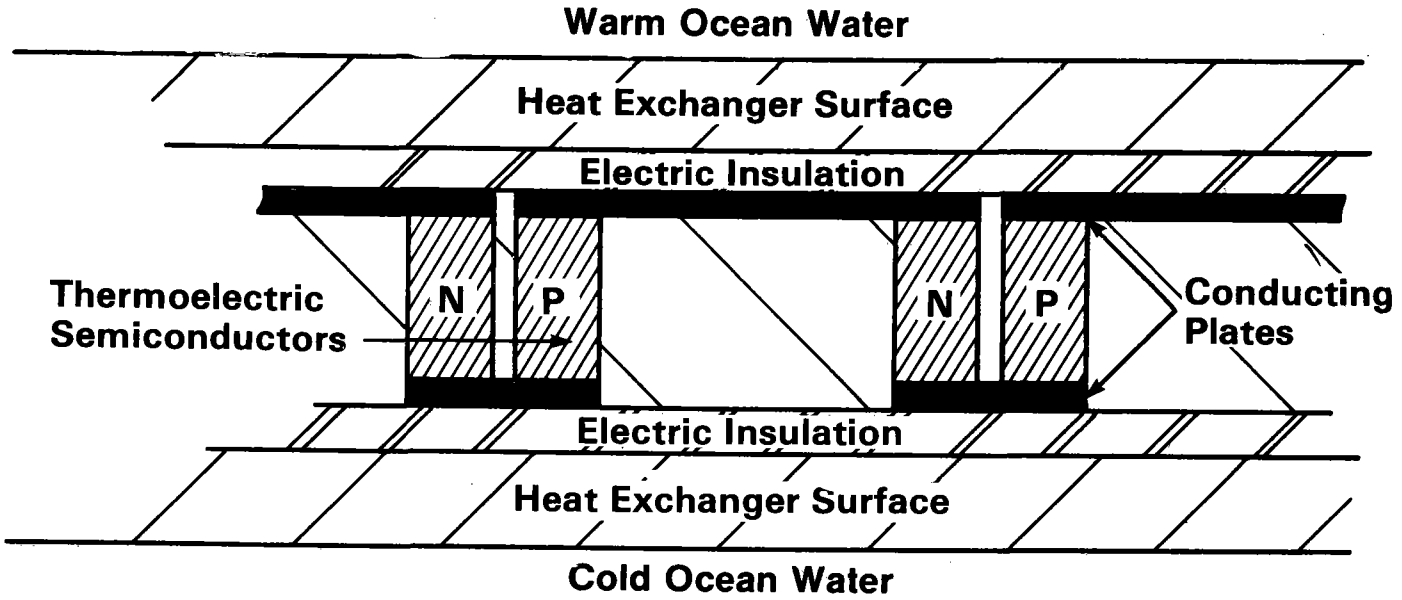

Figure 5-2. STANDARD THERMOELECTRIC GENERATOR

Subscripts:

- in: thermal insulation separating the thermoelectric elements
- c: cold junction of the thermoelectric generator
- n: n-type thermoelectric material
- p: p-type thermoelectric material
- w: warm water flow
- wj: warm junction of the thermoelectric generator
- g: thermoelectric generator

5.3.2 Analytical Model of Thermoelectric Generator

A simple schematic diagram of the thermoelectric generator model is shown in Figure 5-3. The generator performance is determined by equating the heat fluxes, q_w and q_c, to the heat fluxes at the warm and cold junctions, respectively, of the thermoelectric generator.

$$q_w = (T_w - T_{wj})\, H_w \tag{5.1}$$

$$q_w = \frac{K_g \Delta T}{L} + I\alpha_g T_{wj} - \frac{1}{2} I^2 R \tag{5.2}$$

$$q_c = (T_{cj} - T_c)\, H_c \tag{5.3}$$

$$q_c = \frac{K_g \Delta T}{L} + I\alpha_g T_{cj} + \frac{1}{2} I^2 R \tag{5.4}$$

The heat flux through the warm and cold sides of the heat exchanger is determined from the thermal conduction coefficient. The heat flux at the thermoelectric junctions is slightly more complicated, being the sum of thermal conduction, the Peltier effect, and joule heating [10]. The joule heating within the generator is assumed to disperse evenly between the warm and cold junctions.

The lumped-parameters used to describe the thermal and electrical properties of the generator are determined from:

$$K_g = A_n K_n + A_p K_p + A_{in} K_{in} \tag{5.5}$$

$$\alpha_g = \alpha_n + \alpha_p \tag{5.6}$$

$$R = \frac{\rho_n L_n}{A_n} + \frac{\rho_p L_p}{A_p} + \frac{2\ CR}{A_n} + \frac{2\ CR}{A_p} \tag{5.7}$$

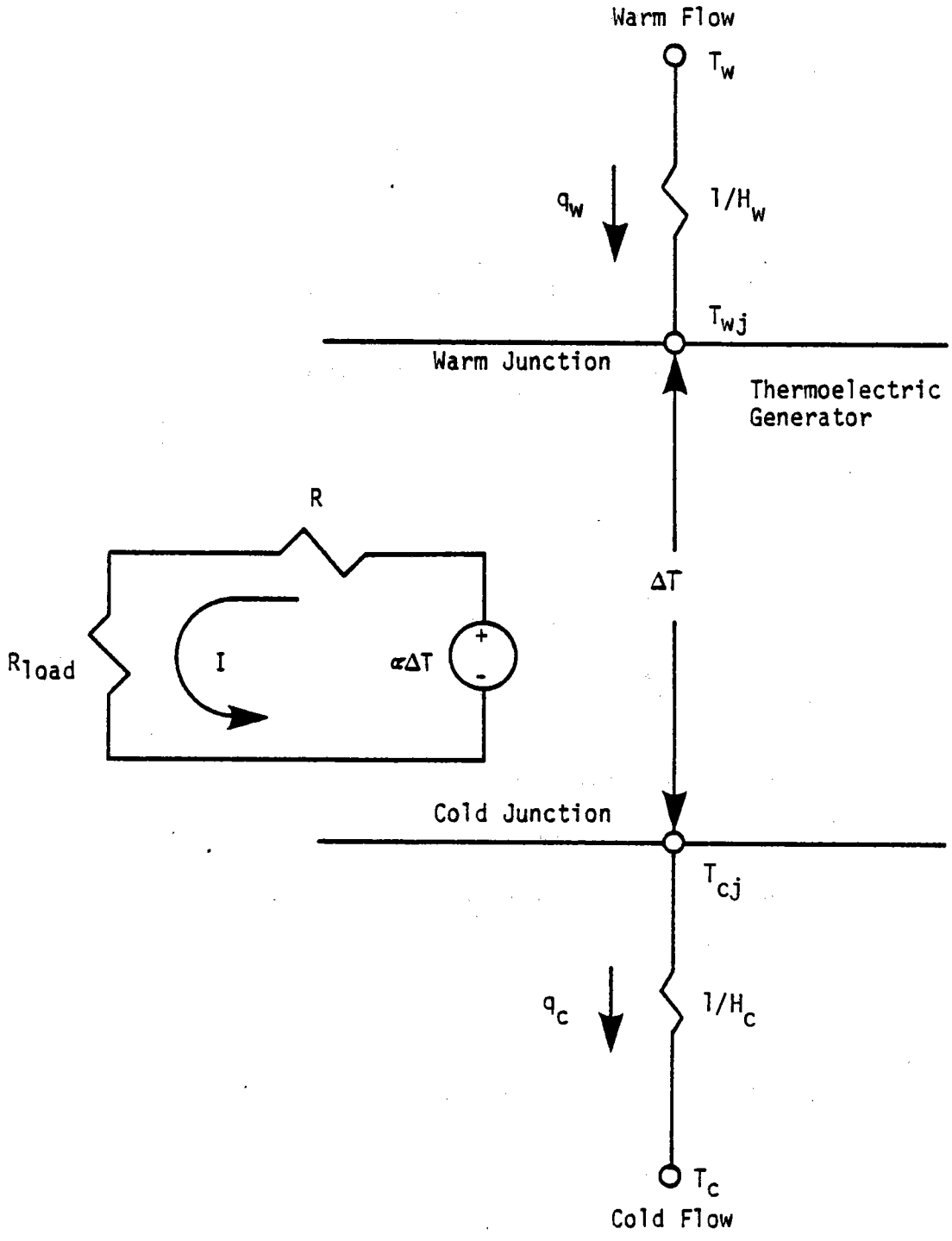

Figure 5-3. SCHEMATIC OF THE THERMOELECTRIC GENERATOR MODEL

Since maximum power output is desired, additional constraints are applied. It can be shown that for maximum power transfer:

$$R_{load} = R \tag{5.8}$$

$$\frac{A_n}{A_p} = \left(\frac{\rho_n}{\rho_p}\right)^{1/2} \tag{5.9}$$

Matching the load to the internal generator is the standard condition for maximizing electrical power. Equation 5.9, defining the ratio of the semiconductor areas, minimizes the generator internal electrical resistance for a given thermoelectric thickness.

The electrical performance for the maximum power output condition is:

$$I = \frac{\alpha\Delta T}{2R} \tag{5.10}$$

$$P = \frac{(\alpha\Delta T)^2}{4R} \tag{5.11}$$

Equations 5.10 and 5.11, together with the material and geometric properties of the thermoelectric generator, the heat exchanger thermal conductivities, and the warm and cold flow temperatures, form a set of sufficient constraints to determine the generator performance. A numerical convergence routine is used to solve this nonlinear set of equations.

5.4 THERMOELECTRIC GENERATOR PERFORMANCE

The power output of the thermoelectric generator is affected by many parameters--so many that a detailed study of each is beyond the scope of this evaluation. This preliminary investigation is directed toward providing a reasonable estimate of the power production potential and understanding of several major design considerations.

For all results presented, the following thermoelectrical properties are used:

p-type thermoelectric:

$\rho = 1.0 \times 10^{-5}$ (Ω-m)

$K = 1.1 \times$ (W/m°K)

$\alpha = 2.0 \times 10^{-4}$ (V/°K)

n-type thermoelectric:

$\rho = 1.0 \times 10^{-5}$ (Ω-m)

$K = 1.1$ (W/m°K)

$\alpha = 2.0 \times 10^{-4}$ (V/°K)

$CR = 1 \times 10^{-9}$ (Ω/m^2)

The necessary heat-transfer coefficients and pumping losses for a plate-fin heat exchanger are given in Kays and London [11]. (The pumping loss calculation assumes an 87% conversion efficiency from electrical power to the water flow.) Aluminum fins, 0.025 inch thick, have been used for determining the heat exchanger fin efficiency.

The properties for the warm and cold water sources are:

	Warm Flow	Cold Flow
Temperature (°C)	25	5
Density (kg/m^3)	1,000	1,000
Dynamic Viscosity (kg/m/s)	1.52×10^{-3}	0.89×10^{-3}
Prandtl Number	12.0	5.9
Specific Heat (J/kg°C)	4,183	4,183

An overview of the system performance is presented in Figures 5-4 through 5-7. Figure 5-4 shows the effect on electrical power output as the thickness of the thermoelectric material is varied. The power output maximizes with an appropriate thickness of thermoelectric material. In the remaining graphs (Figures 5-5, 5-6, and 5-7), the thermoelectric thickness has been optimized to achieve maximum power generation.

Figure 5-5 plots the relationship between Reynolds numbers describing the flows through the heat exchanger and the gross generator output and net electrical output. For this graph, the Reynolds numbers for the warm and cold flows were the same, a constraint which does not yield maximum net power. (For the flow rates considered, a maximum net power of 284 W/m^2 would be realized for a Reynolds number of 3000 in the warm flow and 2000 in the cold flow.)

Figure 5-6 illustrates the volume of thermoelectric material that can be removed (without severely degrading electrical output) by reducing the percentage of area covered with thermoelectric material. As the thermoelectric coverage is reduced, the desired 'maximum power' thickness is also reduced by approximately the same ratio. The limit to the possible reduction in coverage is determined by either the fabrication technology or second-order effects such as contact resistance or the heat transfer through the insulation encasing the elements.

Figure 5-7 shows the power output potential of the thermoelectric generator as the available temperature difference increases. The potential output power increases roughly in proportion with the square of the temperature difference across the heat exchanger. The increased electrical generation potential for larger temperature differences suggests that this generator might be useful in low-temperature applications in addition to OTEC; for example, solar ponds, geothermal fluids, and conventional power plant bottoming cycles. Section 6.0 develops the solar pond application.

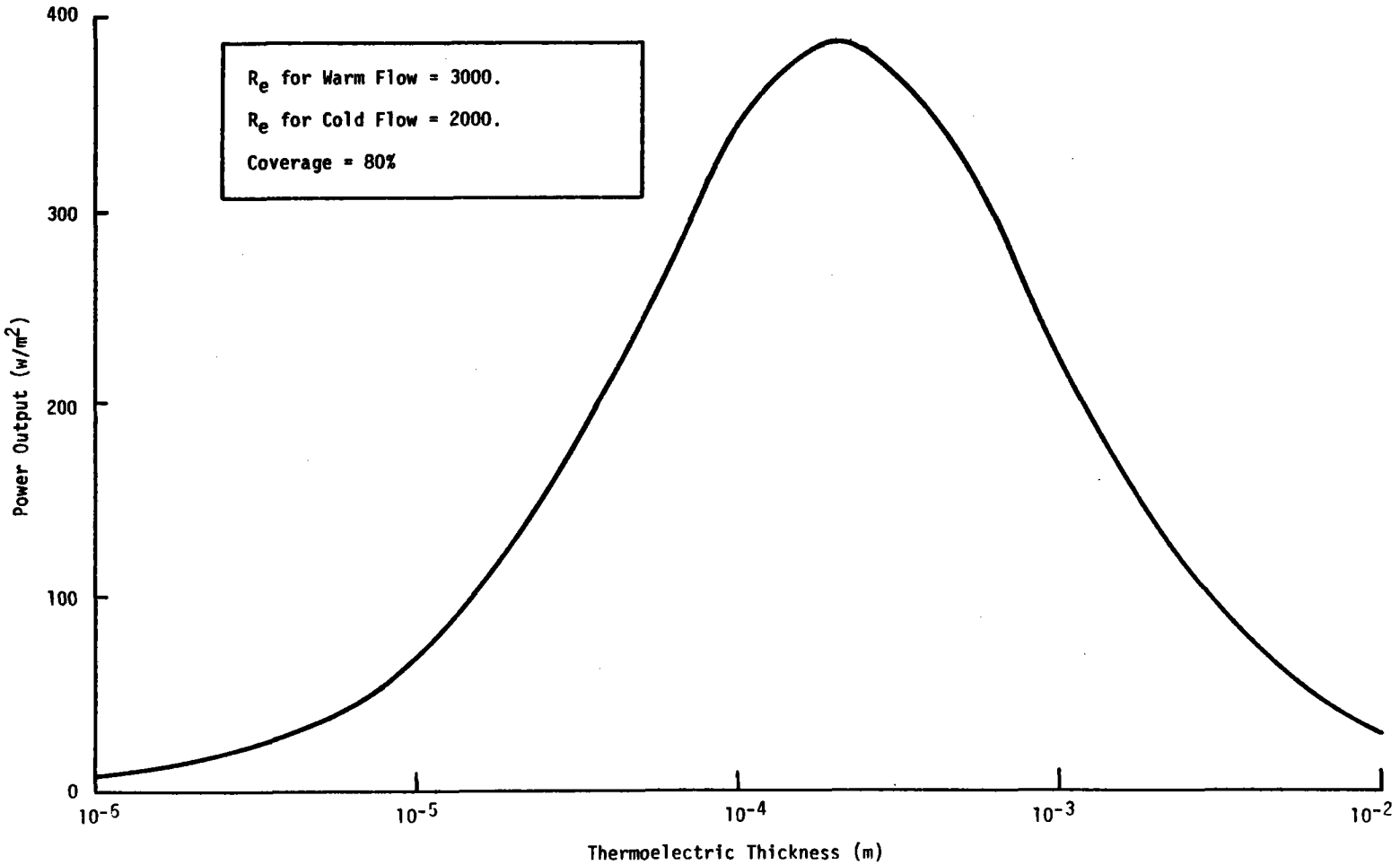

Figure 5-4. POWER OUTPUT VS. THERMOELECTRIC THICKNESS

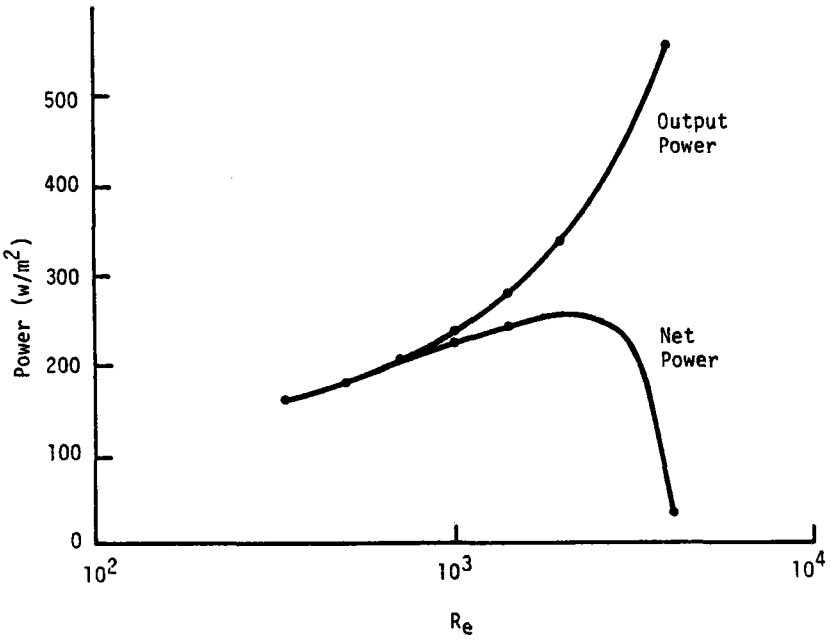

Figure 5-5. GROSS POWER AND NET POWER VS. REYNOLDS NUMBER FOR A THERMOELECTRIC GENERATOR

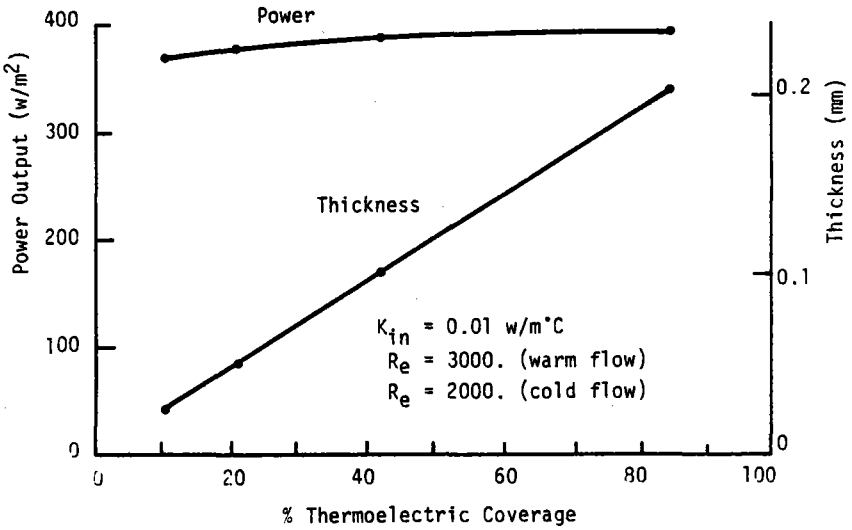

Figure 5-6. EFFECT ON POWER OUTPUT AND MAXIMUM POWER TE THICKNESS AS COVERAGE VARIES

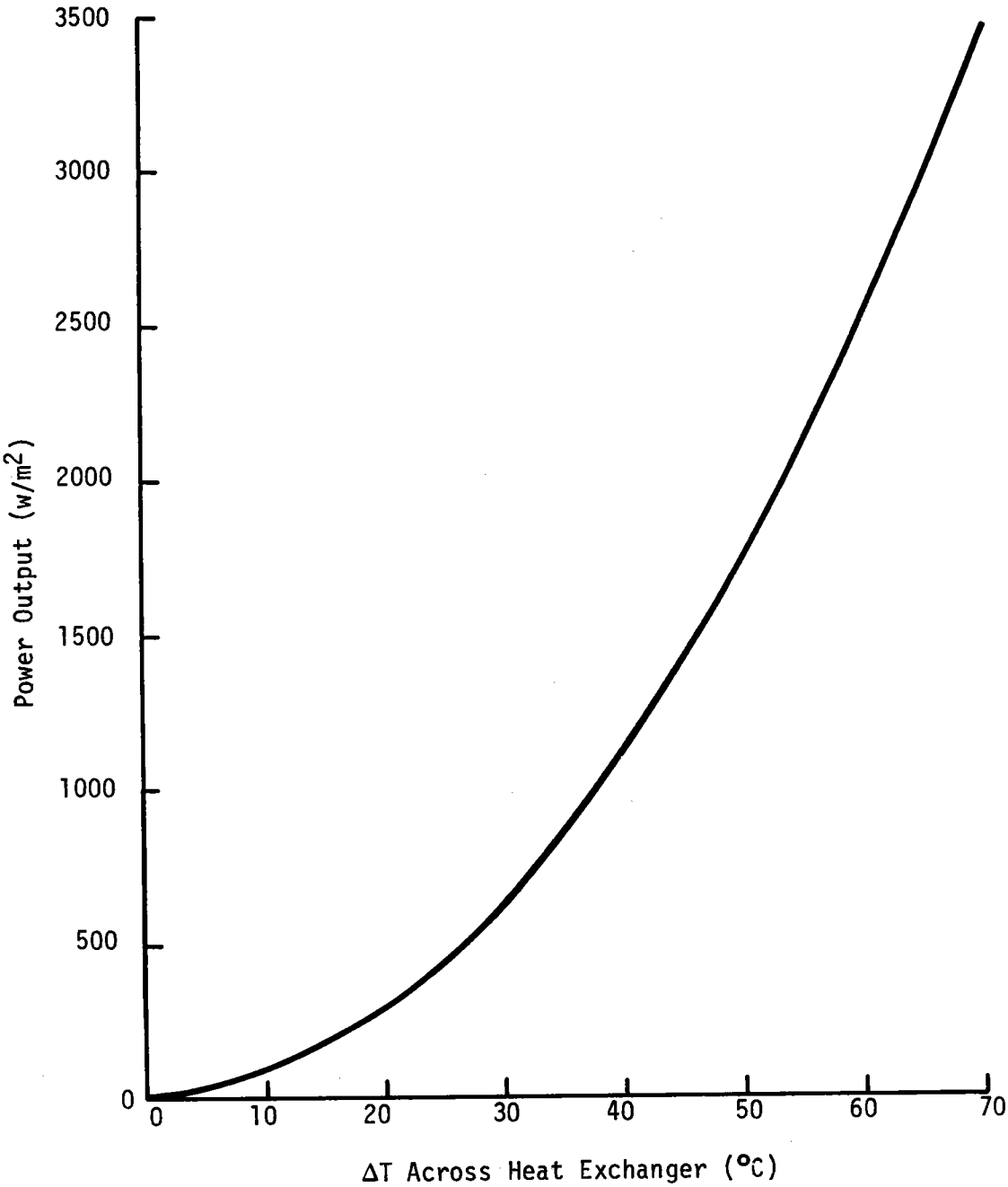

Figure 5-7. GROSS POWER OUTPUT VS. AVAILABLE TEMPERATURE DIFFERENCE

5.5 PRELIMINARY DESIGN OF AN OTEC-TE SYSTEM

A thermoelectric generator module has been designed that is suitable for OTEC [Figure 5-8 (A,B,C)]. This design combines heat exchanger and electric generation functions in one modular system. The module is far more compact than the "conventional" closed-cycle OTEC design. The design has been optimized around a compact plate-fin heat exchanger described by Kays and London for which experimental data were available [12]. Many other heat exchanger designs are available with perhaps equal or better performance. This design is the result of the preliminary analysis described in Section 5.4.

Table 5-2 lists the design parameters and calculated performance for the module. Losses due to joule heating and power requirements for water pumping have been accounted for in the calculation of net electrical power output. No allowance was made for losses due to manifolding or electric power conditioning; however, these should represent only a small additional loss.

Table 5-3 lists the estimated capital costs of two baseline, closed-cycle OTEC system designs prepared under DOE contract--one by the TRW Defense and Space Systems Group and the other by Lockheed Missile and Space Company--and compares these costs with some estimated component costs for a thermoelectric OTEC. Figures 5-9A and 5-9B show artist's conceptions of the two closed-cycle systems. The thermoelectric OTEC includes fewer mechanical components and simpler heat transfer/power generation components. The thermoelectric material costs only $15-60/kW (in 1978 dollars) depending upon the thickness of the semiconductor elements. The thermoelectric OTEC offers the potential for at least a 25% reduction in capital costs over the conventional systems. Additional reductions in capital costs could be realized by designing an entire system around the thermoelectric module.

Substantial advantages in operation and maintenance expenses are expected from the use of modular thermoelectric power generation devices rather than massive turbine-generators. Table 5-4 compares the reliability and maintainability estimates made by TRW for their closed-cycle design with estimates for a thermoelectric OTEC plant from experience in other applications of low temperature thermoelectric devices.

The failure of a major component in a conventional OTEC plant reduces its output power by the amount of generating capacity affected until the component is repaired or replaced. Since the OTEC power plant is intended to provide base load electric power, such reductions in output are serious problems. To reduce the impact of equipment failure, conventional OTEC designs include multiple units so that a single major component failure causes only a fractional loss of power output. The TRW design uses 4 power modules for their 100 MW_e (net) plant, whereas the LMSC design uses 16 power modules for their 160 MW_e plant. Because the power modules in the closed-cycle system utilize a pressurized heat transfer system susceptible to leaks caused by corrosion, an entire module may be shut down because of a single leak.

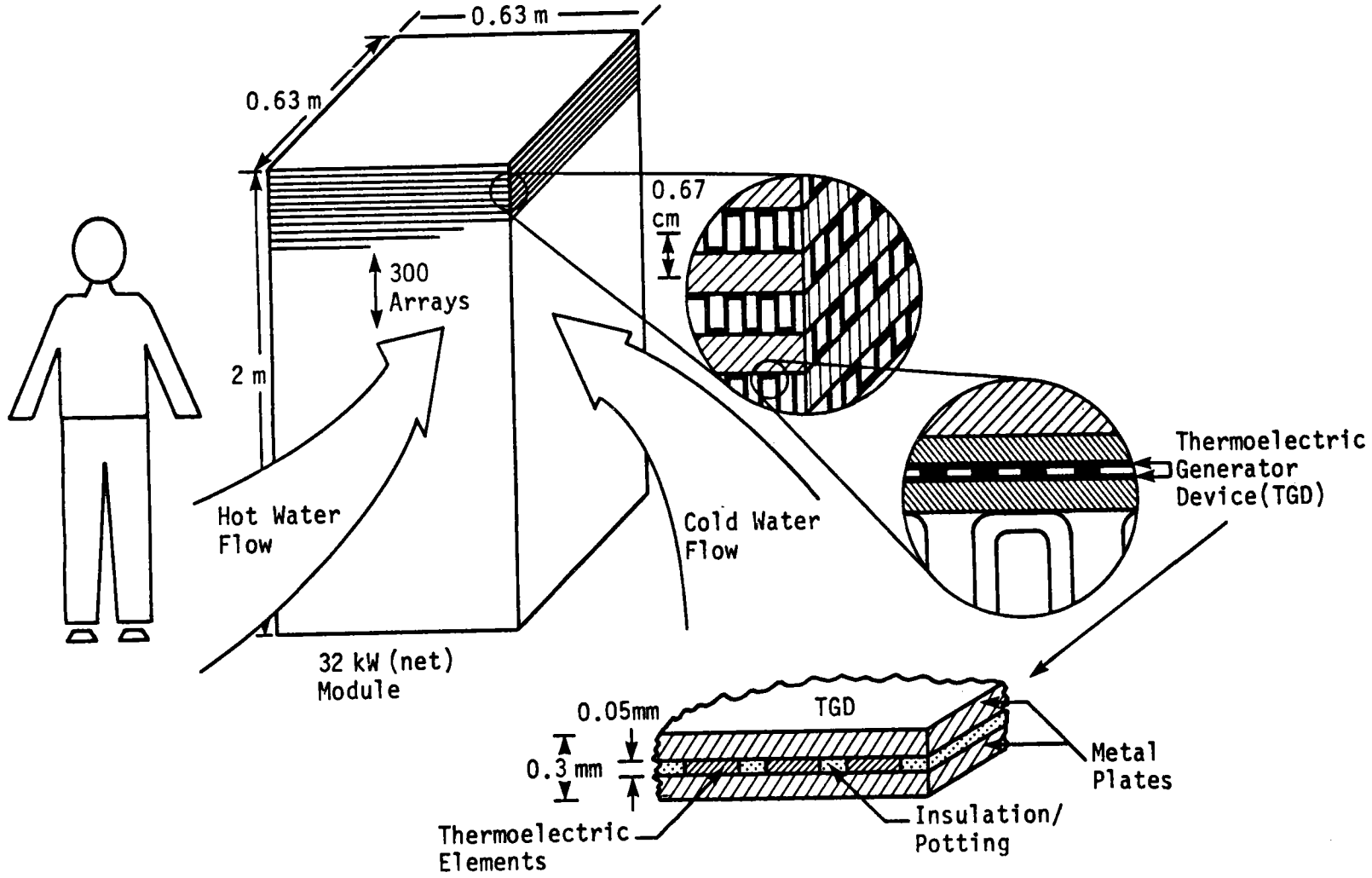

Figure 5-8A. THERMOELECTRIC OTEC MODULE DESIGN

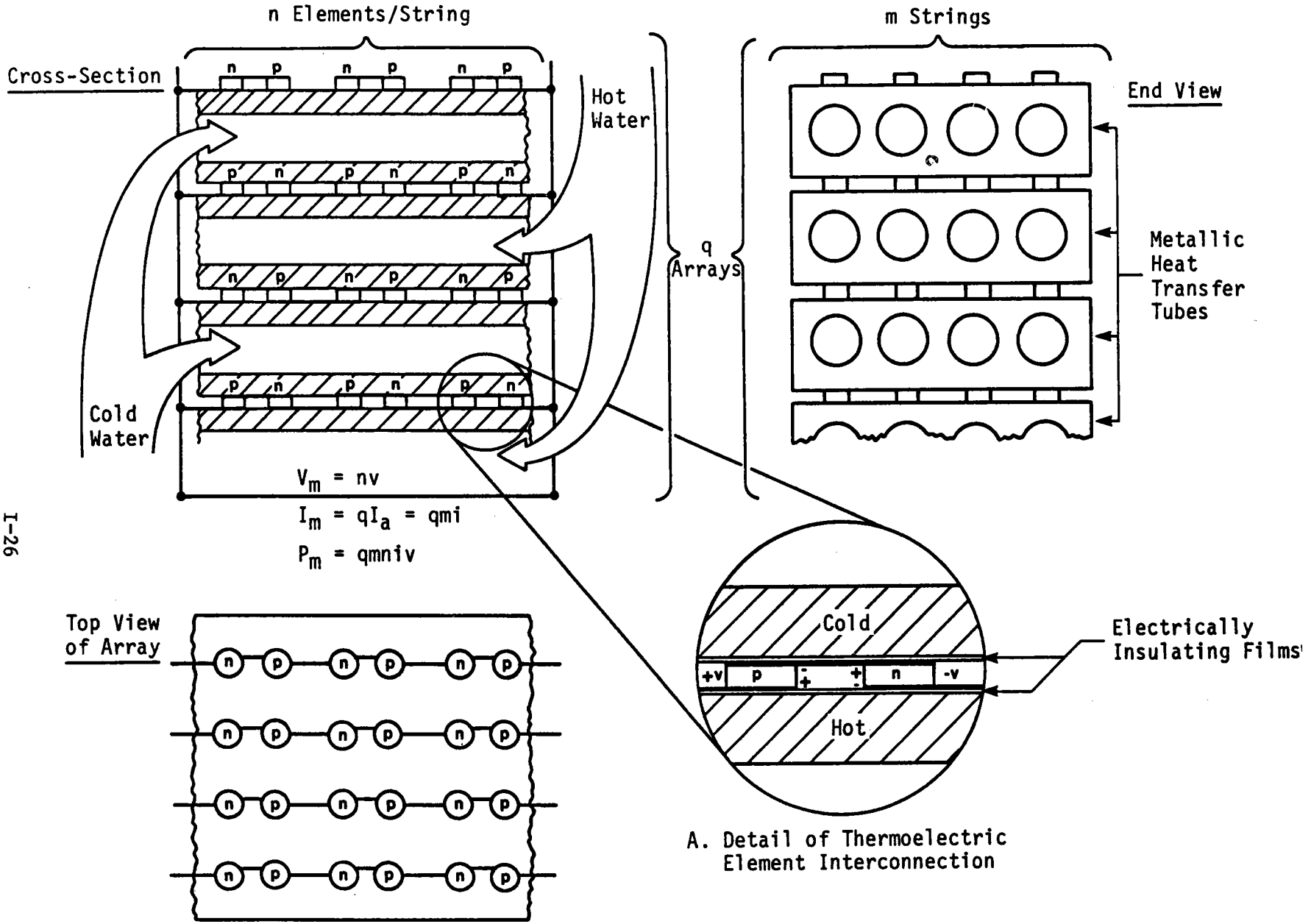

Figure 5-8B. THERMOELECTRIC OTEC MODULE DESIGN

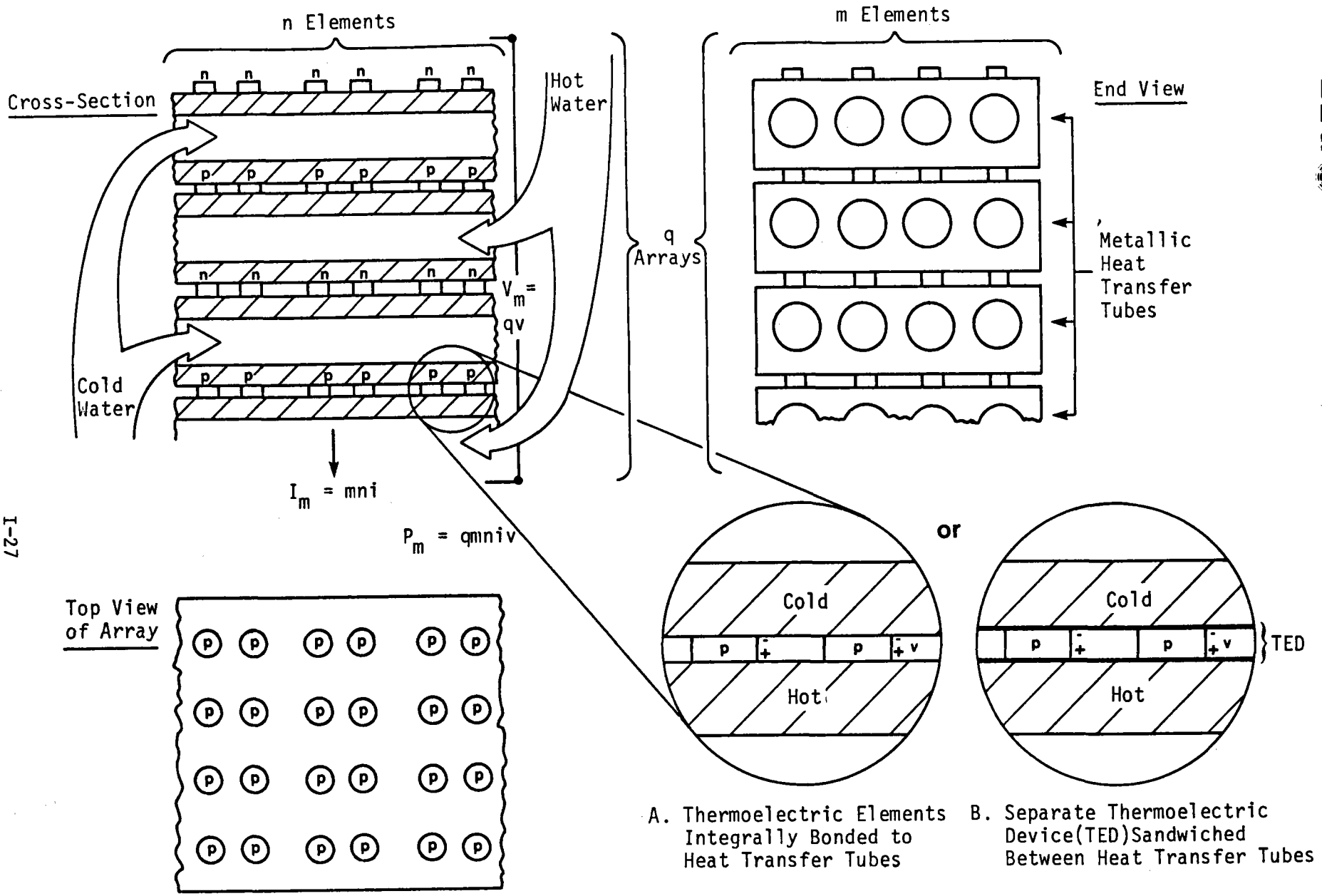

Figure 5-8C. THERMOELECTRIC OTEC MODULE DESIGN

Table 5-2. THERMOELECTRIC ENERGY CONVERSION MODULE FOR OTEC SYSTEM: DESIGN PARAMETERS

Inlet Temperatures	Warm water: 25°C	Cold water: 5°C
Outlet Temperatures	23°C	7°C

Thermoelectric Power Generator

Thermoelectric material properties (typical of bismuth telluride at 20°C)

Figure-of-merit ($°K^{-1}$)	n-type 3.6×10^{-3}	p-type 3.9×10^{-3}
Electrical resistivity (Ω-m)	n-type 10^{-5}	p-type 10^{-5}
Thermal conductivity (W/m°K)	1.1	
Thermal insulation - thermal conductivity (W/m°K)	0.001	
Electrical contact resistance coefficient (Ω-m^{-2})	10^{-8}	

Heat Transfer Tubes

Plate-fin design with perforated fins [10]	
Plate thickness (cm)	0.076
Fin thickness (cm)	0.064
Hydraulic diameter (m)	0.0025
Thermal conductivity of metal (W/m°K)	200

Water Pumps - product of motor and pump efficiencies - 87%

Water Velocity (m/s)	1.07

OPTIMIZED DESIGN - OPERATING PARAMETERS

Water-flow velocity 1.07 m/s (3.51 ft/s)

Heat transfer coefficient (W/m°K) warm side 1485; cold side 11,373

Thermoelectric material

Fraction of area covered by thermoelectric	0.10
Thickness of thermoelectric elements (mm)	0.026

Electric power production (W/m^2) of thermoelectric array

Gross[a]	387 W/m^2
Net[b]	282 W/m^2

[a]Accounts for joule heating losses

[b]Accounts for pumping power losses.

Table 5-3. OTEC SYSTEM CAPITAL COSTS

Module	Ammonia Closed Cycle[a]		Thermoelectric OTEC	
	Aluminum HX (1979 $/kW)	Titanium HX (1979 $/kW)	Commercial Thermoelectrics (1979 $kW)	Advanced Thermoelectrics (1979 $/kW)
Heat exchangers (and thermoelectrics	482-844	567-989	1218	658
Demisters	8-48	8-48	NA	NA
Turbogenerators	84-135	84-135	NA	NA
Seawater pumps	103-241	115-241	395	213
Other Power systems	139-235	130-235	130-235	130-235
Platform	60-362	60-362	60-362	60-362
Cold water pipe	86-96	86-96	86-96	86-96
Mooring/deployment	60-238	60-238	60-238	60-238
Electric cable	121-543	121-543	121-543	121-543
Total	1143-2743	1232-2887	2070-2722	1326-2343
Average	1943	2064	2396	1835

[a]On a module basis, these represent the highest and lowest estimates by four DOE contractors and COE personnel as reported during February 1978. The contractors' names corresponding to the estimates made are priority information and are not presented for that reason.

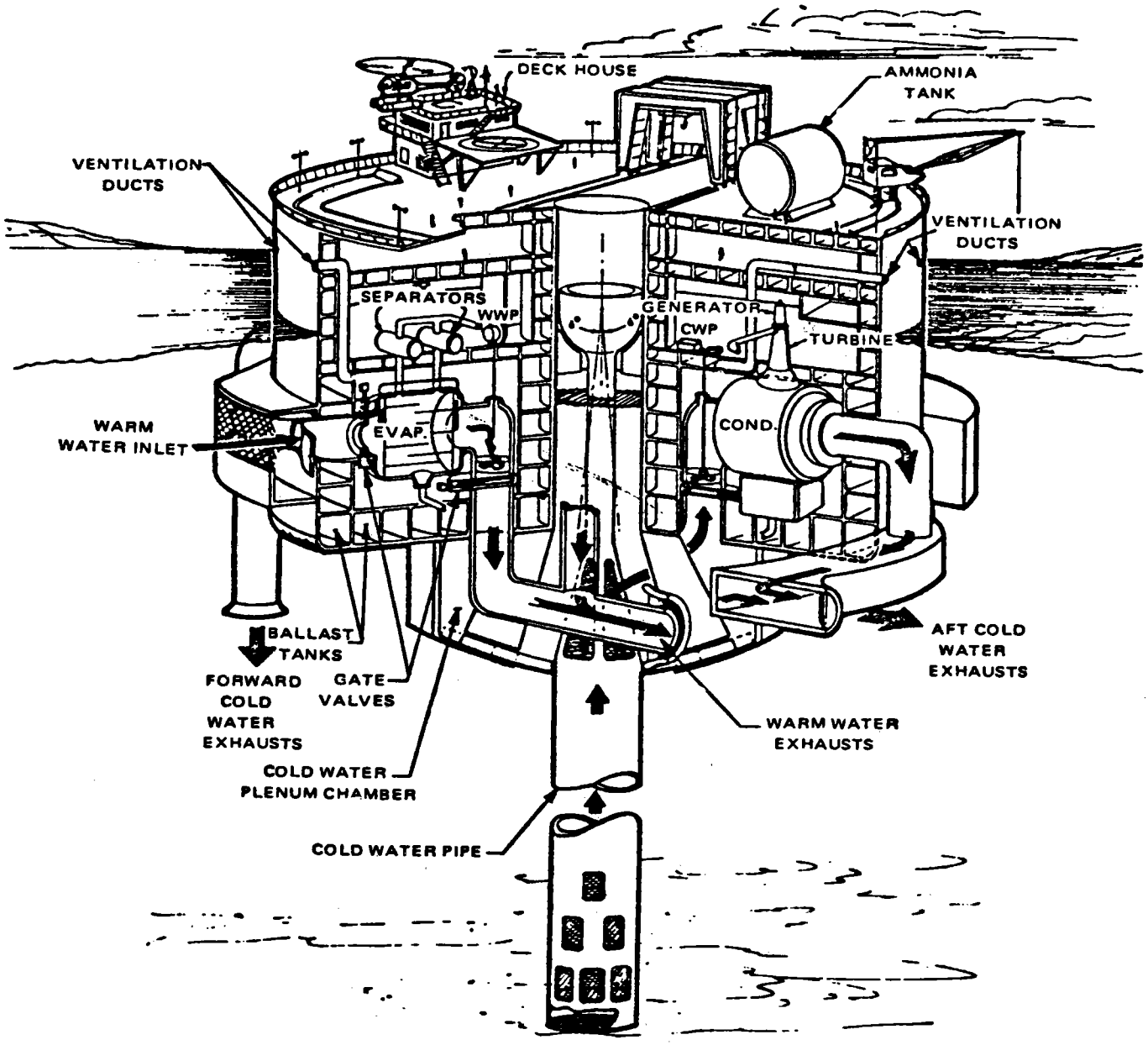

Figure 5-9A. ARTIST'S CONCEPTION OF CLOSED CYCLE OTEC SYSTEM, TRW CORPORATION

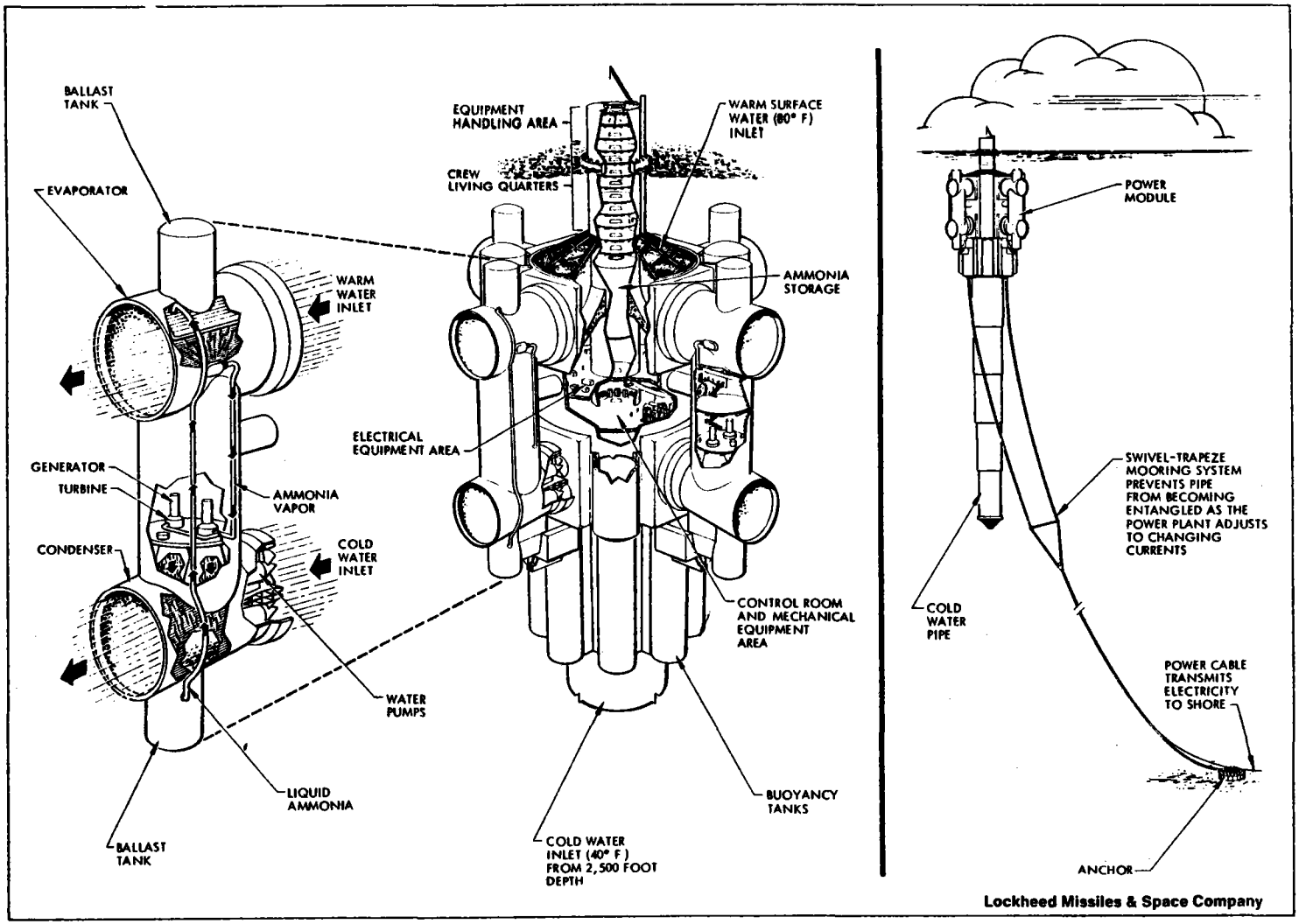

Figure 5-9B. ARTIST'S CONCEPTION OF CLOSED CYCLE OTEC SYSTEM, LOCKHEED MISSILE AND SPACE CO.

Table 5-4. RELIABILITY AND MAINTAINABILITY ESTIMATES FOR TRW AND CLOSED CYCLE AND THERMOELECTRIC OTEC DESIGNS

Component	Closed Cycle			Thermoelectric		
	Number	MTBF[a] (years)	MTTR[a] (days)	Number	MTBF[a] (years)	MTTR[a] (days)
Platform						
Core	1	40	14	1	40	14
Cold water pipe	1	10	19	1	10	14
Auxiliary Systems	-	5	1	--	5	1
Power Module						
Heat Exchangers	8	3	7			
Fluid Transfer Systems	12	1	5	N[b]	1	5
Power Generators	4	1	5	3100	30	1/8
Electrical & Controls	4	5	1	4	5	1

[a]MTBF = Mean Time Between Failures, MTTR = Mean Time to Repair

[b]N, the number of fluid transfer systems to be used in the thermoelectric design, can be varied to optimize reliability.

The 100 MW_e (net) thermoelectric OTEC plant would consist of more than 3,000 power modules/heat transfer units of the type shown in Figure 5-8. A leak in a heat transfer unit could destroy an array but would reduce only marginally the output of the module. Even the failure of one entire module would have no appreciable impact on plant output, and such a module could be replaced.

This example of the application of the thermoelectric generator to OTEC serves to illustrate the advantages of the design, which are summarized in Table 5-5. The thermoelectric conversion of ocean thermal energy to useful electrical power on a large scale is a novel concept which:

- uses proven (thermoelectric) technology,
- is well suited to automated mass production,
- reduces capital costs,
- increases system reliability,
- reduces materials requirements, and
- decreases maintenance costs.

Table 5-5. SUMMARY OF CLAIMS FOR THERMOELECTRIC ENERGY CONVERSION

Design Improvements Over Conventional Energy Conversion Systems	Advantages Gained
Greater design simplicity	Fewer subsystems Less maintenance Less costly design process
Greater design modularity	Mass-producible components Economical module repair/replacement
Greater design reliability	
Low-cost, solid-state energy conversion devices operating at innocuous, low temperatures with long life expectancies	Lower maintenance
Heat transfer systems operating at ambient pressure	Graceful (gradual) failure of components
Inherent redundancy of large numbers of thermoelectric generators connected in series/parallel arrays/modules	Lower levels of unavailability due to scheduled and unscheduled maintenance Higher capacity factor

SERI

SECTION 6.0

STEG - SOLAR POND

6.1 INTRODUCTION

Thermoelectric power generation has been shown to be attractive for OTEC applications. The thermoelectric generator offers longer life and lower initial costs than comparably rated organic Rankine engines. These cost advantages more than compensate for the lower conversion efficiency of the TE generator. In a similar application, a TE generator can be combined with a stratified solar pond. These ponds provide inexpensive solar collection and thermal storage in locations where salt is available at low cost. Potential applications of a solar pond-TE system depend on whether the low collection costs of the solar pond can compensate for the lower efficiency of the TE generator. To evaluate a solar pond-thermoelectric system, a stratified pond model was developed.

6.2 STRATIFIED SOLAR POND SYSTEM DESCRIPTION

A typical salt concentration gradient solar pond is shown schematically in Figure 6-1 [12]. The salt solution is composed of three regions of differing salinity: a surface convecting layer, a nonconvecting salt concentration gradient region, and a lower convection-storage zone. The upper layer is formed by the surface effects of wave turbulence and wind shear. Because it serves no useful purpose, it is normally kept as thin as possible. The nonconvecting region provides the thermal insulation barrier for the convection-storage zone. Heat is extracted from the convection-storage zone by pumping the heated brine to a heat exchanger. The black pond bottom absorbs a significant fraction of the incident solar radiation, which is transferred readily to the salt solution by convection. Thermal loss through the pond bottom is attenuated by the storage and insulating properties of the ground below the pond. For large ponds, the thermal loss through the pond edges is negligible.

6.2.1 Stratified Solar Pond Model

A lumped parameter model, illustrated by the RC thermal network analog shown in Figure 6-2, represents the pond. The salt solution and ground storage are sectioned into several layers represented by nodes in the RC network. The nodes are positioned such that a linear approximation of the temperature gradient within the associated layer is acceptable. Consequently, the two convecting zones are each modeled as a single node and are assumed to be isothermal. The salt-gradient is sectioned into several layers of equal depth and the ground storage is also divided into several uniform layers. For the salt concentration gradient and ground storage layers, the node temperatures are designed to represent the temperatures at the middle of the layer. Heat capacity at each node is determined from its specific heat, C_p; density, ρ; and the layer thickness, ΔX.

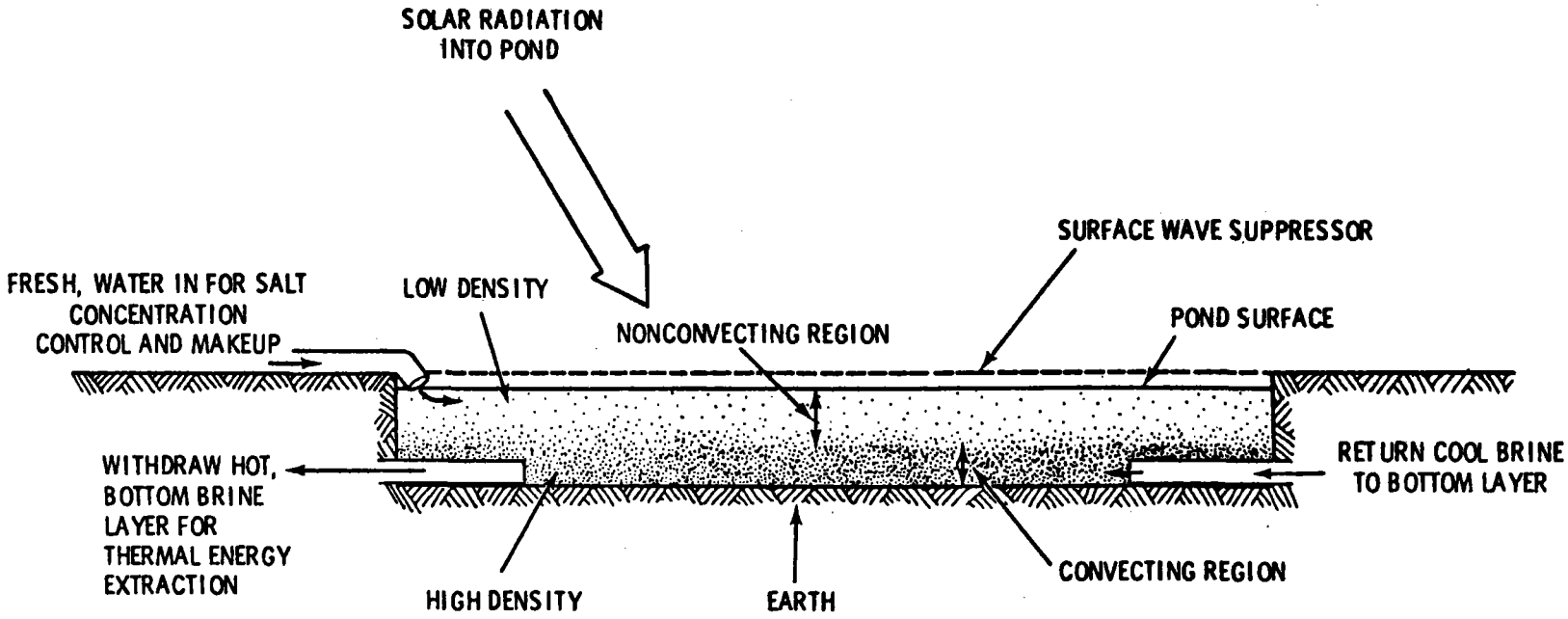

Figure 6-1. STRATIFIED SOLAR POND SCHEMATIC

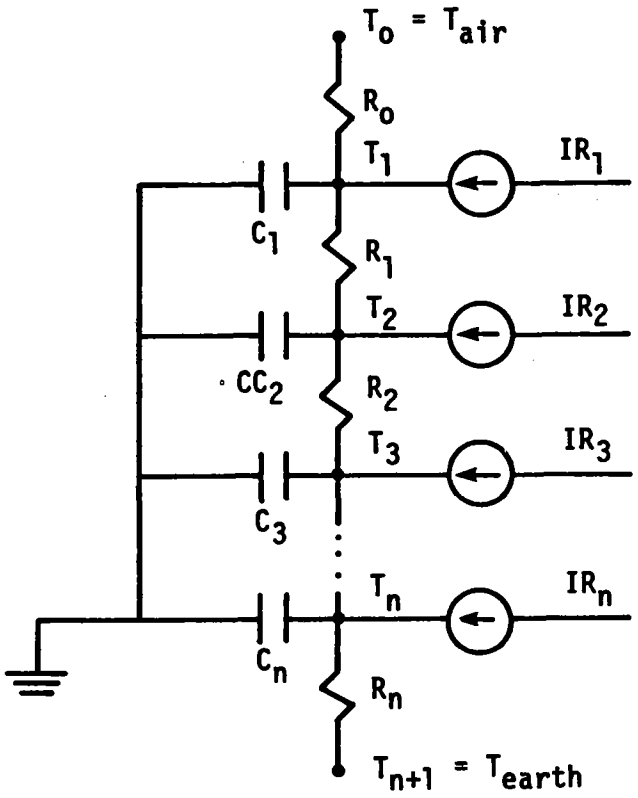

Figure 6-2. LUMPED-PARAMETER MODEL OF A STRATIFIED SOLAR POND

$$C_i = C_{p_i} \times \rho_i \times X_i \tag{6.1}$$

The thermal resistances are determined from the thermal transfer process (conduction, convection, or radiation). For all the resistances except that between the air and pond surface the conduction resistance dominates. In the following expression, R, the thermal conductivity, is

$$R = \frac{X_i}{2K_i} + \frac{X_{i+1}}{2K_{i+1}} \text{ for } i = 1 \text{ to } n \tag{6.2}$$

K is assumed to be arbitrarily large for the two convection zones. The value of R_o, the resistance between the pond surface and air, must account for thermal losses due to convection, evaporation, and radiation. Since experimental observation has reported that the pond surface temperature follows the ambient air temperature rather closely, convection is the dominant heat transfer process. Any value of R_o small enough for the surface temperature to track the air temperature is acceptable because the insulation for the convection-storage region is dominated by the resistance of the nonconvecting salt concentration layer.

Solar radiation absorbed in each node layer is accounted for by the current sources in the RC network. The radiation absorbed on the pond bottom serves as input into the node representing the convection-storage zone. This simplification is possible because the convective heat transfer coefficient between the pond bottom and the convection zone is so large that the pond bottom temperature is in near agreement with the convection-storage zone temperature.

The absorption of solar radiation within the pond is affected by the amount of solar radiation striking the surface, the angle of incidence, and the transmission properties of the salt solution. Transmission characteristics for clear water, described by Rabl and Nielsen, are currently used [13].

6.2.2 Dynamic Solution of the Stratified Solar Pond Temperatures

The dynamic equation that describes each node of the RC thermal network is:

$$\frac{dT_i}{dt} = \frac{T_{i-1} - T_i}{R_{i-1}\, C_i} + \frac{T_{i+1} - T_i}{R_i\, C_i} + \frac{IR_i}{C_i} \tag{6.3}$$

Expressed in state matrix form:

$$\frac{dt}{dt} = [A]\, T + [B] \begin{bmatrix} T_o \\ T_{n+1} \\ [IR] \end{bmatrix} \tag{6.4}$$

with,

$$A_{i\,i} = \frac{R_{i-1} + R_i}{R_{i-1}\,R_i\,C_i} \qquad \text{for } i = 1 \text{ to } n$$

$$A_{i\,i-1} = \frac{1}{R_{i-1}\,C_i} \qquad \text{for } i = 2 \text{ to } n$$

$$A_{i\,i+1} = \frac{1}{R_i\,C_i} \qquad \text{for } i = 1 \text{ to } n-1$$

$$A_{ij} = 0 \qquad \text{Otherwise}$$

and

$$[B] = \begin{bmatrix} \frac{1}{R_o C_1} & 0 & \frac{1}{C_1} & 0 & 0 & 0 & \cdots \\ 0 & 0 & 0 & \frac{1}{C_2} & 0 & & \\ 0 & 0 & 0 & 0 & \cdot & & \\ \cdot & \cdot & \cdot & & & & \\ \cdot & \cdot & \cdot & & & \cdot & \\ \cdot & \cdot & \cdot & & & & \\ & \frac{1}{R_n C_n} & & & & \cdot & \frac{1}{C_n} \end{bmatrix}$$

The solar pond time solution is formed by implicit finite difference equations obtained from the approximation:

$$T\,[\Delta t(m+1)] = T\,(m\Delta t) + \frac{dT}{dt}\,[\Delta t(m+1)]\,\Delta t \qquad (6.5)$$

The resulting expression of the next node temperatures in terms of the current node temperatures and the applied input is:

$$T\,[\Delta t(m+1)] = \left([I] - \Delta t\,[A]\right)^{-1} T\,(\Delta t \cdot m) + \left([I] - \Delta t[A]\right)^{-1} \Delta t[B] \begin{bmatrix} T_o \\ T_{n+1} \\ [IR] \end{bmatrix} \qquad (6.6)$$

The use of implicit finite difference equations allows the simulation time increment to be arbitrarily large without introducing numerical instability. Rapid simulations can be performed with a time increment of a day, week, or even month. Such large time increments are useful because of the large thermal inertia of ponds but would not be possible if conventional explicit difference equations were used to solve the pond model.

6.2.3 Stratified Solar Pond Simulation Applications

The solar pond model presented here can be used to investigate the performance of nonconvecting ponds under realistic weather and load conditions for a diverse range of applications. As presented in Part II of this report, a solar pond/wind turbine hybrid system was investigated for supplying the energy needs of two production facilities in Fort Worth, Tex. Soon to be undertaken is a parametric study of the pond to determine pond geometry under different load and cost constraints. Such an optimized solar pond would be equipped with thermoelectric generators.

6.3 SOLAR POND - THERMOELECTRIC IRRIGATION SYSTEM

Irrigation systems powered by solar energy have been studied or constructed using the following technologies:

- photovoltaic cells,
- shallow solar ponds driving organic Rankine cycle turbines, and
- collectors with engines driving a mechanical pump.

Such systems have been considered primarily for the southwestern United States. In the United States, over 35 million acres are pump-irrigated, representing 260 trillion Btu of energy consumed at an estimated annual cost of $520 million. Most of the energy for irrigation pumping is used by large pumping units with peak ratings of 100 to 300 kW. In Texas and New Mexico, where approximately 32% of the cultivated and pasture acreage is irrigated, natural gas is the main source of pumping energy. In Arizona and California, where nearly all cultivated and pasture acreage is irrigated, electricity is the primary energy source.

Photovoltaic cell-powered irrigation systems will become cost effective with array prices of $500/peak kilowatt, sometime between 1985 and 1990 depending on the fuel cost escalation rate [13]. Therefore, any system with better economics than photovoltaics with battery storage, in the same time frame, should be a viable technology.

Solar ponds have a potential of being a low cost solar collector with inherent thermal storage. Motivated by an apparent cost advantage, Israel and, to a lesser extent the United States, have actively pursued solar ponds. One version of solar ponds, called shallow solar ponds, has been studied by Lawrence Livermore Laboratories (LLL) [15]. Shallow solar ponds are essentially large plastic bags filled with water that collect solar energy. When they are used in conjunction with a nighttime thermal storage pool, the energy drives organic Rankine cycle engines (ORCE), which in turn power the irrigation pumps. A schematic diagram of such an irrigation system is shown in Figure 6-3. Detailed cost figures have been determined by LLL and a summary is given in the Appendix to Part I.

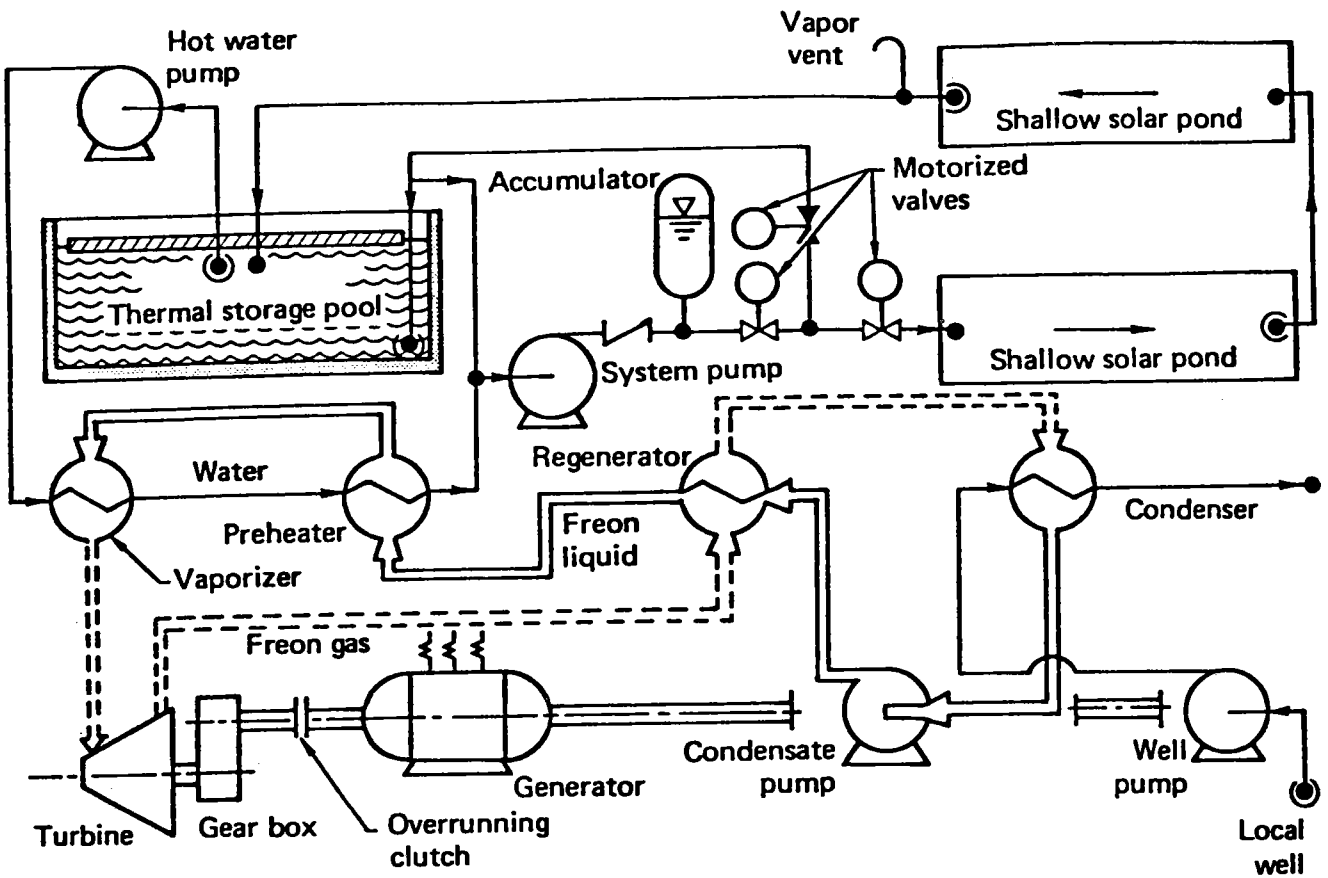

Figure 6-3. SHALLOW SOLAR POND POWER SYSTEM FLOW DIAGRAM

6.3.1 Proposed Scheme - Solar Pond and Thermoelectric System for Irrigation [9]

In this scheme, a stratified solar pond is considered as the low-cost solar collector. If the salt is free or low in cost as in many western states, stratified solar ponds offer the most economical means of solar collection. Because of their large area, they also provide thermal storage. A schematic diagram of a solar pond-thermoelectric system driving an irrigation pump is shown in Figure 6-4. A pump circulates hot water from the bottom of the pond to the heat exchanger (which maintains the temperature on the hot side of thermoelectric generator) and back to the pond. Cold water pumped from the well is used to keep the temperature around 20°C on the cold side, thus eliminating any additional cooling gear. There would be some diffusion of salt from the bottom of the pond to the surface, which would be washed away with fresh water [16]. Salt solution would be added to the lowest layer every few weeks.

The thermoelectric solar pond scheme has several advantages. It is extremely simple and inexpensive to maintain. Because a solar pond has built-in storage for periods when solar insolation is not available (days or weeks depending on pond size), there is no need for a backup. This should be compared to a photovoltaic system, in which solar cells must be supported by batteries and providing storage for a few days becomes very expensive.

All of these factors are particularly attractive in distributed applications such as irrigation systems. Table 6-1 gives estimated solar pond-thermoelectric system unit costs based upon industry projections for the cost of components. The cost of ORC engines, as developed by LLL, [15] is shown in Table 6-2. Capital costs of ORC engines are given in Figure 6-5. Current designs of thermoelectric elements being marketed include 2-mm length elements, although the limit of current technology is generally accepted as 0.75 mm. Thermoelectric material costs, in volume production, are shown in Figure 6-6. It must be recognized that thermoelectrics, though much lower in cost, have only half the efficiency of ORC engines; hence the total system costs need to be compared for any application.

The simplicity of the thermoelectric system can be appreciated better if the thermoelectric conversion system, which consists of n and p thermoelectric elements sandwiched between hot and cold metal plates (Figure 6-7), is compared with the conversion system using ORC engines (Figure 6-8). Hot water from the solar pond provides heat to the hot side (~ 90°C) of TEG and cold water pumped from the well for irrigation may also be used to extract heat from the cold side (~ 15°C).

The strongest argument for thermoelectric power generation systems is economics. Lawrence-Livermore (LLL) studies have shown that the cost of organic Rankine cycle engines (100 kW) cannot decrease by more than about $800/kW for a production of about 10,000 units a year, based on materials and fabrication techniques similar to the refrigeration manufacturing industry, which is already a mature technology [15]. On the other hand, thermoelectric generators are currently manufactured only in small quantities, perhaps a few hundred kW capacity per year. Approximately 95% of the present cost ($8 to

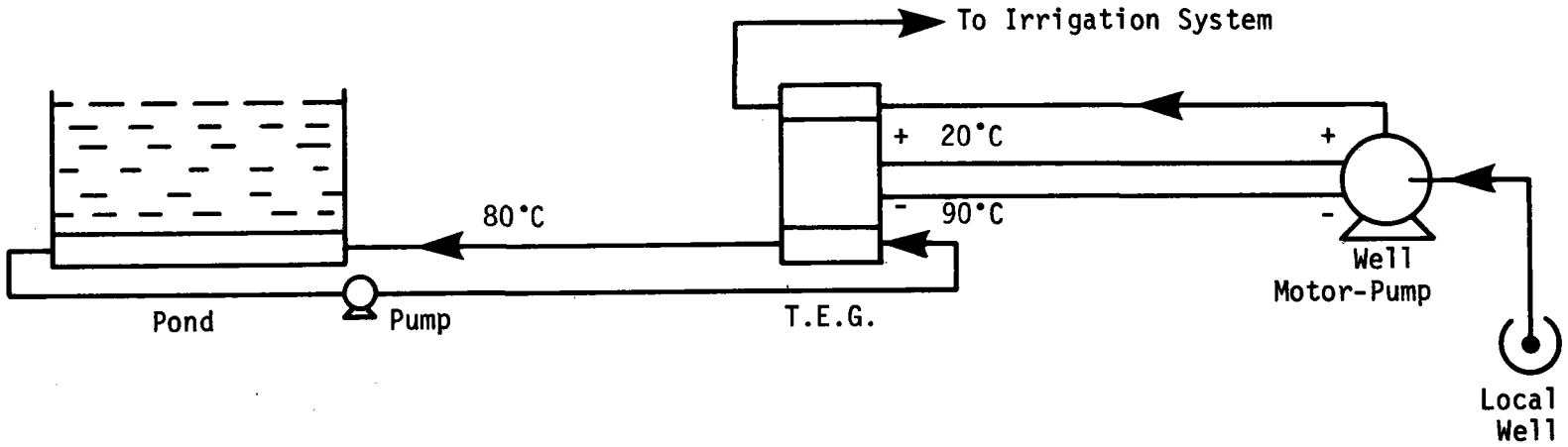

Figure 6-4. STRATIFIED SOLAR POND - THERMOELECTRIC IRRIGATION SCHEME

Table 6-1. SHALLOW SOLAR POND - THERMOELECTRIC POWER SYSTEM UNIT COSTS

Item	Unit	Cost ($/unit)	Time (years)	Maintenance Cost ($/year)
Land acquisition	Acre	1000	---	
Pond construction				
Digging, leveling, and dike construction	ft^2	0.003		
Hypalon liner	ft^2	0.27	20	
Installation	ft^2	0.08		
Tedlar cover	ft^2	0.21	20	
Total Pond Construction Cost:	ft^2	0.563		
Total	ft^2	1.12		250
Conversion Machinery				
Thermoelectrics, controls	kW	170		60
Pumps	kW	350	25	100
Piping	m^2, wetted area	191	30	20
Operating Charges (Total)		10,000/year		

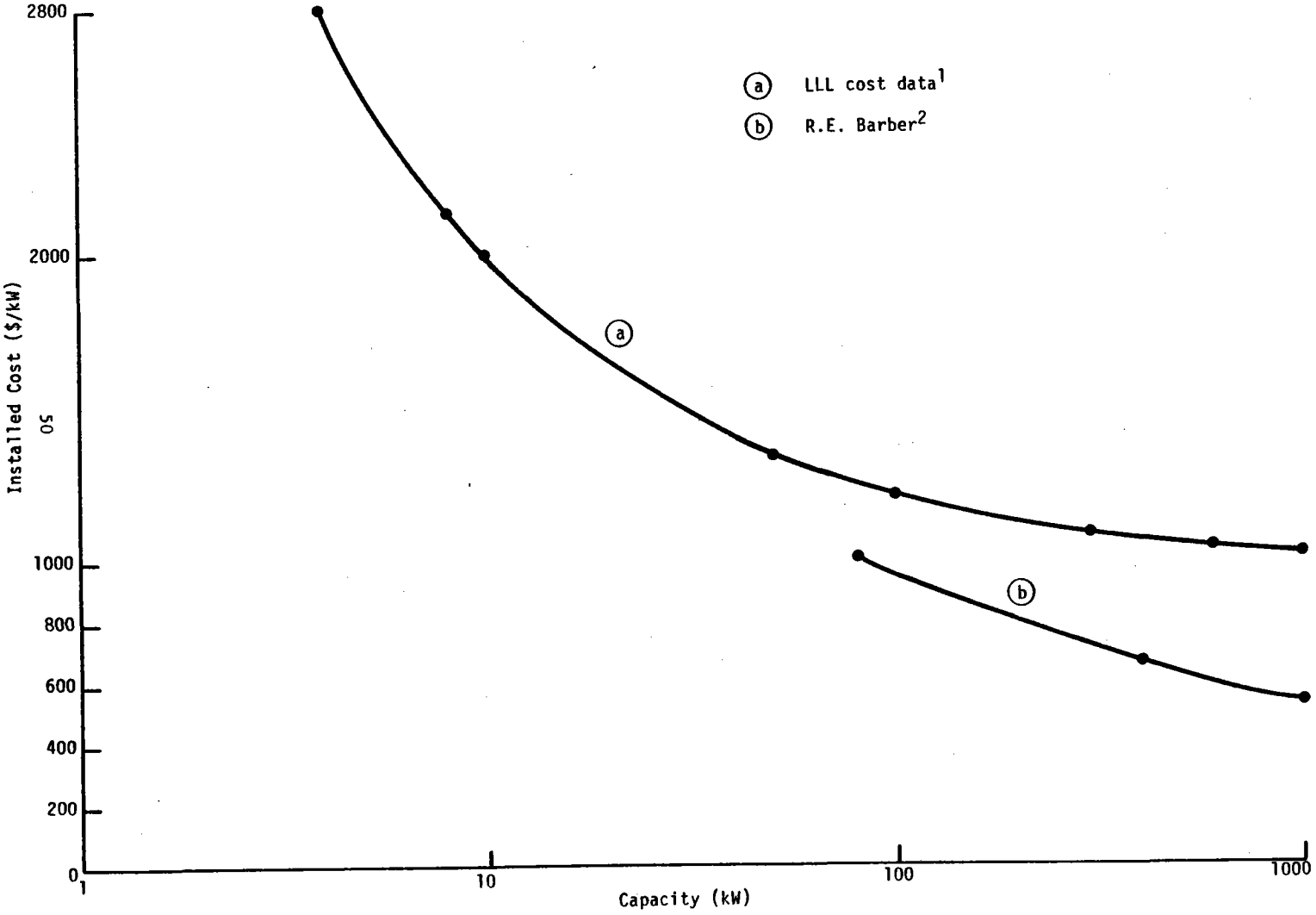

Figure 6-5. COST PROJECTIONS OF ORGANIC RANKINE CYCLE ENGINES

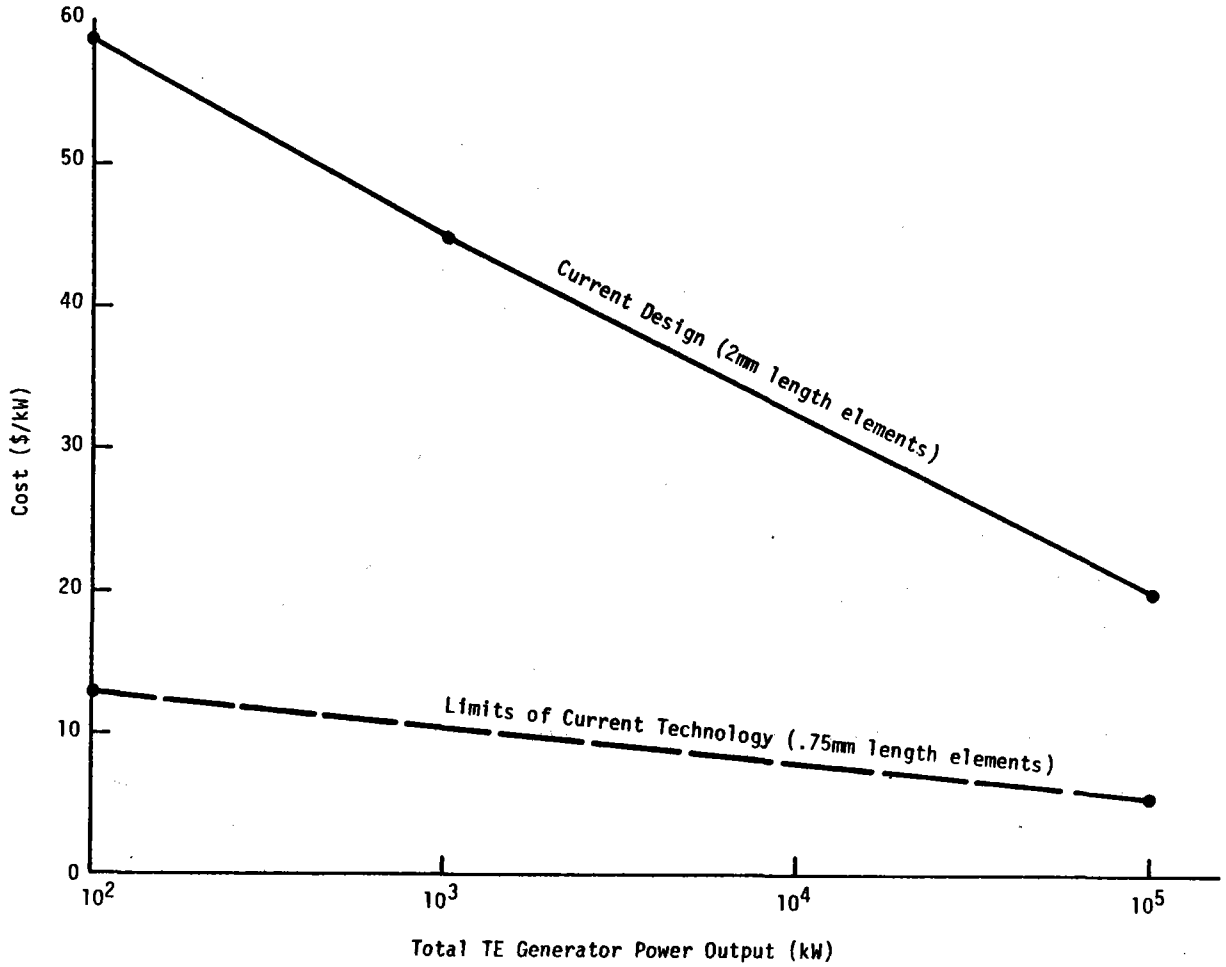

Figure 6-6. THERMOELECTRIC MATERIAL COSTS

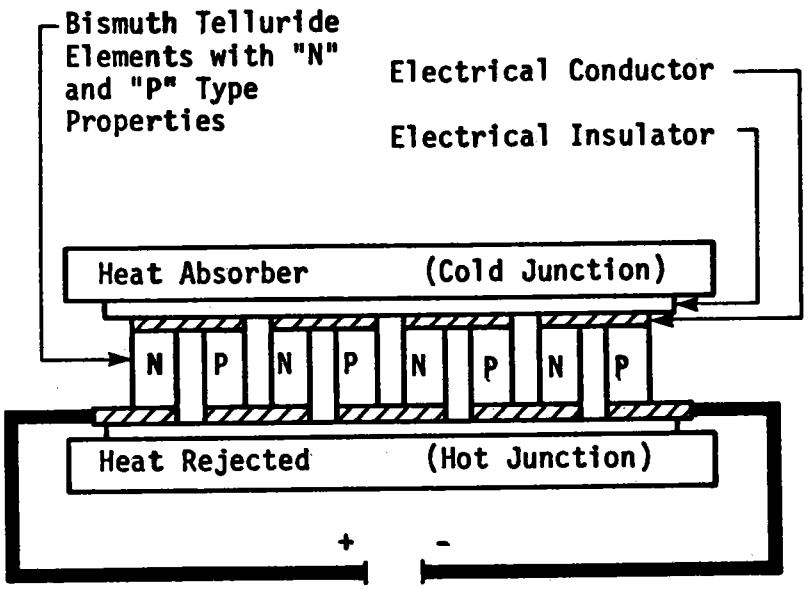

Figure 6-7. TYPICAL THERMOELECTRIC MODULE ASSEMBLY ELEMENTS ELECTRICALLY IN SERIES, THERMALLY IN PARALLEL

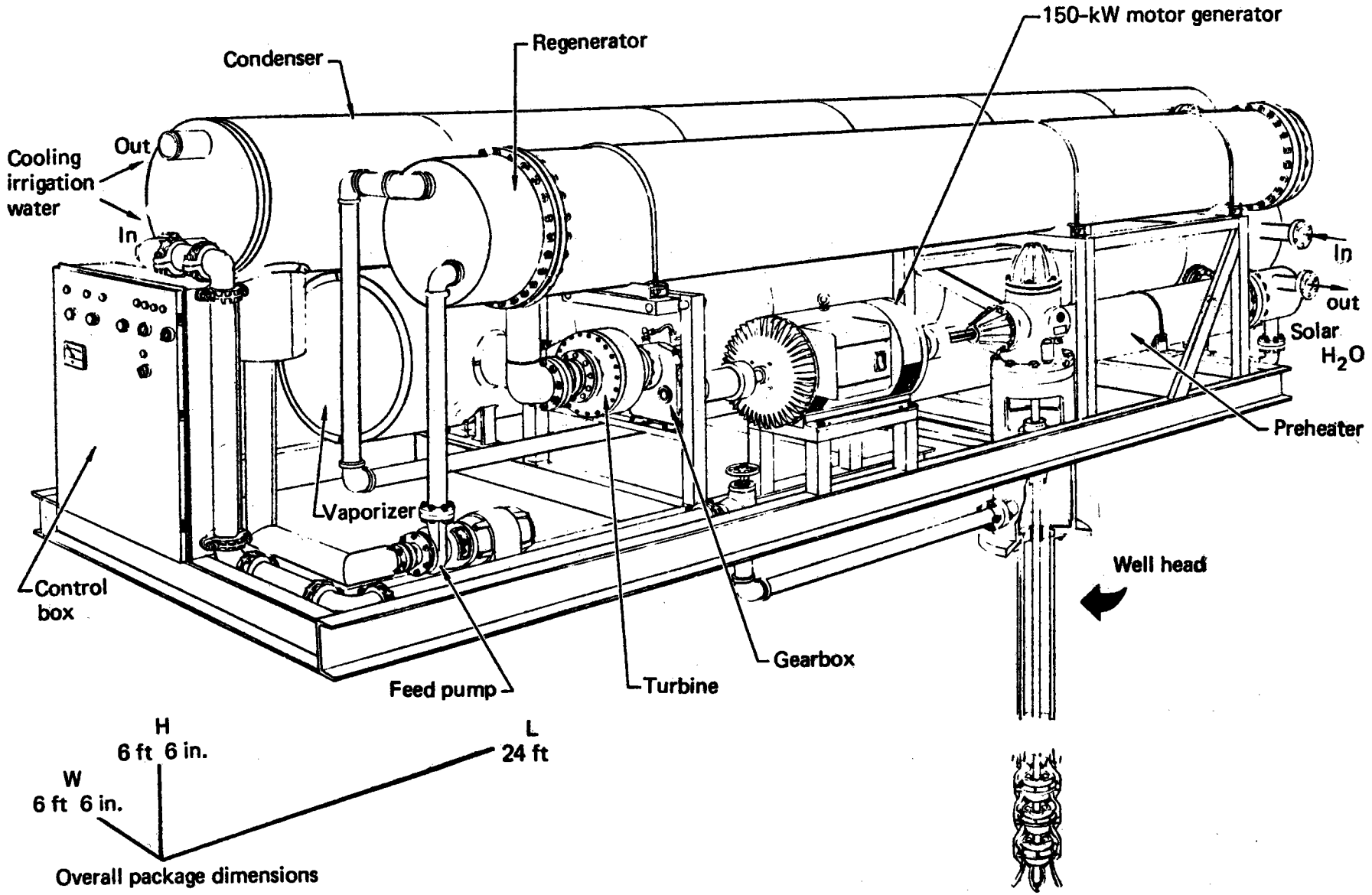

Figure 6-8. ORC ENGINE CONVERSION MACHINERY [15]

$10/W) represents labor and about 5% materials. Presuming an increase in production to even a modest level of 1 MW per year (which is only 10 irrigation systems of 100 kW), the cost of thermoelectric generators may decrease to about $100/kW through automated production techniques. Further, the life of thermoelectrics can be at least 20 years whereas the life of ORC engines is 3 to 5 years at best. Also, maintenance of thermoelectrics is negligible, whereas ORC engines require constant maintenance.

Table 6-2. ORGANIC RANKINE CYCLE ENGINE (CONVERSION) UNIT COSTS

Item	Unit	Cost ($/unit)	Time (years)	Maintenance Cost ($/year)
Turbine and gear box	$(kW)^{1/3}$	3200	--	75
Generator and switchgear	kW	60	--	20
Instrumentation and controls	$(kW)^{1/2}$	1200	--	50
Regenerator	kW/°C	1000	20	--
Other heat exchangers	kW/°C	100	20	--
Installation	kW	200	--	--

Estimated energy costs of three different irrigation systems--shallow solar pond + ORCE, stratified solar pond + ORCE, and stratified solar pond + TEG--are calculated in Appendix I-A. It is important to observe from the calculations shown in Appendix I-A that the cost of the thermoelectric generator is less than 10% of the total cost. Hence the energy cost (¢ /kWh) is not sensitive to the cost of the thermoelectric generator, but to the cost of the solar pond (heat source). Results are summarized in Table 6-3. The stratified solar pond + thermoelectric generator scheme offers the lowest cost. In sizes required for irrigation (20 to 200 kW), thermoelectric generators are expected to be more economic than ORC engines.

Table 6-3. COMPARISON OF ENERGY COSTS FOR DIFFERENT SOLAR POND POWER GENERATION SCHEMES (25 kW CAPACITY)

	Capital Investment ($/kW)	Energy Cost (¢/kWh)
Solar Pond + Thermoelectrics (20% Carnot)	4844	11.2
Solar Pond + Thermoelectrics (30% Carnot)	3476	8.1
Solar Pond + ORC Engine	3485	11.7
Shallow Solar Pond + ORC Engine[a]	6496[a]	17.9

[a] [15].

SECTION 7.0

POTENTIAL FOR NEW MATERIALS AND DEVICES

7.1 MATERIALS

In thermoelectric energy conversion the figure-of-merit, Z, which is proportional to the conversion efficiency, is given by

$$Z = \frac{\alpha^2}{\rho K} \qquad \text{where } \alpha \text{ is the Seebeck coefficient,} \quad \rho \text{ is the electrical conductivity, and} \quad K \text{ is the thermal conductivity.} \qquad (7.1)$$

The classic problem in thermoelectrics is that in solid state the electrical and thermal conductivities are coupled and hence Z is limited. This, in turn, limits the efficiency achievable in converting heat to electricity. The Z values of commonly used thermoelectric materials are shown in Figure 3-1. It was commonly believed in the 1960s that the ZT value does not exceed unity, and it was suspected that there may be some natural limitation to this quantity. However, several investigators have shown that ZT values higher than one can be obtained. In Bi_2Te_3, PbTe, and the so-called selenides, ZT values now are higher than one. Recently a 25% improvement in Z has been reported by Syncal in Ge-Si alloys by doping them with gallium phosphide. Pristoulet and his colleagues in France have reported a ZT value of 1.25 at 1500°K in a compound of silicon and boron (SiB_4). Thus all indications are that there are several materials which have potential for higher efficiency.

An exciting new possibility is the use of amorphous semiconductors for thermoelectric energy conversion. It is well known that amorphous semiconductors, being glasses, have very poor thermal conductivity. It is also known that they can be made conducting by doping. The remaining questionable factor is the magnitude of the Seebeck coefficient in these materials. A very good candidate for investigation is hydrogenated amorphous silicon, now routinely grown by RCA Laboratories for their studies of photovoltaic solar cells. Similarly, ternary chalcopyrite semiconductors are known to have poor thermal conductivities and high Seebeck coefficients [17], and many of them are being investigated for photovoltaic applications. Some of these may be excellent candidates for solar thermoelectric energy conversion in the low temperature range. Organic semiconductors like polyacetylene are showing promise as cheap semiconductors [19]. Because of low thermal conductivity, these also are candidates for thermoelectric energy conversion.

7.2 DEVICE FABRICATION

Because of the limited applications of thermoelectrics, fabrication of devices is labor intensive. With the possibility of applying solar thermoelectrics and other low grade heat to electricity conversion, automated manufacturing techniques similar to those used in the electronics industry are possible.

The cost of material is rather low because thermoelectrics use polycrystalline, cheap materials like Bi, Pb, Te. Thin- and thick-film technologies should be investigated for mass production techniques. A study conducted by General Atomics Company, under subcontract from SERI, showed that the cost of thermoelectric materials can decrease to $20/kW.

SECTION 8.0

FUTURE WORK

Thermoelectric energy conversion is a viable technology for solar energy, but its application must be chosen carefully. It is not economical in technologies using costly collectors because of poor efficiency. In situations where operation and maintenance costs need to be minimized, solar thermoelectrics have an edge over other technologies.

This report has identified two applications of solar thermoelectrics which hold strong promise: OTEC and stratified solar ponds. A preliminary design of an OTEC system will be done next year. The present work on the solar ponds will be extended to optimize total system performance and cost. Additional studies will be undertaken to evaluate other applications including total energy system applications and topping and bottoming cycle applications for solar thermal power plants. There are two nonsolar applications which also deserve study: geothermal conversion and bottoming cycles for conventional power plants.

The cost of thermoelectric devices when they are produced on a large scale is primarily the cost of materials. For low temperature thermoelectrics, the preferred materials are bismuth and tellurium. At present production levels tellurium costs $20/lb in large quantities. Bismuth is cheaper at $1/lb. The costs and availability of these materials under much larger production levels will be investigated.

The concepts proposed in this report will be verified by experiments on prototypes. New concepts for thermoelectric device structures are currently being investigated; for example, thick-film structures which use much smaller amounts of material than present technology but do not degrade performance. These structures present very promising opportunities for cost reduction.

Even with no technological breakthroughs present thermoelectric technology, tailored to interface with solar devices, can be economical in some applications. A preliminary design developed by General Atomics Company for solar pond applications, operating between 80°C on the hot side and 25°C on the cold side, estimates 0.023 lb/W of bismuth telluride. At present day costs per pound of BiTe, and adding 50% for manufacturing costs, it is possible to produce thermoelectric generators for solar pond applications at about 75¢/W. At least one order of magnitude reduction in material cost is possible by thin- or thick-film techniques; hence, this may very well be the most economical conversion technology from low grade heat to electricity. Low temperature devices, such as low cost solar collectors and solar ponds, combined with low temperature solar thermoelectric power conversion, may offer one of the most economical solar technologies for electric power production for the near future.

SECTION 9.0

REFERENCES

1. Coblentz, W. W. U.S. Patent No. 1077219; 1913.

2. Telkes, M. "Solar Thermoelectric Generators." Journal of Applied Physics. Vol. 25; p. 765; 1954.

3. Roselle, F. E. "Recent Terrestrial and Undersea Applications of Radioisotope Thermoelectric Generators." Proceedings of the 13th Intersociety Energy Conversion Conference. August 20-25, 1978, San Diego, CA; p. 1967.

4. Katz, K. "Themoelectric Generators for the Conversion of Solar Energy to Produce Electrical and Mechanical Power." Proceedings of the Conference on New Sources of Energy. Rome, August 1961; Vol. 4: p. 153.

5. Raag, V. System Analysis and Cost Projections for Solar Thermoelectric Devices, Technical Report. Syncal Corporation; September 15, 1978.

6. Chang, T. Solar Thermoelectric Power Generation, Its Present Status and Future Prospect, Technical Report. University of Arizona; May 1977.

7. Drumheller, K. Comparison of Solar Pond Concepts for Electrical Power Generation, Technical Report. Richland, WA: Batelle Pacific Northwest Laboratories; October 1975; BNWL-1951.

8. "Ocean Thermal Energy Conversion - Environmental Development Plan." Washington, D.C.: U.S. Department of Energy; March 1978.

9. Jayadev, T. S.; Benson, D. Patent disclosure filed, October 1978.

10. Angrist. S. W. Direct Energy Conversion. Allyn and Bacon; p. 140; 1971.

11. Kays, W.; London, A. L. Compact Heat Exchangers. McGraw Hill; p. 219; 1964.

12. Stryus D. L.; Saworski, R.; Harling, O. K. The Nonconvecting Solar Pond. Richland, WA: Batelle Northwest Laboratories; January 1975; BNWL-1891.

13. Nielson, C. E.; Rabl, A. "Solar Ponds for Space Heating." Solar Energy. Vol. 17: pp. 1-12; Pergamon Press; 1975.

14. Matlin, R. W.; Katzman, N. T. The Economics of Adopting Solar Photovoltaic Energy Systems for Irrigation. M.I.T. Lincoln Laboratory; July 1977; COO/4094-2.

15. Platt, E. A.; Wood, R. L. Engineering Feasibility of a 150kW Irrigation Pumping Plant Using Shallow Solar Ponds. Lawrence-Livermore Laboratory; April 1978; UCRL-52397.

16. Nielson, C. E. "Salt Gradient Solar Pond Development." Washington, D.C.: Annual Solar Heating and Cooling Meeting; September 1978.

17. Pastoulet, B. "Preparation of Refractory Thermoelectric Materials by C.V.D.--Application to Solar Energy Conversion." Extracted abstracts, The Electrochemical Society, Inc., fall meeting; October 17-22, 1976.

18. Shay, J. L.; Wernick, J. H. Ternary Chalcopyrite Semiconductors: Growth, Electronic Properties and Applications. Pergamon Press; p. 211; 1976.

APPENDIX I-A

COST CALCULATIONS OF THREE SCHEMES FOR A 25-kW SOLAR POWERED IRRIGATION AND POWER GENERATION SYSTEM

Solar Pond + Thermoelectrics

Solar Pond + ORC Engines

Shallow Solar Pond + ORC Engines

I-A.1 CAPITAL COSTS OF A 25 kW SYSTEM

I-A.1.1 Cost Equation

$$\text{Capital Cost } C_{Cap} = \frac{C_{col}}{\eta I} + C_{con} + C_{other}$$

where

C_{cap} = Capital cost \$/kW S-E
C_{coll} = Cost of collector in \$/m^2
η_{S-E} = Efficiency of conversion = $\frac{\text{electric power output}}{\text{solar input}}$
I = Insolation in W/m^2 averaged over the whole year
C_{con} = Cost of converter in \$/kW
C_{other} = Cost of pumps, plumbing, site preparation, etc.

I-A.1.2 Operating Conditions

$I = 0.25$ kW/m^2, $C_{other} = 700$ \$/m^2

Hot water = 80°C
Cold water = 18°C
ΔT = 62°C
Carnot efficiency = 17.5%

Thermoelectric generator efficiency:

20% of Carnot = 3.5%
30% of Carnot = 5.25%

Organic Rankine Cycle Engine Efficiency, 40% of Carnot = 7%

I-A.1.3 Efficiency (solar to electric)

Solar pond + TE (20% Carnot) = 0.25 x 0.035 = 0.009
Solar pond + TE (30% Carnot) = 0.25 x 0.0525 = 0.013
Solar pond + ORC Engine = 0.25 x 0.07 = 0.0175

I-A.1.4 Cost Assumptions

Solar pond (C_{coll}) = 10\$/m^2 where salt is free
25kW DRC engine (C_{con}) = 1000 \$/kW [Ref. 15 and Figure 6-5]
Thermoelectric generator (C_{con}) = 200\$/kW
Cost of plumbing, instrumentation (C_{other}) = 200\$/kW

I-A.1.5 Capital Cost Calculations

1. Solar pond + TEG (20% Carnot)

$$C_{cap} = \frac{C_{col}}{\eta_{S-E}} + C_{con} + C_{other}$$

In this case, $C_{cap} = \frac{10}{0.25 \times 0.009} + 200 + 200 = 4444 + 200 + 200$

$= 4844$ \$/kW

(It has to be noted that cost of TEG is insignificant as compared to pond costs.)

2. Solar Pond + TEG (30% Carnot)

$$C_{cap} = \frac{10}{0.25 \times 0.013} + 200 + 200 = 3076 + 200 + 200$$

$= 3476$ \$/kW

3. Solar Pond + ORC Engine

$$C_{cap} + \frac{10}{0.25 \times 0.0175} + 1000 + 200 = 2285 + 1000 + 200$$

$= 3485$ \$/kW

4. Shallow Solar Pond + ORC Engine [15]

$C_{cap} = 3879 + 1721 + 896 = 6496$ \$/kW

I-A.2 ANNUAL COST CALCULATIONS

Cost due to investment:
Fixed Charge Rate: Capital Recovery Factor + Taxes, etc.
Assume 5% for taxes and other expenses

Capital Recovery Factor for equipment lasting 20 years	= 11.7%
Capital Recovery Factor for equipment lasting 5 years	= 26.4%
FCR for equipment lasting 20 years	= 16.7%
FCR for equipment lasting 5 years	= 31.4%
Life of Solar Ponds	= 20 years
Life of Thermoelectrics	= 20 years
Life of ORC Engines	= 5 years

O&M for Thermoelectric Systems = 10% of annual fixed costs
O&M for ORC Systems = 20% of annual fixed costs.

I-A.2.1 Annual Cost of Solar Pond + Thermoelectrics (20% Carnot)

Both solar pond and thermoelectrics last for 20 years.
FCR = 16.7%
Annual cost = Fixed charges + O&M
= 4844 x 0.167 + 10% of fixed charges
= 4844 x 1.1 x 0.167 = $889

I-A.2.2 Annual Cost of Solar Pond and Thermoelectrics (30% Carnot)

Annual cost = 3476 x 1.1 x .167 = $638

I-A.2.3 Annual Cost of Solar Pond + ORC Engines

ORC Engines last for five years, operating at 90% load factor.

FCR for solar ponds, as before = 16.7%
FCR for ORC engines = 31.4%
O&M = 20% of annual fixed charges.
Fixed cost = (2285 x 0.167) + (200 x 0.167) + (1000 x 0.314)
= 381 + 33 + 314 = 728
Annual cost = 728 x 1.2 = $873

I-A.2.3 Annual Cost of Shallow Solar Pond + ORC Engines

Annual cost = [(3879 + 896) x .167] + [1721 x .314]
= 797 + 540 = $1337

I-A.3 ENERGY COSTS

Because the thermoelectric system has very low maintenance, the system could provide energy at a capacity factor of 0.9. As compared to that, ORC engine system has a higher maintenance and hence can operate at a capacity factor of 0.85 or less.

$$\text{Cost of Energy } (¢/\text{kWh}) = \frac{\text{Annual changes } (\$/\text{year})}{\text{No. of hours x capacity factor}}$$

1. Solar pond + TEG (20% Carnot)

$$\text{Cost of Energy} = \frac{889}{87.60 \times .9} = 11.2¢/\text{kWh}$$

2. Solar Pond + TEG (30% Carnot)

$$\text{Cost of Energy} = \frac{638}{87.60 \times .9} = 8.09¢/\text{kWh}$$

3. Solar Pond + ORC Engine

$$\text{Cost of Energy} = \frac{873}{87.60 \times .85} = 11.7¢/\text{kWh}$$

4. Shallow Solar Pond + ORC Engine

$$\text{Cost of Energy} = \frac{1337}{87.60 \times .85} = 17.9¢/\text{kWh}$$

GA-C15168
(11-78)

APPENDIX I-B

THERMOELECTRIC APPLICATION TO SOLAR POWER

By

J.M. Neill, N.B. Elsner, and D.L. Sonn

GENERAL ATOMIC PROJECT 3062

NOVEMBER 1978

GENERAL ATOMIC COMPANY

1. SUMMARY

This report describes preliminary studies to identify and quantify the applicability of thermoelectric devices coupled to solar energy systems. These studies were performed by General Atomic (GA) for the Solar Energy Research Institute (SERI).

The studies include cost/technical models of three reference systems, an electric generating plant with a thermoelectric topping cycle, a process heat plant utilizing the reject energy from a thermoelectric system, and a solar pond which drives a low-temperature thermoelectric system. The studies also include estimates of the cost of thermoelectric generators (TEGs) produced in quantities up to 10^8 watts.

It is shown in the studies that with automated and large-scale production of thermoelectric materials and modules, TEGs can be made for well under $100/W(e). The efficencies achievable for low-temperature solar pond are about 2.7% for a temperature difference of 55°C and appear attractive enough to warrant exploration of this application in more detail.

The topping cycle application shows a modest cost incentive, which may be enhanced if less conservative loss assumptions are used in the system performance analysis, if modest projections in material properties are made, and if systems smaller than the reference systems studied in this report are considered.

2. INTRODUCTION

This report documents studies performed for the Solar Energy Research Institute (SERI), under Work Order No. 1295, dated August 8, 1978. The purpose of the study is to identify and quantify the applicability of thermoelectric devices coupled to solar energy systems. Specifically, General Atomic (GA) was requested to:

1. Conduct system analysis, using computer modeling techniques, to assess quantitatively the potential efficiencies of solar thermoelectric generators (a) with current materials and technology, and (b) with advanced concepts.
2. Generate realistic cost and performance projections for selected solar thermoelectic generator (TEG) concepts including production up to 10^8 watts.
3. Provide a description of the current state-of-the-art in thermoelectric technology.
4. Provide a discussion of probable advances in the technology (improved material conversion efficiencies, lower cost materials, advanced designs) and identify areas of research which, if supported, would likely accelerate these advances.

The information thus developed was to be used as part of a SERI assessment of the technical feasibility and economic competiveness of solar thermoelectric generators.

It was necessary to devise some solar thermoelectric systems that could be analyzed to assess the applicability of the coupling. This required identification of the characteristics of thermoelectric generators so as to choose the systems directly. Thermoelectric devices are less efficient than photovoltaic cells and the leading thermodynamic power conversion systems. Therefore, the use of thermoelectric devices in solar applications would appear justified where their other characteristics have applicability. These other characteristics include:

1. Thermoelectrics are passive systems requiring little maintenance and operator control. (This is not true of Rankine or Brayton power conversion systems.)
2. Thermoelectrics utilize thermal energy and can therefore operate from either concentrated insolation or thermal storage.
3. Thermoelectrics can operate at high temperature - up to 1100°C. (This is not true of photovoltaics. In fact, even thermodynamic power conversion systems are limited because of heat exchanger wall stresses when heat is transferred to a pressurized working fluid.)
4. Thermoelectrics can reject heat at reasonably elevated temperatures - >200°C. (This is not so with photovoltaics.)
5. Thermoelectric systems are modular, and their costs and size scale linearly with output power, thus facilitating development and demonstration. (This is not the case with thermodynamic power conversion systems.)

Based on these characteristics, three reference solar thermoelectric systems were selected and are described in Section 4. They include an electric generating system (case 1) with and without a topping cycle, a solar process heat system (case 2) with and without a topping cycle, and a solar pond concept (case 3).

Present and future thermoelectric material and fabrication costs have been developed. These data, together with a description of the cost bases and methodology for cost projection, are described in Section 5. The reference cases have been analyzed and modified where necessary, and the results are reported in Section 6. Conclusions from these results are reported in the same section.

A description of present and future thermoelectric technology is given in Section 7. This description covers present thermoelec-

tric material properties, future advances, and other advances in the state-of-the-art that bear on the cost or performance.

In section 8, overall conclusions regarding the applicability of TEGs to solar power sources are given. Work that should be done either to exploit or delineate that applicability is described.

3. THERMOELECTRIC MATERIALS AND PROCESSES CURRENTLY IN USE

3.1. INTRODUCTION

The figure of merit (Z) versus temperature for the thermoelectric alloys, available today, is plotted in Figs. 1 and 2 for P-type and N-type alloys, respectively. As can be seen, the $(Bi,Sb)_2(Se,Te)_3$ alloys have the highest figure of merit of all the alloys developed thus far. Presented below are the main characteristics of the alloys utilized in TEGs today. Most of the discussion is devoted to the $(Bi,Sb)_2(Se,Te)_3$ alloys because they have a greater chance of being employed in a solar-powered generator and are further along in development for large-scale, low-cost use.

3.2. $(Bi,Sb)_2(Se,Te)_3$ ALLOYS

The $(Bi,Sb)_2(Se,Te)_3$ alloys are normally prepared by Bridgman casting. In this process, an ampule of molten alloy is slowly lowered from the furnace and the material is grown with the desired anisotropic columnar grains. These cast forms are not mechanically strong, and they cleave very easily between the columnar grains as well as transgranularly on planes parallel to the columnar growth. The reason for the weak mechanical properties in the one direction is shown schematically in Fig. 3. Fortunately, however, the columnar growth is oriented parallel to the current flow and, if a large (in cross-sectional area) thermoelectric element does delaminate, the mechanical separation is not noticeable electrically or thermally since the resulting two elements are in parallel. If a small (in cross-sectional area) thermoelectric element delaminates, however, a high resistance or open circuit occurs, as shown in Fig. 4.

The exact compositions of $(Bi,Sb)_2(Se,Te)_3$ alloys are not fixed and vary depending upon the use. The N-type alloy is typically rich

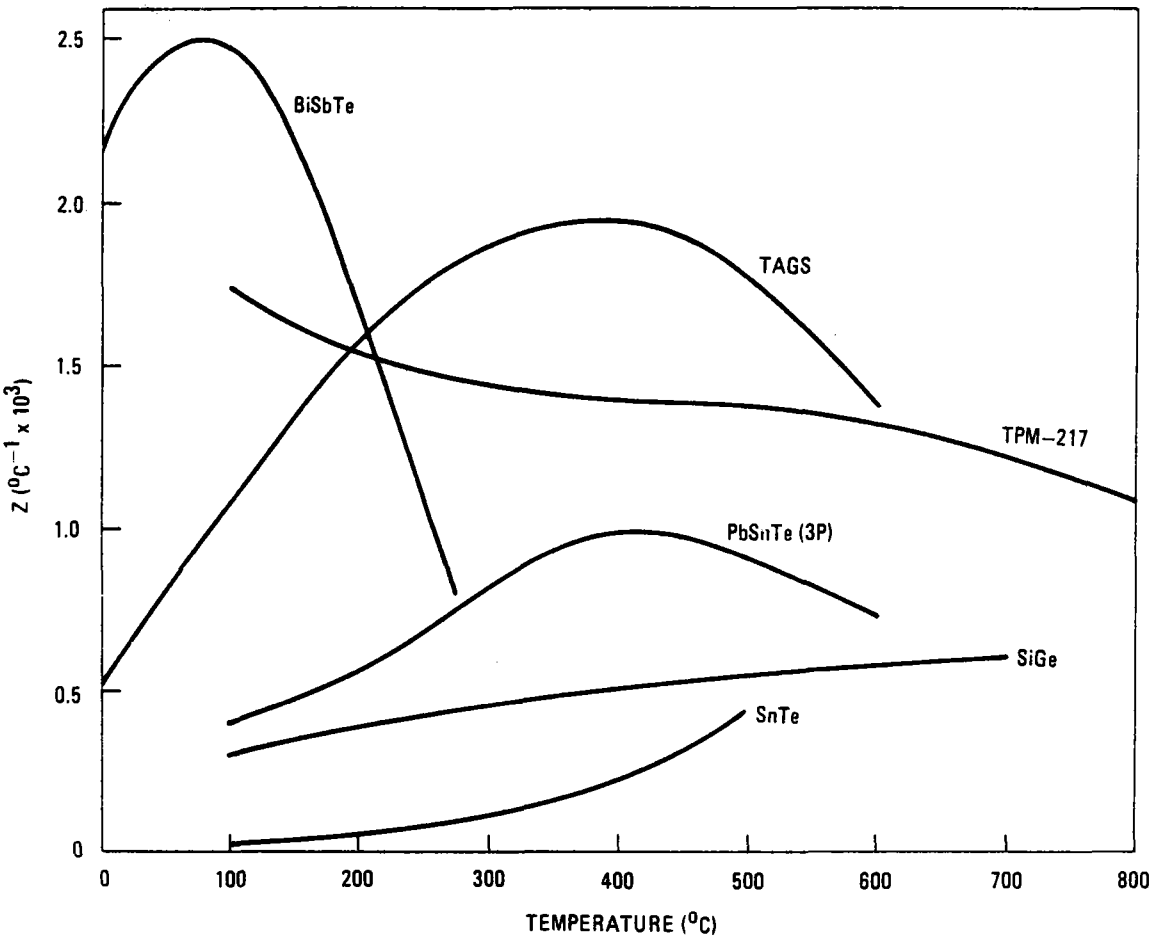

Fig. 1. Figure of merit of P-type thermoelectric alloys

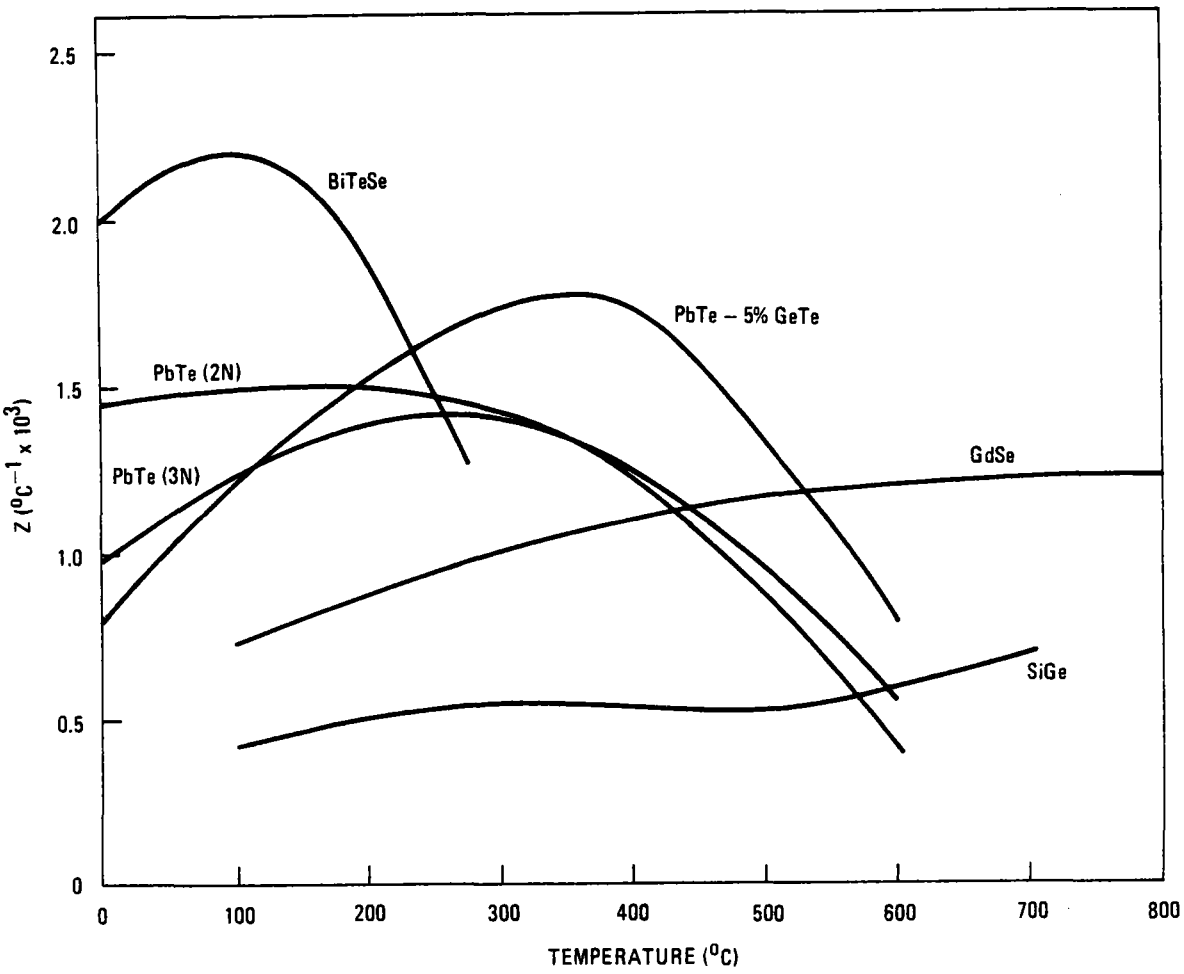

Fig. 2. Figure of merit of N-type thermoelectric alloys

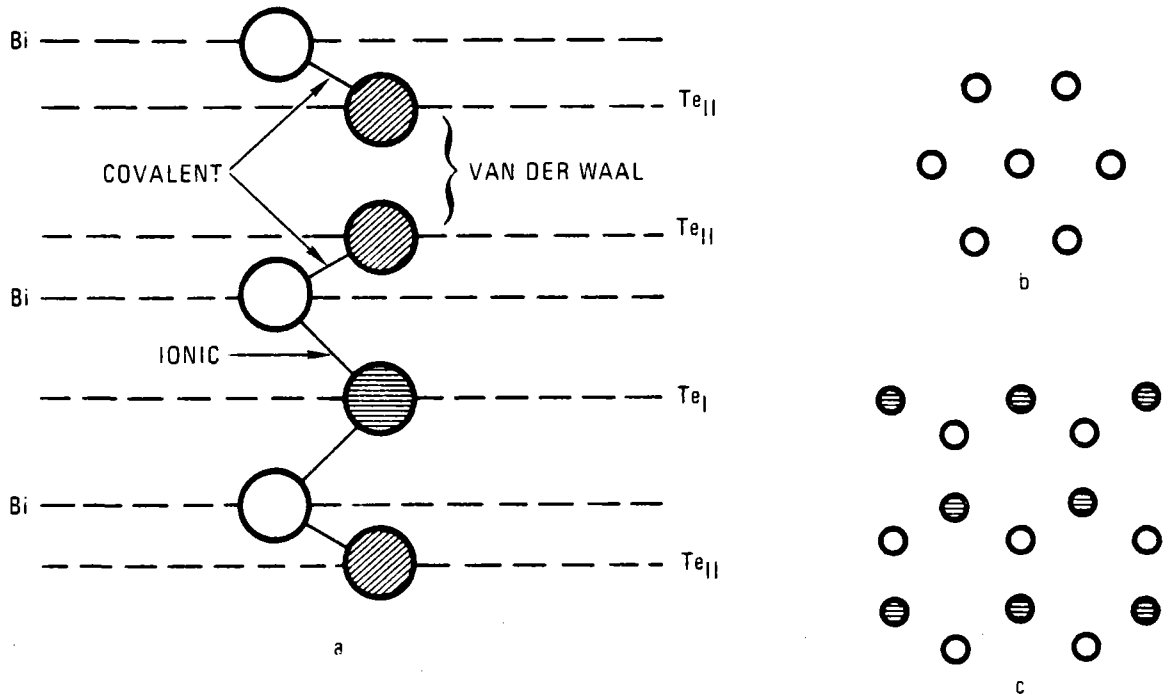

Bi_2Te_3 and Sb_2Te_3 possess tetradymite structure of Bi_2Te_2S. Bi and Te atoms are distributed in layers (a). Each layer consists of atoms of one kind distributed in a plane hexagonal lattice (b). The layers are displaced with respect to one another so that each atom of a given layer has three neighbors in the next layer (c).

In discussion of bonds in Bi_2Te_3 and Sb_2Te_3 one must consider:

1. bonds between identical atoms in one layer
2. bonds between neighboring layers of Te_{II}
3. bonds between Te_{II} and Bi layers
4. bonds between Te_I and Bi layers as well as between Te_I and Sb layers.

The distance between identical atoms in one layer (4.38 Å, b) is close to van der Waals' radii of Te or Bi, and the distance between Te_{II} atoms in neighboring layers (3.72 and 3.62 Å for Bi_2Te_3 respectively) is close to the distance between atoms of neighboring chains in pure Te (3.74 Å).

We may conclude, therefore, that there is practically no binding between atoms in the same layer, and that small residual forces act between Te_{II} and Te_{II} layers.

Fig. 3. Bismuth telluride structure

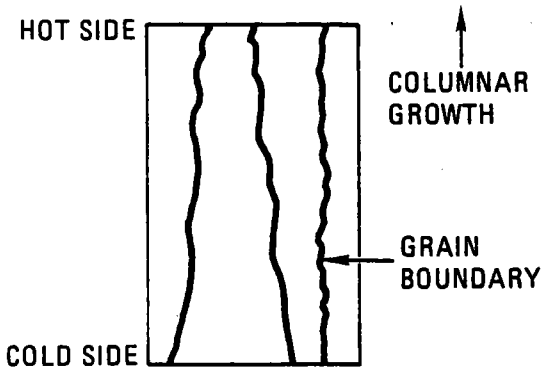

In a thermoelectric element that has sufficient cross-sectional area, delamination between the columnar grains does not affect the thermoelectric properties.

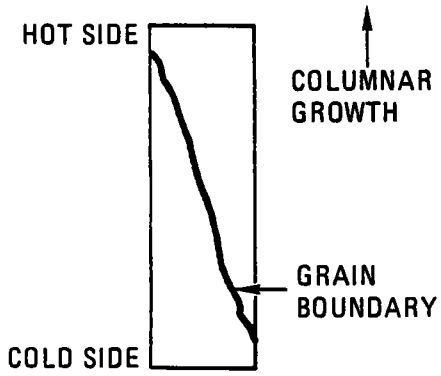

In a thermoelectric element that has a small cross-sectional area, delamination will cause either a high thermal and electrical resistance or an open circuit.

Fig. 4. Comparison of elements that are small and large in cross-sectional areas

in Bi_2Te_3 (80 to 95%) and may contain small amounts of Bi_2Te_3 and Sb_2Te_3 in solid solution. The P-type alloy is typically 75% to 90% Sb_2Te_3 and may contain small amounts of Bi_2Te_3 and Bi_2Se_3 in solid solution. The most promising alloys developed to date are solid solutions of three separate compounds (see Ref. 1):

$(Bi_2Te_3)_{90}(Sb_2Te_3)_5(Sb_2Se_3)_5$ + iodine doping (N-type), and

$(Sb_2Te_3)_{72}(Bi_2Te_3)_{25}(Sb_2Se_3)_3$ + Pb doping (P-type).

These Bridgman cast alloys yielded a figure of merit of 3.2 X 10^{-3}/K and 3.4 X 10^{-3}/K, respectively, at room temperature. These values are higher than commercially available Bridgman cast alloys.

While the Bridgman cast material has size limitations ($\geq$0.50 in. X 0.050 in.), it is currently by far the least expensive process for producing $(Bi,Sb)_2(Se,Te)_3$ alloys. With a development effort, it should be possible to produce the powder-metallurgy-prepared material at very low cost. Automated powder presses are in existence today that can be employed in this process.

Techniques for fabricating the Bridgman cast or powder-metallurgy-prepared elements into low-cost compact modules have been developed and qualified. The manufacturing sequence in fabricating these modules is shown in Fig. 5. Radio-thermoelectric generators (RTGs) containing these modules have operated for several years with little or no degradation. These same types of modules have been operated up to 350°C in accelerated testing for many thousands of hours with no degradation. Normally, $(Bi,Sb)_2(Se,Te)_3$ alloys are not used above 280°C because no gain in efficiency is obtained.

As the need for thermoelectric elements of small cross section and/or high strength developed, it was apparent that Bridgman cast alloys could not be used since the small elements have little strength and produce high-resistance anomalies. The development of fine grain $(Bi,Sb)_2(Se,Te)_3$ alloys has allowed fabrication of elements of very

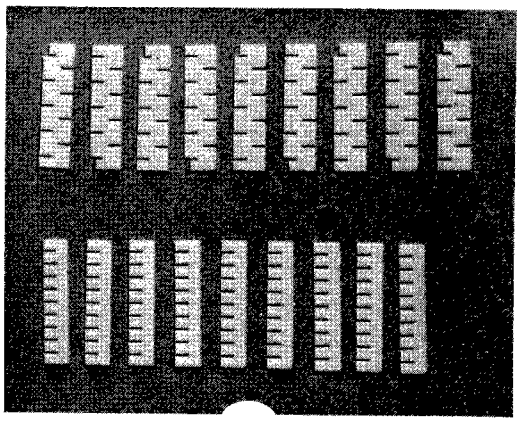

(a) Egg crate components

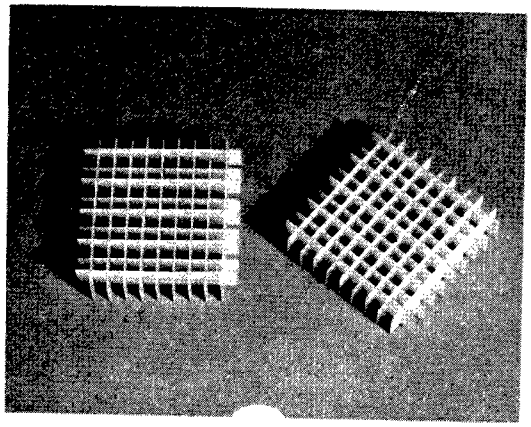

(b) Assembled egg crates

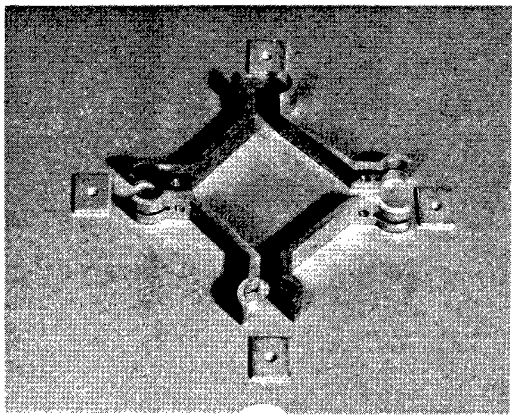

(c) Plasma spraying and sanding fixture, side supports

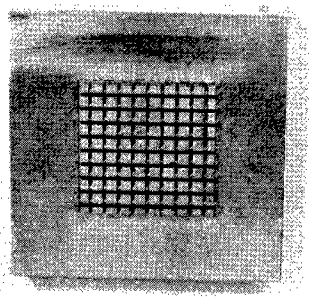

(d) Plasma spraying fixture, bottom support

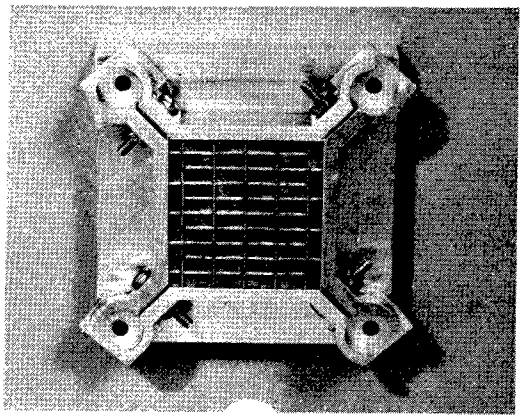

(e) Elements assembled into egg crate and tooling for plasma spraying

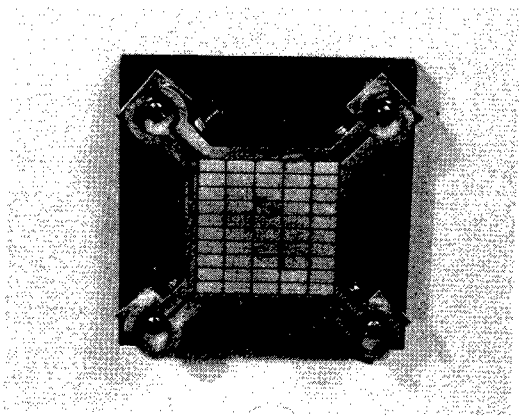

(f) Completed module after sanding

Fig. 5. Fabrication process for assembling low cost thermoelectric module

small cross section (0.006 in. X 0.006 in.) that either produce high voltages when used for power or can make use of high voltages when used for cooling.

While powder metallurgy alloys allow a breakthrough in miniature device technology, the figure of merit of the N-type material is decreased by approximately 25% at room temperature. At elevated temperatures (T_H = 280°C), however, the powder metallurgy alloys are equal to or better than the Bridgman cast materials because the powder-metallurgy-prepared alloys have a lower thermal conductivity at higher temperatures.

In converting the $(Bi,Sb)_2(Se,Te)_3$ family of alloys into a powder metallurgy product, special processing techniques and quality control procedures are mandatory to ensure a mechanically sound product.

3.3. PbTe-BASED ALLOYS

The PbTe-based alloys consist of N-type PbTe, P-type PbTe, and P-type PbSnMnTe. All three alloys are isotropic in structure and the cast and powder-metallurgy-prepared materials are similar in thermoelectric properties. Typically, they are used in the powder metallurgy condition. The N-type material is slightly Pb rich, is readily prepared by powder metallurgy techniques, and is not crack sensitive. The P-type PbTe, however, is Te rich and crack sensitive. The PbSnMnTe alloy which is Sn rich was developed to replace P-type PbTe. Although its figure of merit is slightly less than PbTe, it is much more fabricable and is compatible with Fe (P-type PbTe is only compatible with W and Mo).

The PbSnMnTe alloy precipitates a small amount of MnTe in early life with a small change in thermoelectric properties, while the

other two alloys are stable in properties if they are in contact with compatible materials.

The PbTe-based alloys have been used in most of the space RTGs. Large-scale powder metallurgy processing could be applied to the N-type PbTe and P-type PbSnMnTe alloys to greatly lower production costs, but development is required with PbSnMnTe to enhance its ability to be fabricated into low-cost modules.

3.4. SiGe ALLOYS

The SiGe alloys are normally prepared by powder metallurgy techniques; however, the parameters for the pressing operation are very restrictive compared to PbTe alloys. The pressing temperature for SiGe alloys is much higher, ~1280°C, and the resulting resistivity is dependent on the density obtained.

During gradient operation, the N-type SiGe precipitates phosphorous and the P-type material boron as a function of time and temperature. This precipitation of the dopants (decrease in carrier concentration) causes the thermoelectric properties to change, with an overall decrease in the figure of merit.

The SiGe can be operated over the largest ΔTs of any thermoelectric alloys developed thus far, and this attribute is fortunate because the figure of merit of SiGe alloys is so low that large ΔTs are needed to obtain competitive efficiencies. At >950°C in an inert atmosphere, the vaporizing Si and Ge species attack quartz insulations to produce the volatile species SiO and GeO. Coatings of Si_3Ni_4 have been used to suppress this interaction. The SiGe generators fabricated by RCA Corporation for the Department of Energy (DOE) for space applications have been extremely expensive and, for this reason, DOE has dropped SiGe alloys from further use. For terrestrial applica-

tions, the SiGe alloys could be adapted to a low-cost generator. The English have developed relatively inexpensive compact-type SiGe modules. In this construction, multiple N-type and P-type legs and contacts are pressed simutaneously and the ceramic Forsterite is used to separate the N-type and P-type legs.

3.5. TAGS

The alloy $(AgSbTe)_{15}$ $(GeTe)_{0.85}$ (TAGS) (undoped) has a favorable figure of merit up to 550°C. However, from a practical standpoint, the alloy is limited to lower temperatures. At 375°C and above, the vaporization weight loss is significant. Operation of the alloy in an inert atmosphere versus vacuum allows its use up to 450°C. In gradient operation the alloy undergoes large changes in thermoelectric properties. These changes are accompanied by precipitation of phases rich in Ag, Sb, and Te.

TAGS can be fabricated by cast or powder metallurgy techniques. The alloy is somewhat crack sensitive and resembles P-type PbTe in mechanical properties.

While the alloy has obvious limitation, it has been used successfully in space generators (where the element legs are cast individually), and with some development it could be fabricated into a compact-type module for low-cost terrestrial application.

3.6 $(Cu,Ag)_3Se$ ALLOY

The $(Cu,Ag)_2Se$ alloy has been under development since the mid-1960s and its first RTG use is planned for the early 1980s. It is a self-doping alloy that is Se rich. The alloy has the unique property of diffusing the excess Cu and Ag to the colder end in a matter

of minutes. The Cu is seen to grow out of the material in the form of whiskers. Another unique property is that the alloy is current sensitive; the ratio of current x length/area must be considered in designing a device. At temperatures below ∿600°C, this dependence is of less concern.

The alloy is fabricable by powder metallurgy techniques and is similar to N-type PbTe in mechanical properties. Thus, the use of this P-type alloy over P-type PbTe or PbSnMnTe is a definite advantage with respect to thermoelectric and mechanical properties and probably has the most potential of any P-type alloy [beside P-type $(Bi,Sb)_2(Se,Te)_3$] being employed in a low-cost, compact-type module. Design studies performed by GA indicate that the N-type PbTe can be used with $(Cu,Ag)_2Se$ in such a module, and this module can be cascaded with the lower temperature $(Bi,Sb)_2(Se,Te)_3$ alloys, which, as noted in Section 3.2, can be fabricated into low-cost compact modules.

3.7. Gd_2Se_3 ALLOY

The alloy Gd_2Se_3 (also undoped) is being developed along with $(Cu,Ag)_2Se$. This alloy is expensive in raw material costs and difficult to process by powder metallurgy techniques. The Gd is an active getter for oxygen, and this contamination severely affects the thermoelectric properties. The alloy can be operated at high temperatures (∿1200°C) and, if the cost of Gd can be reduced, the alloy could possibly be used in solar applications; however, this cost reduction would have to be accompanied by a reduction in fabrication costs.

3.8. OTHER ALLOYS

Studies on $FeSi_2$ and $CoSi_2$ (and alloys of these compounds) as thermoelectric alloys for waste heat applications have been carried

out. The figure of merit of these materials is lower than that of SiGe alloys and, therefore, large ΔTs are required to obtain useful efficiencies.

4. REFERENCE SYSTEMS AND TECHNICAL APPROACH

4.1 SOLAR POWER TOPPING SYSTEM

Case 1, a solar electric plant, is illustrated in Fig. 6. This case was selected to determine whether a TEG can play a useful role as an electric topping cycle. Figure 6 shows that the focused insolation impinges on the thermoelectric cells at 1100°C and is rejected to a salt (HITEC*) heat exchanger at 577°C. The rejection temperature is high enough that the hot salt can heat steam through a salt-to-steam generator to drive a conventional high-pressure steam turbine. Because the solar collector field has a high capital cost, the Rankine power cycle was chosen for its high efficiency and includes reheat as well as four stages of feedwater heating. This cycle, illustrated in Fig. 7 achieves a net efficiency of 39.20%.

Case 1 was analyzed for three plant sizes, 2MW(e), 10MW(e), and 100MW(e) both with and without the thermoelectric topping cycle. One reason for investigating a range of plant sizes is that the smaller units are likely to be distributed and meet local power demands (e.g., individual plant needs). Thus, it may not be necessary to associate an electric distribution system (grid) with such a plant, and the user may be prepared to pay more per kilowatt-hour of capacity than for a large, centralized power plant that requires a grid.

The second reason for studying a range of power plant sizes is that the Rankine cycle efficiency declines as the turbines become smaller. Typically, the turbine blade heights become smaller while tip clearances and associated losses stay roughly the same. It is

---

*HITEC, the trade name for the salt supplied by the Dupont Company, comprises an eutectic mixture of sodium nitrate, sodium nitrite, and potassium nitrate.

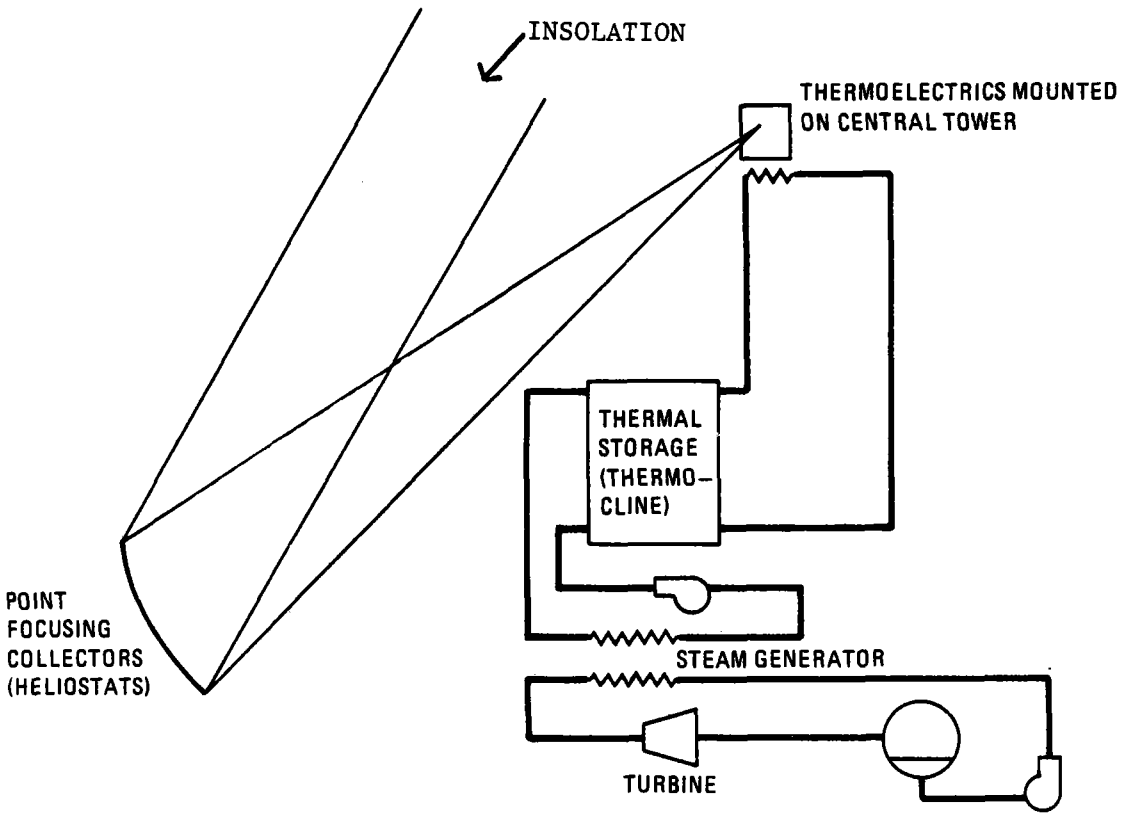

Fig. 6. Reference case 1: solar electric plant with topping cycle

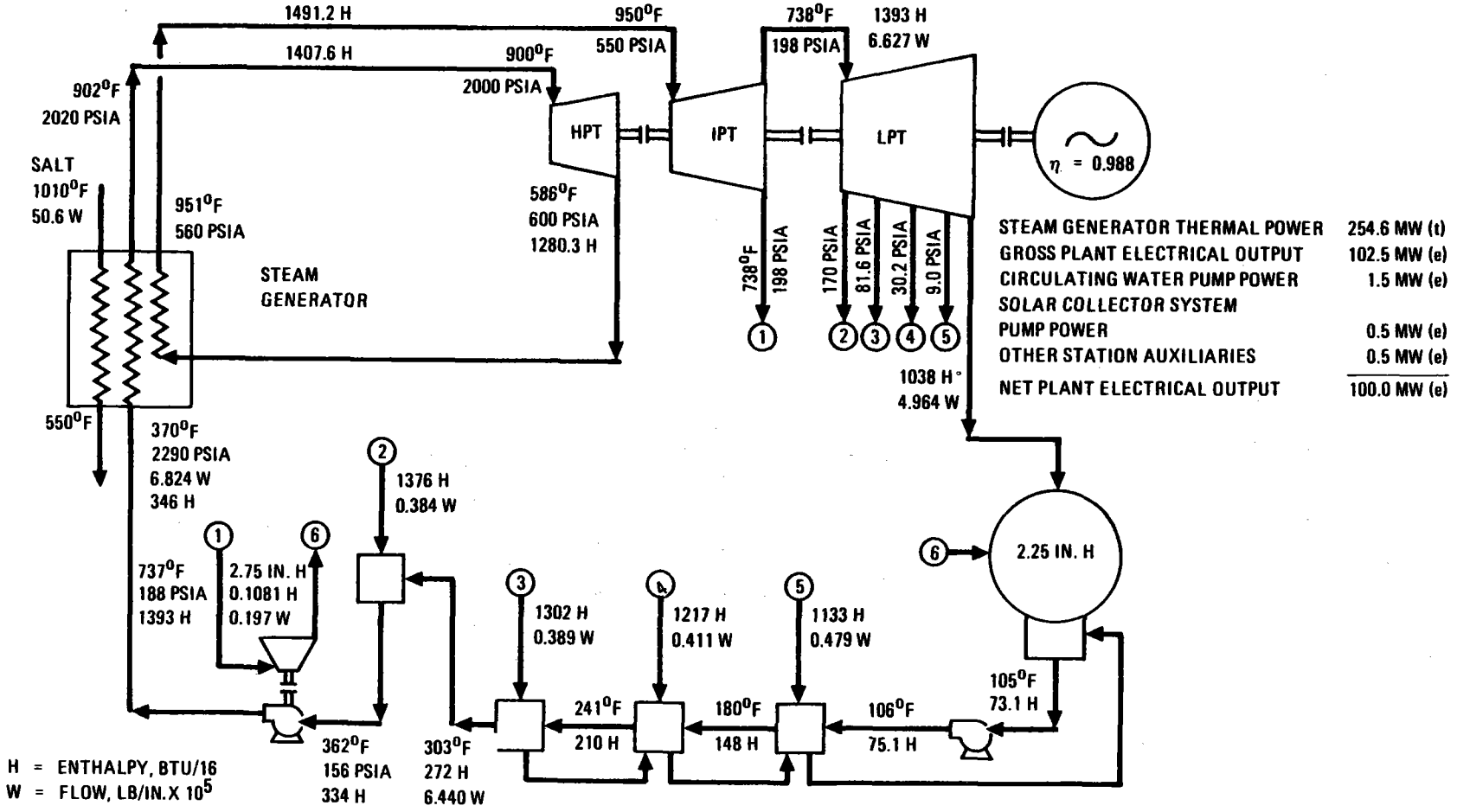

Fig. 7. Reference 100 MW(e) steam cycle power conversion system

possible to reduce this effect by utilizing a high-speed turbine which drives a 60-Hz electric generator through reduction gears. Such gearboxes can be costly and their reliability is questionable. It is not surprising, then, that such small steam turbines are not readily available and their capital cost per kilowatt-hour is much higher. Figure 8 illustrates these points from a summary complilation of available literature on turbogenerator set costs and efficiencies. Efficiencies in the 10-MW range have dropped substantially; in fact, to avoid excessively small components, nonreheat cycles are employed.

The analysis has used a point-focusing system as the reference solar collector. Data on the performance and cost of the collector system were taken from Ref. 2 and include an overall light-to-heat-collection efficiency of 53.1%. The latter value includes an allowance of 15% for cosine losses. Line focusing systems such as the GA patented fixed-mirror solar concentrator (FMSC) concept (Refs. 3 and 4) were not included because their lower solar concentration factor does not permit a high temperature topping cycle. While such line focussing systems are well suited for themoelectric/process heat applications due to their modularity, it was decided to retain the point focusing system as the reference collector for case 2 in order to avoid confusing the evaluation of thermoelectrics with the economics of another solar collector. Present collector costs for central power systems are still uncertain, and it seemed undesirable for the thermoelectric economic evaluation to be trapped in a collector cost uncertainty band.

The reference collector system employed thermal storage to provide a continuous service period of 14 hr for a solar input (assumed constant) for 9 hr. This storage was used to maintain the electrical output of the plant constant. In effect, this meant that the topping thermoelectrics operated for 9 hr only, during which time the bottom-

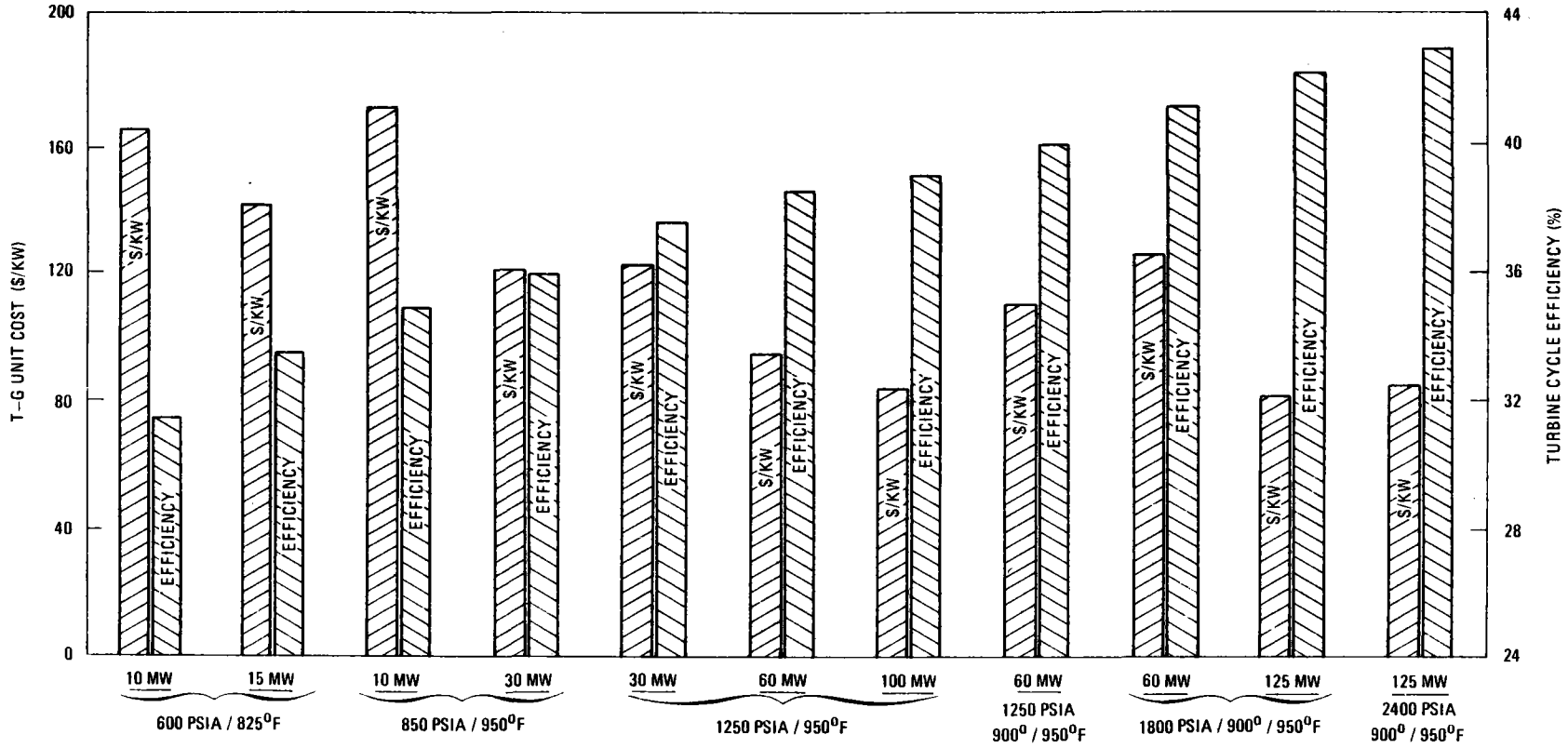

Fig. 8. Costs and turbine cycle efficiencies

ing cycle ran at less than rated conditions (∿80%). No loss of efficiency in the Rankine cycle was assumed. For the remaining 5 hr, the steam turbogenerator set ran at design power.

4.2 SOLAR TOTAL HEAT SYSTEM

Case 2 is based on the idea that an industrial user of heat might install a solar total heat system if faced with the loss of his present heat source, e.g., because of unavailability of natural gas or low-sulphur oil. Since the user will most likely need electricity and will need it mostly when the heat is being utilized, the concept of a local (instead of centralized) electric use tied to the heat source emerges.

Figure 9, taken from Ref. 5, provides a measure of the quantity of heat used in the United States as a function of its terminal (supply) temperature. It is important to note that 50% of the total heat used in the U.S. (including preheat requirements) is needed at 550°F or less, and without preheat 30% is needed at 500°F or less. These observations suggest that a solar system which collects heat at as high a temperature as can be conveniently and economically stored and which then passes the heat through a thermoelectric system that rejects the heat at a 550°F process delivery temperature has potential applicability. Therefore, the system depicted in Fig. 10 was devised. It comprises a central receiver system in which the focused insolation is passed through a thermoelectric topping cycle over the same temperature range as that of case 1. Case 2 is also analyzed without the topping cycle.

The heat transport fluid employed is HITEC, which may also be stored. Thermal storage for 16 hr is planned, consistent with two-

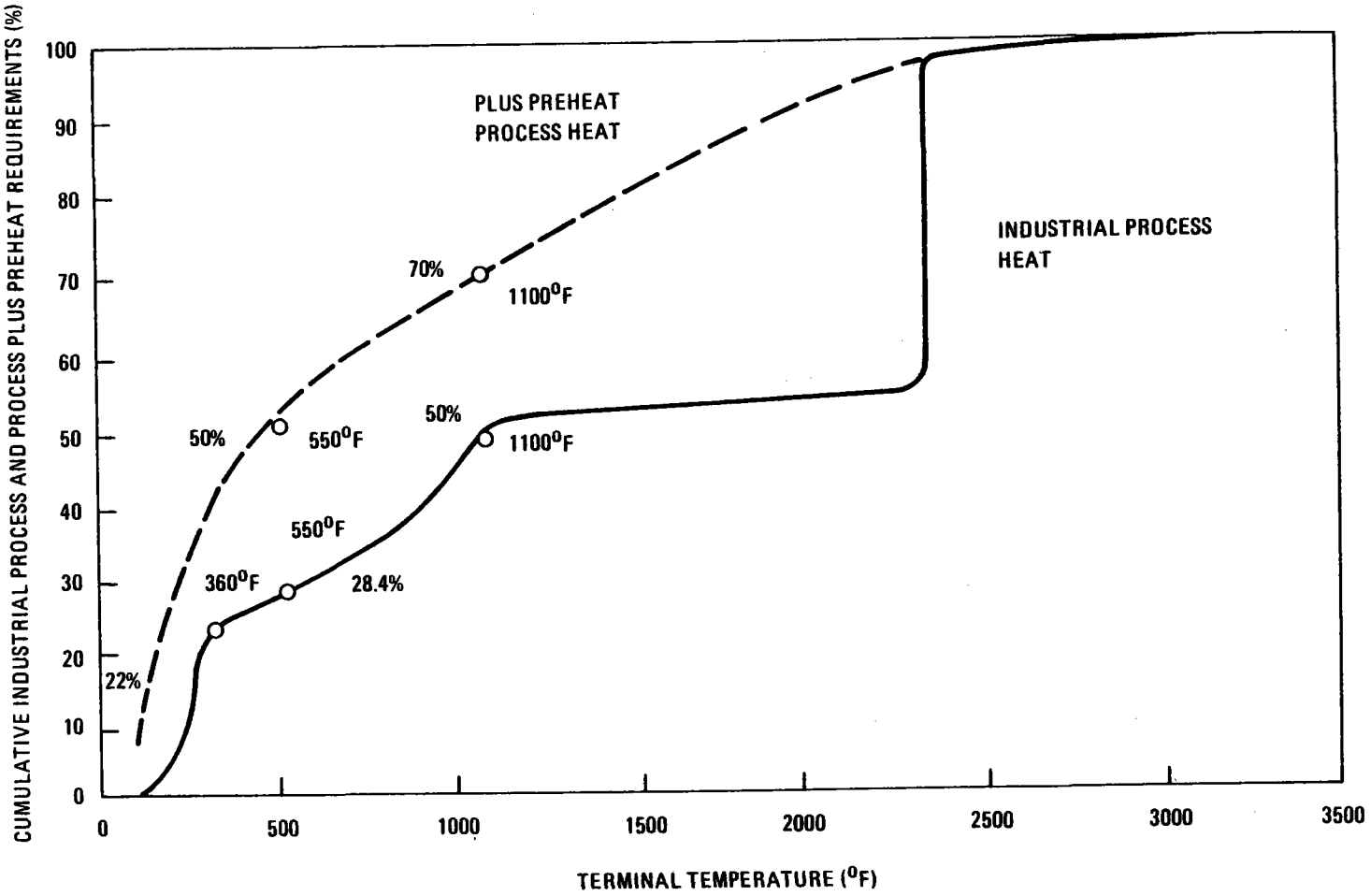

Fig. 9. Temperature spectrum of survey data base industrial process and preheat requirements (60° to 3300°F)

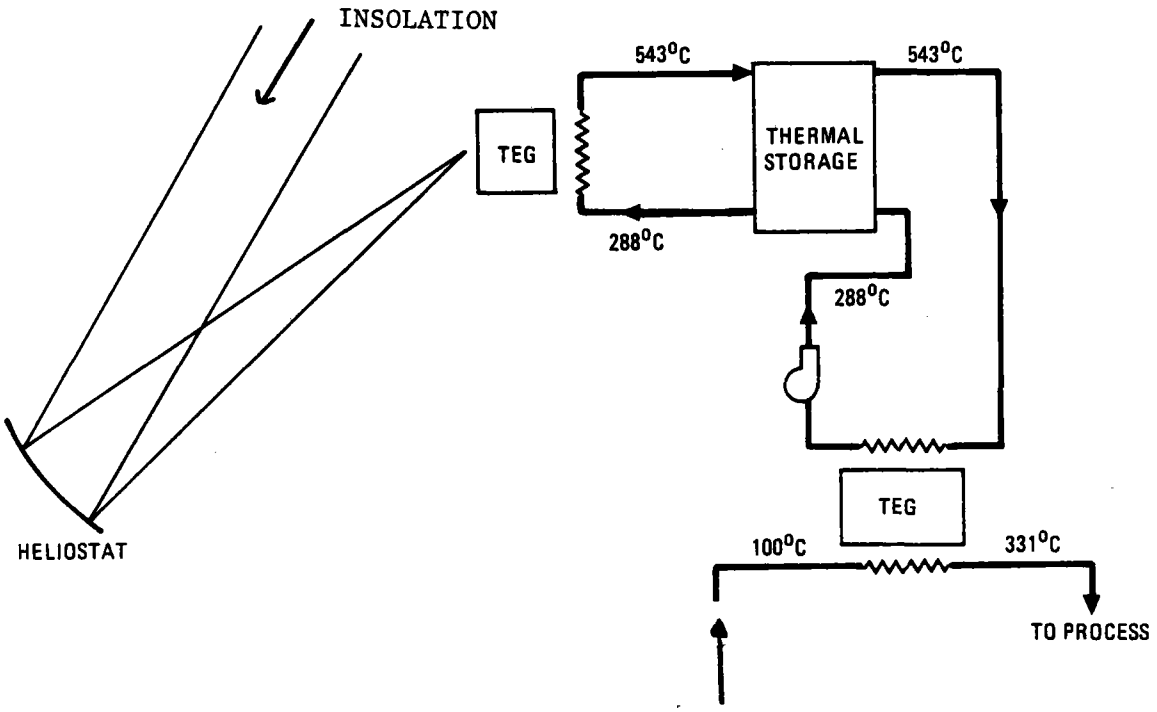

Fig. 10. Solar total heat system
(with topping cycle)

shift operation of the plant. The salt is pumped from storage to a low-temperature thermoelectric generator, which rejects heat over a range but allows it to be delivered to the process at 331°C (628°F). The use of pressurized water as the medium transporting the heat to the process is suggested, but the cost and technical studies here have not included this rejection heat exchanger, which is in contact with the cold side of the TEGs. The plant is sized for a 1-MW(e) output from the bottoming cycle TEGs, which is consistent with a 21.83-MW(t) delivered heat rate to the process. A return temperature of 100°C from the process to the TEGs was assumed.

In scoping out the work on this program, it was proposed to study a variant of case 2 in which the heat from the bottoming cycle TEGs was utilized for either space heating or air-conditioning. Figure 11, illustrates this system, but its costs were not determined due to lack of time. However, in this variant system, a 100-W(e) output, to be used locally, was the reference concept and the rejection heat temperature was 187°C, i.e., convenient for steam heating or for absorption refrigeration. The average lower rejection temperature of this case 2 variant allowed a bottoming cycle efficiency of 7.27% to be achieved compared to the 4.23% efficiency of case 2 proper.

4.3 SOLAR POND

Case 3 is a concept suggested for study based on the idea that if one can make a very cheap collector and heat storage system such as a solar pond, then one can afford an inefficient power conversion system provided its capital cost is low. General Atomic has performed this study only from the point of view of determining the TEG requirements, materials, sizes, and costs, and then determining the permissible collector cost for a given installed capital cost target of $2,000-W(e) commensurate with a distributed-type plant.

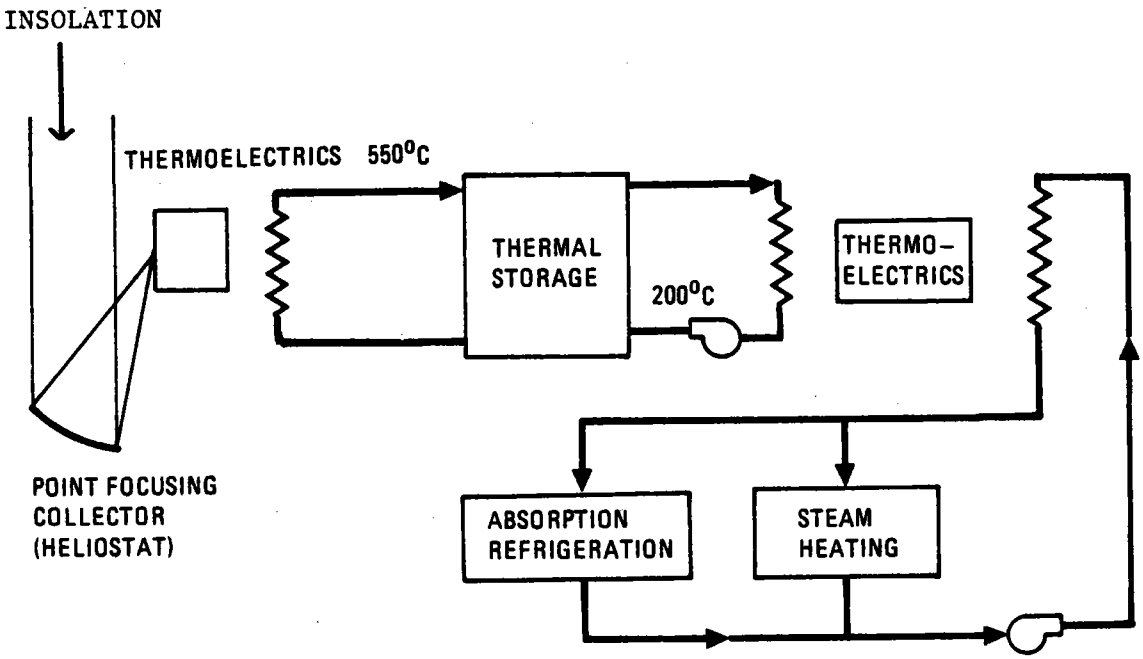

Fig. 11. Solar total heat system for space heating/cooling end use

The pond is assumed to have cold and hot temperatures of 20°C and 85°C, respectively. A temperature drop of 5°C on hot and cold ends is allocated to permit transfer of heat to the TEGs. Thus, the TEG observes a net temperature difference of 55°C.

4.4 TECHNICAL APPROACH

The THEAT computer code (a proprietary GA code) was employed to calculate the optimal design parameters of the thermoelectric generators, whether single or multistaged. The code computes the TEG output and number of elements required for a set of independent variables describing the thermoelectric element cross-sectional area, length, interstage temperature, number of circuits, etc. The code is, in turn, coupled to an optimization search algorithm to maximize an objective function, which may be either the TEG efficiency, the volume weighted efficiency, or any other function desired. Tabular thermoelectric data are interpolated and integrated over the temperature range of their use. References for the materials data employed and the results obtained are given in Section 5. Figures 1 and 2 show the present-day values of the figure of merit for various P-type and N-type thermoelectric materials, respectively, as a function of temperature, expressed as

$$Z = \frac{\alpha^2}{\rho\kappa}$$

where α = the Seebeck coefficient,

ρ = the electrical resistivity, and

κ = the thermal conductivity

The parameter Z is a convenient measure of the performance of the thermoelectric material: the higher the Z, the better the TEG performance. Thus, Figs. 1 and 2 were employed as a guide to selecting thermoelectric materials for the differing temperature ranges of the applications exemplified in cases 1 through 3.

5. THERMOELECTRIC MATERIAL COST AND MARKETS

Thermoelectric system costs have been studied to provide data for the reference cases described in Section 4.

Thermoelectric materials Bi, Te, Se, Si, and Ge, when processed into purity levels of 99.999%, are available in limited quantities and require 6 month lead purchasing times. The reasons for this are many. Most of these elements are the byproduct of primary mining operations in which a major metal is extracted. The primary demand for the TEG materials is made by industries that utilize only trace material quantities, such as in the manufacture of drugs and pharmaceutical products. Since the purity levels demanded for TEGs require several separation processes to eliminate impurities, labor becomes a pacing portion of the cost of manufacture. Raw materials, as found in the combined form, are estimated to be in excess of the gigaton level. Separation processes presently employed yield less than 2 metric tons of TEG material annually at levels of 99.999% purity. Thus, it is necessary that 700 tons of raw material be used to obtain this 21 tons (3%) of five-nines pure material. The bulk of the raw material, with purity levels less than five-nines purity, is sold as prime material to industries where the impurities would not adversely affect it products. Most of the impurities found in TEG materials cannot be tolerated since they add uncontrolled dopant levels. Present day raw material resources, if processed to reasonable levels, could yield sufficient quantities of TEG to supply power at a competitive price and volume.

The total yearly throughput of a typical processor is in the range of less than five tonnes. Further processing to deliver the desired purity level, 99.999% gives low yields, and the resulting high labor to material ratio makes large orders unattractive. The primary users are pharmaceutical manufacturers where trace material quantities are employed.

Typical of the pricing structure is tellurium, with a base quoted price of $13.50/lb in lots of less than 100 lb. A marginal discount structure is applied yielding $12.15/lb in lots of 1000 lb. The material to process labor ratio is 40/60. To find what pricing structure for TEGs would exist under the mature, competitive, high-volume production conditions necessary to produce material in sufficient quantities for the reference cases, the following calculation was used:

$$\text{material} = 0.40\ (\$12.15) = \$4.86,$$
$$\text{labor} = 0.60\ (\$12.15) = \$7.50.$$

Material

Apply 5% discount per 50,000 lb on a sliding scale to reflect raw material process increase throughput.

Labor

Apply sliding scale of 60% to 10% on materials to reflect automated process and decrease of labor content.

Table 1 illustrates the resulting costs for tellurium for finished TEGs in terms of the weight of the finished product as a function of the market size.

5.1 CONDITIONS/ASSUMPTIONS

The pricing structure used in the SERI case studies is valid only when the following assumptions are included:

1. Extraction of raw materials at high throughput volumes is accomplished using mass production/extraction techniques.
2. The market for some conductor thermoelectric materials is constant and forecasted to be relatively predictable.
3. Capital equipment has largely been written off, reflecting a mature industry.
4. Profit margins are low, reflecting competitive supply conditions.
5. Labor content in extraction and manufacturing processes is

TABLE 1

TELLURIUM PRICING STRUCTURE

REFLECTING INCREASED THROUGHPUT SLIDING SCALE

Lot Size (lb)	Market Price ($)	Material (%)	Labor (%)	Material Content ($)
100	13.50	40	60	5.40
1,000	9.25			
10,000	7.80			
50,000	6.71			
100,000	5.37			
200,000	3.87			
500,000	3.10			
750,000	2.43			
1,000,000	2.04			
2,000,000	1.84			
>2,000,000[(a)]	1.29	90	10	1.16

(a) At >2,000,000 lb: material content = 0.90 ($1.29) = $1.16/lb

labor content = 0.10 ($1.29) = .13/lb

$ 1.29/lb

proportionately low, reflecting high yields, limited rework, and controlled procedures.

6. Learning has been accomplished and further development is not required.

Pricing data were generated for other thermoelectric materials subject to the above conditions/assumptions. These cost data, in terms of the weight of finished TEG products, are given in the following tables and were utilized in the calculations reported in Section 6.

5.2 SUMMARY OF TEG PRICING STRUCTURE

	Si	Ge	Bi	Te
Pounds	$/lb	$/lb	$/lb	$/lb
Less than 1,000	7.20	22.80	7.45	9.45
3,000	6.00	19.00	6.30	7.80
30,000	4.32	13.70	5.67	6.71
100,000	3.89	12.33	4.54	5.37
300,000	3.50	11.10	3.41	3.87
500,000	2.70	8.60	2.73	3.10
1,000,000	1.54	4.90	1.80	2.04
2,000,000			1.13	1.29

TAGS

Te	200,000 lb	$ 3.87/lb
Ge & dopant	40,000 lb	11.10/lb
Sub total	240,000 lb	$ 5.08/lb
Labor 8%		.42
Price @	240,000 lb	$ 5.50/lb

2N

Te	200,000 lb	$ 3.87/lb
Pb	20,000 lb	2.80/lb
Sub total	220,000 lb	3.77/lb
Labor 8%		.30
Price @	220,000 lb	$ 4.07/lb

BiTe

Bi	400,000 lb	$ 2.73/lb
Te	250,000 lb	3.87/lb
Sub total	650,000 lb	$ 3.17/lb
Bi	1,000,000 lb	$ 1.80/lb
Te	670,000 lb	2.04/lb
Sub total	1,670,000 lb	$ 1.90/lb
Bi	2,000,000 lb	$ 1.13/lb
Te	1,340,000 lb	1.29/lb

SiGe 50/50 Alloy

Si	400,000 lb	$ 3.10/lb
Ge	400,000 lb	8.60/lb
	800,000 lb	$ 5.85/lb
50/50 Alloy		
Si	1,000,000 lb	$ 1.54/lb
Ge	1,000,000 lb	4.90/lb
	2,000,000 lb	$ 3.22/lb
65/35 Alloy		
Si	520,000 lb	$ 2.70/lb
Ge	280,000 lb	11.10/lb
	800,000 lb	$ 5.64/lb

65/35 Alloy

Si	1,300,000 lb	$ 1.54/lb
Ge	700,000 lb	6.75/lb
	2,000,000 lb	$ 3.36/lb

$(Cu,Ag)_2Se$

$(Cu,Ag)_2Se$	400,000 lb
$(Cu,Ag)_2Se$	1,000,000 lb
$(Cu,Ag)_2Se$	2,000,000 lb

Pricing references for this study are based on manufacturing cost data compiled for the manufacture of thermoelectric generators over the past 12 years. Base case studies were derived from manufacturing experience from the following companies:

General Atomic Company	San Diego, CA
General Instrument Company	Newark, N.J.
Teledyne Isotopes	Westwood, N.J.
The 3M Company	St. Paul, Minnesota
RCA Corporation	Harrison, N.J.

The experience used ranged from product inspection to production on a pilot line basis and the transformation from limited quantities to standard market requirements. For example, a typical pilot line produces 12 thermoelectric generators per year with an average output of 100W each. Typical present-day production is 20 thermoelectric generators per month, or 240 TEGs per year, with an average power output of 100W. The average selling price is $2800 for 100W of power or $28/W. Yearly sales for an average supplier are $700,000. Market conditions presently support approximately five suppliers yielding $3.5 million in annual sales. Supplementing these standard products are applications for power shelters, buoys, cathodic protection, and standby-emergency power sources.

5.3 EFFECT OF IMPURITIES AND COST IN $(Bi,Sb)_2(Se,Te)_3$ ALLOYS

Typically the higher purity materials (four to six nines pure) are used in preparing thermoelectric alloys. If less-pure materials are utilized (such as three nines pure) the unknown variable is what effect the remaining trace elements have on the thermoelectric properties. If the trace elements act as dopants their contribution will be large. However, quite often many elements have little or no effect on the properties of thermoelectric materials. Once the role of the typical impurities in the raw materials is known, less-pure starting materials can be utilized with large reductions in materials cost.

5.4 MARKET REVIEW

Thermoelectric generators are presently being sold to a variety of customers and markets that are just developing and will be rapidly expanding in the next 5 years. Of particular interest is the fact that the need of TEG energy sources in the range of 20 to 300W is directly tied to the changeover to solid-state electronic components from vacuum tubes in communication and instrumentation equipment. Prior to the use of solid-state components, all remotely located equipment was designed to use either very low power (less than 10W) and thus capable of operating off batteries, or very high power (500W and up) thus needing diesel generators. With solid-state components and the increased sophistication of equipment, the power levels have now moved into the region of 10 to 200W where only TEGs have demonstrated acceptable reliability and economic advantages. A brief review of the present applications, typical customers, and markets is given below.

For power levels from 10 to 300W, TEGs are the most reliable and least expensive source of power for long duration of operation in unattended remote areas. This has been proved by existing sales records

and requirements. Under 10W, wind-driven generators, primary and secondary batteries, and solar cells become economically attractive. For requirements over 300W, engine generators become competitive. In the future, some competition may come from fuel cells. In summary, the four general market areas are:

1. Power for remote electric or electronic devices.
2. Electric current for cathodic protection (electrically reversing galvanic corrosion) for pipelines and gas well casings.
3. Power for buoys.
4. Power shelters.

5.4.1. Power for Remote Electric or Electronic Equipment

5.4.1.1. VHF Communication. Solid-state VHF communication equipment for base-to-mobile and mobile-to-mobile stations is often located on mountain tops to take advantage of the better area coverage made possible by having the antenna at the highest point in the area. Applications, therefore, tend to predominate in mountainous, low-population areas. Typical users are the U.S. Forestry Service, Nevada Highway Patrol, Dome Communication, and Transwestern Pipeline. Power needs are between 20 and 60W in most cases, and occasionally to 200W.

5.4.1.2. UHF Communication. Specifically, the market for UHF communication is remotely located microwave repeaters. The penetration here to a large extent depends on the acceptance of all-solid-state equipment. Any repeater system with a tube (TWT or Klystron) in the transmitters will require more than 300W, and will not be economically suitable. Repeater systems are now obsolete. First-generation, all-solid-state repeater systems have power requirements of 150 to 250W and can thus profit by the TEG economic advantages.

5.4.1.3. Wire or Cable Communications. A large part of telephone communications is still being carried into remote areas via carrier

current on open lines or cables. In many cases, power for the needed repeaters is fed on the same lines or cables. On some installations in very remote areas, this is not practical, and TEGs are an economical solution. Power levels are 10 to 50W.

5.4.1.4. Telemetering and Remote Control. The combination of sensitive sensors, solid-state logic, low power analog-digital converters and solid-state controlled high frequency links has made possible relatively inexpensive remote telemetering systems for seismic studies, flood control, soil studies, snow-depth monitoring, weather data gathering, and other studies requiring remote sensors where the power levels lie in the economical TEG regime. Typical customers are New Mexico Institute of Mining and Technology, University of Alberta, University of Sydney, U.S. Department of Agriculture, and U.S. Army Corps of Engineering. Similarly, TEGs can power remote control systems on pipelines, electric utilities, and railroads.

5.4.1.5. Marine Navigation Aids. Thermoelectric generators are suitable power sources for the Cubic Decca Mini Fix and Radydist electronic navigation systems. Flashing lights, radio beacons, and fog horns can also be operated from TEGs. Typical customers are Decca Navigator, Computing Devices of Canada, Brown & Root, U.S. Navy, and Canadian Government Hydrographic Service.

5.4.1.6. Aeronautical Navigational Aids. All solid-state "fan" marker beacons (a part of the instrumented landing systems) are now coming into use. These can be powered economically from TEGs.

5.4.1.7. TV Translator. In communities located in valleys far from TV stations, an inexpensive way to get a good TV signal is to place a TV receiver-TV transmitter combination on a mountain top where a strong TV signal can be received and rebroadcast directly to the community. Such a device is called a TV translator. There are now over

2200 low-powered translators in operation, many of these requiring only 5W of power. Therefore, TEGs are suitable sources of power.

5.4.1.8. Railroad Signaling. The railroads use large quantities of primary and secondary batteries for track signaling and therefore it would seem to be a good market for TEGs. In the U.S. this has proved difficult for two reasons. When batteries are still the only source of power, costs are so low it is difficult to justify TEGs, and in other areas batteries have been replaced by ac power. Because railroads already have pole lines along the track, ac power costs are as little as $250 per mile. Outside the U.S. this is not necessarily true, and signaling may still be an attractive market, especially if prices can be reduced.

5.4.2. Cathodic Protection (CP) Current for Pipelines and Natural Gas Well Casings

Pipelines, well casings, and other underground metal structures can corrode due to an electric current generated in the same manner as a dry cell in a flashlight. Metal ions are removed from the section of pipe that is electrically anodic and deposited at the section that is electrically cathodic. If an externally generated current is applied in the correct manner, the entire pipe becomes cathodic and corrosion is prevented. TEGs are a natural source of this current for remote gas wells and gas pipelines because fuel is available from the protected line or well, and electrical output is matched, that is to say...cathodic protection requires high currents and low voltage. In the U.S., pipelines have been and will probably continue to be a limited market because CP can be applied as far apart as every 20 miles and sites can be planned at points where commercial power is available. In foreign areas such as North Africa, Iran, and Australia, commercial power is not readily available and TEGs find more applications. Since gas wells have to be where the gas is found, commercial

power is seldom available. The TEGs fill an economic need because replacement of a corroded well casing costs $12,000 to $20,000, and a complete CP installation costs $3,000 to $4,000.

5.4.3. Power for Buoys

A study by Travelers Research under contract to the U.S. Coast Guard has shown that TEGs are the most suitable source of power on buoys from approximately 6 to 100W. Potential applications are for oceanographic data gathering, automatic weather repeaters, navigation aids, water pollution studies, etc.

5.4.4. Power Shelters

There is a growing demand for all-weather buildings, prewired and equipped with TEGs for remote locations.

Users such as RCA, Alaska Communications, MTS, and Collins Radio have shown a keen interest in and need for packaged TEGs, i.e., fuel supply and equipment in a single enclosure or housing. A major volume of sales and dollars is potentially available here.

5.5 CONCLUSIONS

Thermoelectric generators of economically competitive power could exist under the following conditions:

1. Raw material extraction must be expanded to adopt high-volume, large-throughput techniques currently applied to materials such as copper, coal, and aluminum.
2. The capital expense of mining and manufacture would be reflective of a firm market.
3. The manufacture and assembly of TEGs would be based on high-

volume throughput conditions beyond those present in the industry today.

4. Incentives for manufacture would be provided by either private industry or the government.

If these conditions are met, then TEGs for large power application will be competitive.

6. CALCULATED DATA

6.1. CASE 1, SOLAR POWER TOPPING SYSTEM

The initial calculations of this system employed a two-stage TEG comprising an upper stage of SiGe and a lower stage of CuAgSe (P leg) and GdSe (N leg). These calculations utilized an input temperature of 1100°C, the upper limit for SiGe, and a constant heat rejection temperature of 577°C. The latter is 34°C higher than the hot salt temperature to allow for conduction across the cold shoe, the heat exchanger wall, and the salt film coefficient. The thermoelectric property data for the SiGe are from Ref. 6. Although more recent data (Ref. 7) exist on SiGe with gallium doping which show an improvement in performance of approximately 20%, these later data do not extend to 1100°C and thus were not utilized.

Initial calculations employed a 10% thermal bypass and 10% added internal resistance to account for contact losses. The resulting optimized efficiency was 6.35% and had an interstage temperature of 900°C. When costs of this system were calculated, the cost of the stage 2 material appeared excessive; therefore, all remaining topping cycle calculations were made with a single stage of SiGe covering the range 1100° to 577°C.

By minimizing materials requirements through increasing the power density at only very modest loss of efficiency, it appears now that CuAgSe and GdSe could have been employed as a cost-effective second stage. In addition, since the salt is heated from 287°C to 543°C, the topping cycle rejection temperature should have covered a broader range and not have been a fixed quantity. Therefore, topping cycle efficiencies achievable are higher than those reported below. However, time precluded investigation of these alternatives on this program.

The topping cycle finally calculated and employed in the cost/technical evaluations comprised the parameters presented in Table 2 based on a 100-MW(e) plant total output.

TABLE 2

CALCULATED TOPPING CYCLE PARAMETERS

Performance Data	
Solar flux	950W for 9 hr
Electrical output[(a)]	100 MW for 14 hr total
Thermoelectric output	19.87 MW(e) for 9 hr
Steam turbine net electrical output	80.13 MW(e) for 9 hr
	100 MW(e) for 5 hr
Thermoelectric efficiency	5.43%
Rankine system efficiency[(b)]	37.03%
Overall plant efficiency	42.50%
Light-to-heat conversion efficiency	53.10% (Ref. 2) (including a 15% allowance for cosine losses)
Thermal requirements	336.0 MW(t) for 9 hr
Insolation requirement	689.3 MW(t) for 9 hr
Salt thermal storage	1275 MW-hr
Collector mirror area requirement	72.56×10^4 m^2
Input salt heater rating	346.1 MW(t)
Solar System	
Heliostat area	38 m^2
Number required	19,095
Thermoelectric	
(Single-Stage Cascade Unit)	
Input temperature	1100°C

TABLE 2 (continued)

70.90×10^6 P legs of SiGe	0.25 cm^2 area x 3.1 cm long
70.90×10^6 N legs of SiGe	0.20 cm^2 area x 3.1 cm long
Rejection temperature	577°C
Storage System	
Hot tank/cold tank (each)	59888 cu ft (4 hot and 4 cold)
Internal diameter	42.4 ft
Height	42.4 ft
Storage temperature	545.3°C
Salt pump power	700W
Steam Rankine System	
Gross electrical efficiency	40.27%
Power to auxiliaries	2.5 MW
Net electrical efficiency	39.20%
Electrical power	
Day	80.13 MW for 9 hr
Night	100 MW for 5 hr
Wet tower cooling	

(a)Plant is configured as a peaking plant rather than a base-load plant, i.e., 14 hr operation per 24 hr day.
(b)Referred to input heat source to thermoelectrics.

Table 3 gives the results obtained for a 100-MW(e) plant without a topping cycle.

TABLE 3

CALCULATIONS FOR PLANT WITHOUT TOPPING CYCLE

Rankine system efficiency	39.20%
Overall plant efficiency	39.20%
Thermal requirements	396.8 MW(t) for 9 hr
Insolation requirements	747.3 MW for 9 hr
Collector mirror area requirement	78.66×10^4 m^2
Number of helisotats (each 38 m^2) required	20701
Input salt heater rating	396.8 MW(t)

The above system was recalculated for different size plants which were accompanied by a change in turbogenerator efficiency. Table 4 illustrates the change in Rankine cycle efficiency and overall plant efficiency. The table also includes two cases for comparison. One is a case with increased thermal storage which causes the TEGs to produce a larger proportion of the daytime (9 hr duration) power. The other case is one in which there is no storage whatsoever. The point about this case is that the turbogenerator set is sized for an output which is constant throughout the operational period, unlike the topping cycle systems with thermal storage.

Some additional costs were assigned to the TEGs, apart fro: their material and fabrication cost, to provide for the interfacing of the dc output from the units to the 24-kV, 60-Hz turbogenerator output. This interfacing ilustrated in Fig. 12, comprises 4 x 5 MVA inverters; 4 x 5000 A circuit breakers, and 2 x 10 MVA, 600-V, 24-kV, three-phase

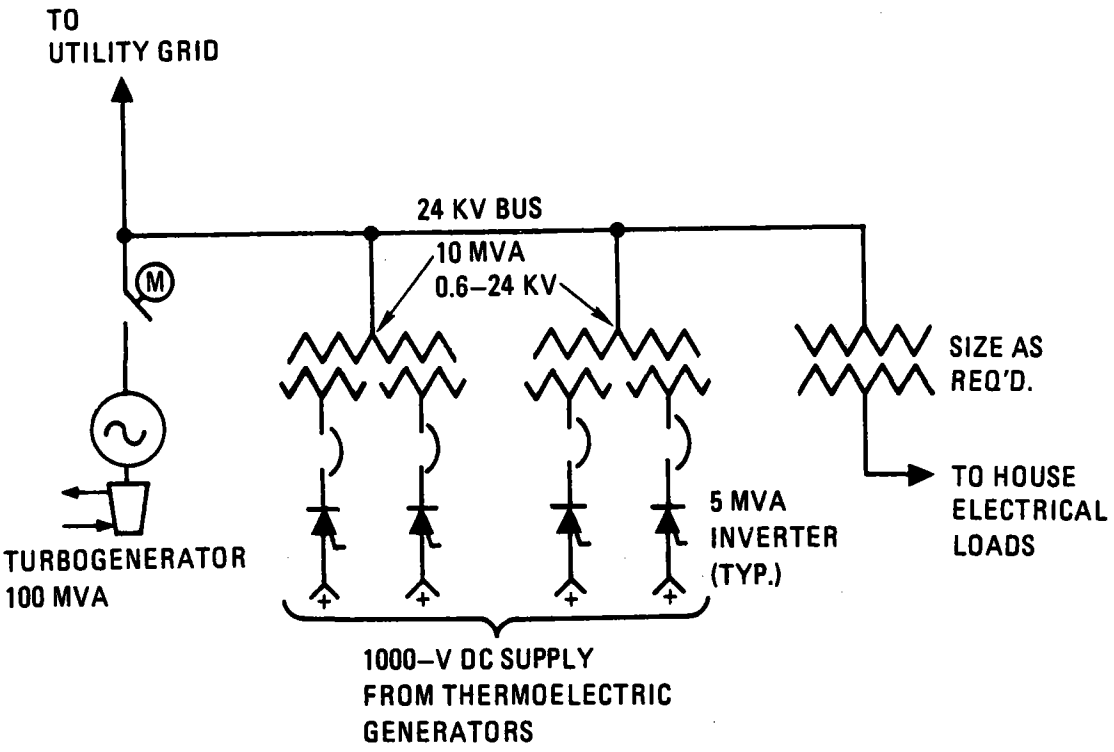

Fig. 12. Single-line diagram of
TEG electrical interfacing

transformers. The base price for this equipment if $1.314m. For plants smaller than 100 MW(e) total, cost scaling employed a 0.7 exponent on the power. No allowance for losses in this equipment was made although such losses lie between 6% and 10%.

TABLE 4
POWER RATING AND EFFICIENCY OF
SOLAR THERMOELECTRIC SYSTEMS

	Power Rating (MW)				
	100	10	2	2	2
Storage time, hr	5	5	5	15	0
Net steam turbine efficiency, %	39.20	34.08	27.10	27.10	27.10
Overall plant efficiency, %	42.50	37.66	31.06	31.06	31.06
Percentage of power by TEGs during day, %	19.9	22.4	27.2	46.6	12.8

Table 5 compares the capital cost of the various solar power systems with and without thermoelectric topping cycles. The thermoelectric cost data were taken from the tabular information presented in Section 5. The reference case is taken from Ref. 2 and describes a 100-MW(e) plant in which steam instead of salt is the primary working fluid. It has a lower overall plant efficiecy than the 100-MW(e) systems described here and therefore has a higher direct capital cost (e.g., $1744/kW versus $1510/kW). However, it provides useful base point solar cost data for the calculations reported here.

The cost data of Table 5 show how the direct capital cost [in $/kW (e)] increases substantially as the system power rating is reduced. Note that in each case, the cost of the TEGs is predicated on a total (production) output of 100 MW(e). Despite the modest power cost of the thermoelectric generator, the resulting cost incentive

TABLE 5

SOLAR POWER PLANT COST DATA (IN $/kW)

Plant Rating, MW	100	100	10	10	2	2	2	2	100 (Ref. Case)
	w/o	TEG	w/o	TEG	w/o	TEG	w/o	TEG	--
Storage Time, hr	5	5	5	5	5	5	0	0	5
Land	5	5	6	6	7	7	5	4	5
Structures/Improvements	51	51	128	128	244	244	244	244	51
Turbine Plant	290	290	579	579	938	938	938	853	242
Electric Plant	88	88	176	176	285	285	285	272	88
Collectors	629	580	724	655	910	794	585	510	695
Salt Heater Steam Generator	96	90	157	147	282	264	169	154	185
Tower	124	119	261	248	491	459	371	347	124
Thermal Storage	96	96	211	211	402	402	0	0	215
Distributables	78	78	129	128	207	203	155	148	86
Balance of Plant	53	53	133	133	253	253	253	253	53
TEGs + Power Cond.	0	54	0	67	0	83	0	83	0
Total Direct Cost	1510	1504	2504	2478	4019	3932	3005	2868	1744
Cost Advantage of System with topping cycle, %	--	0.4	--	1.0	--	2.2	--	4.6	

for a topping cycle is generally small. It is largest when there is no storage at all. These calculations show a reduction of 4.6% in direct capital cost for a 2-MW(e) plant without storage.

It is believed that the model does not fully illustrate the advantages of a TEG because the system employing TEGs is burdened by the cost of a full-size steam turbine and electric generator except in the case of zero thermal storage. A better model would be a system in which the TEGs are purely additive; i.e., they produce additional power during the insolation period only. To compare such a system with a system without TEGs would require comparison of plants having different output power time profiles, and this necessitates some time-dependent weighting of the values of the output power, a task outside the scope of this study.

The conclusions drawn from these results are:

1. There is a modest cost incentive for a thermoelectric topping cycle which is enhanced when
    a. There is no storage at all
    b. The plant is base loaded.
    c. The bottoming cycle efficiency is low.
    d. The output during the insolation period is valued at a greater amount than that generated outside the period.
2. Topping cycles with higher intrinsic efficiencies for the same rejection temperature will show a larger incentive provided their unit capital cost [$/kW(e)] is less than the unit capital cost of a steam Rankine power conversion system.
3. The unit capital cost of solar power systems increases as the plant size decreases.
4. The solar plant efficiency decreases as the size of solar power system decreases.

6.2 CASE 2, SOLAR TOTAL HEAT SYSTEM

This system was calculated with and without a thermoelectric topping cycle comprising SiGe elements which were heated to 1100°C by focused insolation and had a constant heat rejection temperature of 577°C. The latter is 34°C more than the temperature of the hot salt which is subsequently stored. The storage system temperature parameters in case 2 are the same as in case 1.

For the bottoming power system, the TEG was considered as three links so that the hot and cold temperatures could be adjusted reflecting that heat is supplied and removed over a temperature range. A ΔT of 10°C of both cold and hot sides was introduced to allow for conduction and film temperature drops. From the resulting net temperature ranges in each link, appropriate thermoelectric materials were chosen (see Figs 1 and 2) and multistaged TEGs utilized where appropriate. The thermoelectric elements, which had slightly different sizes in each link, were normalized to the same dimensions for manufacturing convenience. The data obtained for this solar process heat system are given in Table 6.

TABLE 6

SOLAR TOTAL HEAT SYSTEM DATA

Performance Data	
Solar flux	950 watts for 9 hr
Electrical output	1 MW(e) for 16 hr
	2.328 MW(e) additional for 9 hr
	with topping cycle, 0 MW(e) without
High-temperature	thermoelectric efficiency 5.432%
Low-temperature	thermoelectric efficiency 4.312%
Thermal requirements	42.87 MW(t) with topping cycle,
for 9 hr	40.59 MW(t) without

TABLE 6 (continued)

Insolation requirements	80.73 MW(t) with topping cycle,
for 9 hr	76.43 MW(t) without
Salt thermal storage	159.8 MW-hr
Heat delivered to process	21.83 MW(t) for 16 hr,
	with and without cycle
Solar System	
Heliostat area	38 m^2 (point focusing system)
Number required	2236 with topping cycle,
	2117 without
Thermoelectrics	
Topping cycle	
Input temperature	1100°C
1.651×10^6 P-leg SiGe	0.25 cm^2 area x 3.1 cm long
1.651×10^6 N-leg SiGe	0.20 cm^2 area x 3.1 cm long
Rejection temperature	577°C
Bottoming cycle	
Link 1, single state	
TAG P-leg	Ref. 8 data
2N N-leg	Reg. 9 data
T_{hot}	490.5°C
T_{cold}	302.2°C
Efficiency	3.990%
Link 2, single stage	
TAG P-leg	
2N N-leg	
T_{hot}	405.3°C
T_{cold}	225.3°C
Efficiency	4.303%

TABLE 6 (continued)

Link 3, two stages	
TAG P-leg	
2N N-leg	
$(Bi,Sb)_2(Se,Te)_3$ P-leg	Ref. 10 data
$(Bi,Sb)_2(Se,Te)_3$ N-leg (stage 2)	Ref. 10 data
T_{hot}	320.2°C
$T_{intermediate}$	204.8°C
T_{cold}	148.3°C
Efficiency	4.410%

The thermoelectric data of Table 6 are approximated in summary form by the following:

7.08×10^6 P-leg TAG	0.08 cm^2 area x 0.2 cm long
7.08×10^6 N-leg 2N	0.12 cm^2 area x 0.2 cm long
34.3×10^6 P-leg $(Bi,Sb)_2(Se,Te)_3$	0.05 cm^2 x 0.3 cm long
34.3×10^6 N-leg $(Bi,Sb)_2(Se,Te)_3$	0.08 cm^2 x 0.3 cm long
Overall efficiency	4.234%

The total system cost (Table7) was calculated using the thermoelectric cost data of Section 5 and as much of the base solar cost data (Ref. 2) as possible.

Table 7 presents the system cost data. It was assumed that the bottoming cycle electricity was used in the process plant and that the topping cycle output was available for export. Thus, the topping cycle requires a more costly electrical plant, with step-up transformers and switchgear to interface with an outside grid. The total cost difference between the two cases is $1311 thousand, which represents $563/kW for the topping cycle. The topping cycle thermoelectric

generators and their power conditioning equipment are also relatively less costly at $169/kW(e) than the $301/kW(e) of the bottoming cycle. This reflects the higher effectiveness of the TEGs at elevated temperature and the scaling advantage that accrues to the power conditioning equipment.

The above capital costs have been converted to an operating cost using a fixed capital charge rate of 15%, a capacity factor of 90%*, and an electrical credit of 5¢/kW-hr. In obtaining the data of Table 8, operating and maintenance costs were ignored. The calculations in Table 8 do not include the cost of an input heat exchanger; they do include costs for items such as site, land preparation, structures, etc., that would be borne by the owner in constructing a new process plant using oil or gas as the fuel source.

The costs of Table 8 are not very different from the costs projected for synthetic natural gas of $4 to $5/$10^6$ Btu in 1978 dollars (Ref. 9). Moreover, the plant owner has major control over the availability of his energy source (except for cloud cover) and is not subject to escalation in the price of his fuel. An advantage of 6.0% in favor of the topping cycle is seen, i.e., slightly larger than for case 1. If the electricity produced by the plant were locally consumed, then the topping cycle would not carry grid interfacing equipment and would show a larger cost advantage.

The conclusion drawn from these case 2 results is that there is a modest incentive for a topping cycle in a process heat system of this size [21.83 MW(t)], which is enhanced:

1. When the electricity produced is consumed at the plant.
2. When the cost of alternative daytime electricity is higher than nighttime electricity.
3. When the efficiency of the topping cycle is higher than the 5.43% employed in these calculations.

---

*Applied to the process heat delivery period of 16 hr

TABLE 7

TOTAL HEAT SYSTEM ($1000)

[2].83 MW(t) and] MW(e)]

	With 2.328 MW(e) Topping Cycle	Without Topping Cycle
Land	59	55
Structures	916	886
Turbine plant	0	0
Electric plant	238	69
Collectors	6,798	6,437
Salt heaters	1,617	1,617
Tower	2,545	2,476
Thermal storage	2,240	2,240
Distributables	846	790
BOP	450	450
TEGs and power conditioning equipment	301	301
	393 (a)	0
Direct cost	16,403	15,311
Indirects (20%)	3,281	3,062
Total cost	19,684	18,373

(a)Topping cycle

TABLE 8

OPERATING COST ESTIMATES FOR SOLAR PROCESS HEAT SYSTEM

[21.83 MW(t)]

		With Topping Cycle	Without Topping Cycle
Capital use charge,	$1000/yr	2953	2756
Electrical credit,	$1000/yr	607	263
Net yearly cost,	$1000/yr	2346	2439
Delivered heat cost,	$/10^6 Btu	5.99	6.37

6.3 SOLAR POND SYSTEM, CASE 3

For the solar pond, bismuth telluride was selected as the thermoelectric material to cover the net range 80°C to 25°C. However, it was deemed appropriate to utilize properties somewhat enhanced over those normally used. Factors of 1.27 and 1.22 were applied to the Seebeck coefficient for the P and N material, respectively. This gave an average combined Z of 3.50×10^{-3}, defined as

$$Z_{\text{average}} = \left(\frac{\alpha_P - \alpha_N}{\sqrt{K_P \rho_P} + \sqrt{K_N \rho_N}} \right)^2$$

Values of Z in excess of 3.5×10^{-3} have been observed in some laboratory tests so that the extrapolation is not considered excessive. In addition, the contact resistance was taken as zero instead of the 10% used in cases 1 and 2. However, the bypass heat flow of 10% was retained.

For a 100-MW(e) plant, the following results were obtained:

5.26×10^9 P-legs BiTe 0.05 cm^2 x 0.2 cm long

5.26×10^9 N-lege BiTe 0.07 cm^2 x 0.2 cm long

Total of 2.311×10^6 lb of BiTe or
$1.927m at $0.834/lb
Efficiency = 2.721%

The above costs correspond to $19.3/kW(e), which is remarkably low. The thermoelectric elements are very small and the power density is high in order to achieve this low a capital cost. Since the solar pond is taken to have hot and cold temperatures of 85°C and 20°C, respectively, it is not clear that the assumed inlet and outlet ΔT of 5°C will be sufficient to transfer the heat from the fluid to the thermoelectric elements and vice versa. This can be better assessed by a systems study that optimizes overall $/kW(e) and accounts for pumping power, determines the outlet water temperature on hot and cold sides, and recognizes the degradation in efficiency as the ΔT between fluid and element increases. It should also be noted that the heat flux on the thermoelectric elements is $5.82 W/cm^2$ or a solar concentration of 61.

A computation was perfomed for a 2-MW(e) plant to establish a goal for permissible collector costs. A target cost of $2000/kW(e) was assumed for this small plant operating in a distributed mode, i.e., not burdened by distribution costs from a centralized plant. The TEGs will require electrical conditioning equipment, which is scaled from the 20-MW(e) cost of $1314 thousand for such equipment:

$$\frac{1314}{2000} \times \left(\frac{2}{20}\right)^{0.7} = \$131/kW.$$

The TEG cost including electrical conditioning is (19 + 131) = $150/kW(e). It is clear that the cost of the electrical conditioning equipment is high enough to motivate a more direct use of the TEG dc electric output.

The permissible collector cost, assuming other plant costs to be

minor, is then calculated from

$$\frac{(2000 - 150) \times 0.950 \times 0.02721 \times 0.4}{10.76} = \$1.78/\text{sqft.}$$

where 0.950/10.76 = solar flux in kW/ft^2,

0.02721 = system power conversion efficiency,

0.4 = assumed light-to-heat collection efficiency.

In other words, the efficiency of the thermoelectric units and their capital cost should be compatible. For application to a solar pond, the critical factors in this computation are clearly the light-to-heat collection efficiency of the pond and the conversion efficiency of the TEGs.

7. TECHNOLOGY ADVANCES

7.1 INTRODUCTION

In the late 1950s and early 1960s it was anticipated that large gains would be made in improving the basic thermoelectric properties and in fabricating thermoelectric materials into useful hardware. The gains made thus far have been smaller than initially projected and have been mostly in the design and fabrication of operating hardware for high-reliability applications.

Since the early 1960s, when fundamental thermoelectric alloy development was at its maximum, considerable solid-state theory has developed. It is expected that much of this theory can be used to conceive new alloys, increase system efficiencies, and improve the basic thermoelectric material parameters.

7.2 ULTRAFINE GRAIN MATERIAL

One approach for improving the figure of merit is to reduce the lattice thermal conductivity K_L. Indeed it has been reduced through solid-solution alloying, which is discussed below. Another approach to reducing K_L is to take advantage of grain boundary scattering of phonons. This method of K_L reduction was analyzed by Goldsmid and Penn (Ref. 10), and their results, shown in Fig. 13, indicate that significant improvements can be obtained. The single-hatched area in the figure represents the reduction in thermal conductivity due to point-imperfection scattering. The double-hatched area indicates the reduction due to boundary scattering. Confirmation of this theoretical anaylsis with experimental data on a one-for-one basis has not been performed; however, it is known that the $(Bi,Sb)_2(Se,Te)_3$ alloys presently in use at GA are lower in K/Total than the conventionally used Bridgman cast alloys. Thus, there is some indication that the approach is valid.

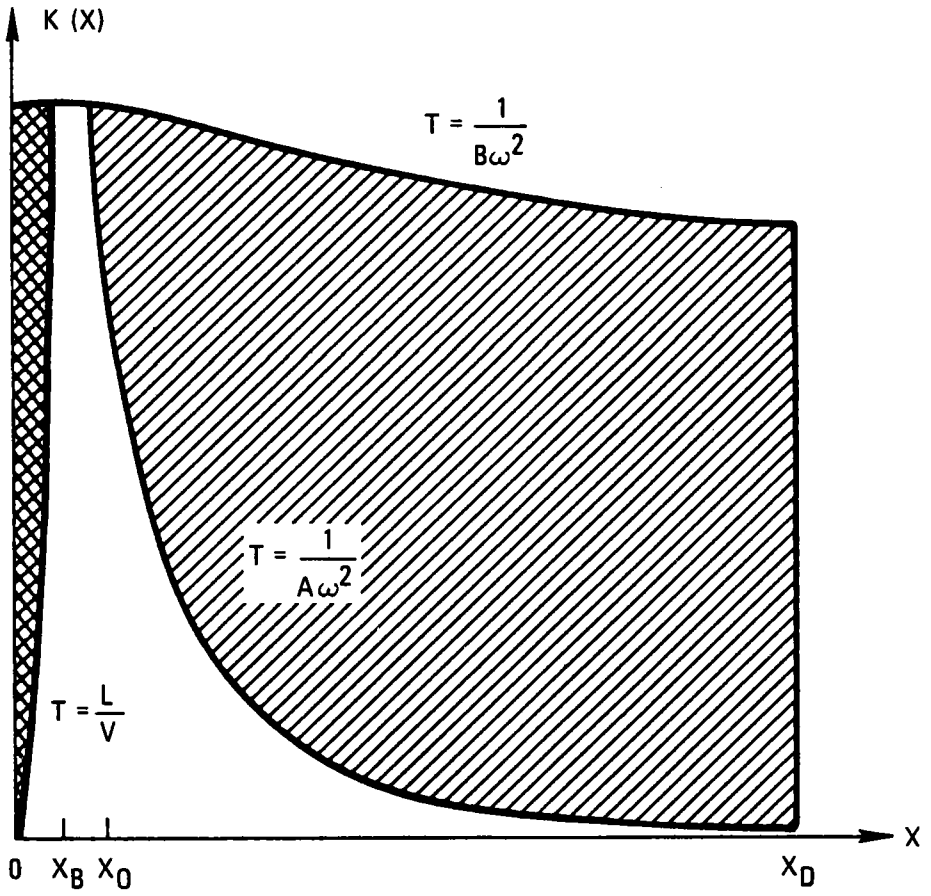

The single-hatched area represents the reduction in thermal conductivity due to point-imperfection scattering. The double-hatched area indicates the reduction due to boundary scattering.

Fig. 13. Schematic plot of thermal conductivity against reduced phonon frequency

In addition to $(Bi,Sb)_2(Se,Te)_3$ alloys, the ultrafine grain material approach is applicable to other alloys and no doubt is being pursued by many investigators. General Atomic, under DOE funding (FY-1978 and 1979), has made some gains. This approach to fabrication of thermoelectric materials can probably also enhance the materials mechanical properties since grain size and strength are inversely proportional. The drawbacks to fabricating ultrafine material are that it is more expensive, the increased surface area increases the potential for more contamination, and the fabricating temperatures must be rigidly controlled to avoid grain growth.

7.3 SOLID SOLUTION ALLOYING

Alloying of compounds/elements that are isomorphic with one another has been used extensively to improve thermoelectric properties, predominately with K_L (lattice). The most impressive development in this area was the alloying of elemental Si and Ge.

Gains can probably be made in adding small amounts of compounds/elements to existing alloys. In this approach, the additives have limited solubility and cause large strains in the lattice. Prior work with GeTe additions to PbTe, and As_2Te_3 additions to $(Bi,Sb)_2(Se,Te)_3$ alloys, indicates that this approach has promise.

7.4 NEW ALLOYS

The rare earth chalcogenides appear to show promise by the development of Gd_2Se_3 (by 3M) and Ce_2S_3 (by GA). Both of these alloys are capable of high-temperature operation ($\geq$ 1100°C and can probably be alloyed with other compounds to enhance their thermoelectric properties.

The $FeSi_2$ and $CoSi_2$ alloys are made up of inexpensive materials

and can be manufactured easily. Further alloy development or modification with these materials could provide a breakthrough in very low cost fabrication technology.

The Brewer-Engels theories of alloying have shown some success in predicting alloy behavior, and perhaps some of this theory can be applied in designing more efficient thermoelectric compounds.

7.5 AMORPHOUS ALLOYS

The electronics materials industry was surprised by the discovery and behavior of amorphous Si. It is probable that amorphous alloys will play a major role in thermoelectricity. Amorphous alloys would no doubt have a much lower K_L regardless of what happens to the electronic properties. The arguments presented in Section 7.2 are probably applicable to these materials. As the amorphous materials are studied and understood, it seems logical that this basic knowledge will be beneficial in formulating new thermoelectric compounds.

7.6 RADIATION PROCESSING

Thermoelectric alloys could possibly be improved through selected radiation damage. A very small amount of effort was directed toward this goal in the early 1960s, but the results were inconclusive. The extensive basic knowledge developed in the past 15 years should help determine whether some form of radiation processing can contribute useful properties.

7.7 CASCADING OR SEGMENTING OF THERMOELECTRIC MATERIALS

Cascading or segmenting of one or more thermoelectric materials over a broad range of temperatures was proposed in the late 1950s, but little effort has been directed toward the engineering and fabrication development of operating hardware. Conceptual design studies

show that efficiencies ranging up to 15 to 20% can be obtained with materials that exist today. Technology programs are required to develop these concepts into useful hardware.

Work was initiated by GA in 1977 in cascading $(Bi,Sb)_2(Se,Te)_3$ alloys with N-type PbTe and P-type $(Cu,Ag)_2Se$, and demonstration modules should be operating in 1979. Material efficiencies up to 13% (with system efficiency of 11%) are expected, and no doubt higher efficiencies can be obtained if other thermoelectric alloys are considered.

8. CONCLUSIONS/RECOMMENDATIONS

In assessing the applicability of thermoelectric systems to solar energy supplies, it is clear that the choice of model has a significant impact on the conclusions. Three representative systems (models) have been studied in a short period of time, and the conclusions below are drawn from the data generated. General Atomic is confident that changed raw material production processes and automation of TEG fabrication and assembly can lead to such drastic reductions in thermoelectric unit costs that the units are primarily material cost limited. Costs well under $100/kW(e) can be achieved, so that the TEG efficiency and not cost is the key factor in assessing its application.

The topping cycle application for a large, central solar power plant does not take advantage of the TEG characteristics of low operational and maintenance costs that arise from the absence of dynamic components. This suggests that smaller plants be considered, but because bottoming cycle power conversion efficiency declines and unit capital cost increases as plant size is reduced, the incentive for a thermoelectric topping cycle is increased but to a much lesser extent than would otherwise be expected. The incentive for a topping cycle is increased when the solar heat is used mostly for process heat and electrical generation is incidental to that end use. A 6% cost advantage is seen for a 22-MW(t) process heat plant. In that plant, the electricity is produced only when the process is operational. Such use is more consistent with a stand-alone plant, where electricity is consumed locally and the plant size cannot justify the operational and maintenance staff needed by mechanical power conversion equipment.

The process heat plant studied also employed thermoelectrics as an intermediate power conversion system in which the rejected heat was used in an industrial heat application. The tie between locally

produced and consumed electricity and heat was fully met by such an application. However, the economic case for this application rests largely on justifying the solar plant. Present fossil fuel costs still show lower end costs. More definitive conclusions on this process heat application must be drawn from a detailed study on a specific situation where factors considered are life cycle costs*, environmental effects, fossil fuel availability, etc.

An extension of the solar process heat system model to lower powers and to space heating and air conditioning is expected to show more favorable technical and economic promise for thermoelectrics. The solar process avoids expensive mechanical power conversion equipment of lower efficiency; it provides for locally produced and consumed electricity with minimal operating and maintenance costs. Moreover, the lower rejection temperature permits higher thermoelectric efficiencies and hence greater electric credits. It is recommended that this application be examined in follow-on studies.

The study of a solar pond was conducted to assess the possibility of fabricating inexpensive thermoelectric elements to yield a system with sufficient efficiency. The results appeared favorable provided that low collector costs can be achieved for the solar pond application, and subject to achieveing modest advances in thermoelectric performance (bismuth telluride) and obtaining small ΔTs on the input and output sides of TEG. This favorable conclusion suggests that thermoelectrics for ocean thermal gradient application be explored.

The recommendations for future work listed below are separated into three categories: (1) system analysis, (2) materials and fabrication, and (3) other applications.

---

*Allowing for solar component lifetime and tax incentives

8.1 SYSTEMS ANALYSIS (FUTURE WORK)

Recommended topics for systems analysis are:

1. Determine the collection efficiency of a solar pond.
2. Determine the cost of solar collectors for a solar pond application.
3. Prepare a conceptual design of a thermoelectric generator for a solar pond application with enough mechanical and flow detail to determine temperature drops, TEG efficiency pumping power, heat exchanger area size, and estimated cost.
4. Determine the topping cycle efficiencies achievable with thermoelectrics having properties improved over present state-of-the-art, using less conservative assumptions and accounting for a range of heat rejection temperatures.

8.2 MATERIALS AND FABRICATION (FUTURE WORK)

Recommendations for materials and fabrication studies include the following:

1. The $(Bi,Sb)_2(Se,Te)_3$ alloys are the most promising alloys for the solar pond and other low-temperature applications. The inexpensive fabrication techniques developed thus far should be studied to determine where these processes can be scaled up or modified to take advantage of the large increases in production. The alloys themselves should be optimized for the exact temperatures over which they will operate so that maximum efficiency can be obtained. With respect to research and development, a basic program should be initiated to further enhance the properties of the alloys.
2. Further alloy development should be directed toward both low-temperature and high-temperature operation.

Typically, low-temperature alloys have exhibited the best figures of merit, and results of this study indicate that the lower temperature applications will have a higher payoff potential. The TAGS alloy, plus its major constituents GeTe and $AgSbTe_2$, are starting points for formulating new compositions. Recent work by the Russians with GeTe-InTe solid solutions indicates that further gains can be made with this family of alloys. High-temperature alloys that have been developed are relatively simple compounds and possibly the figure of merit could be increased through the avenues outlined in this report. The improvement in the quality of rare earth metals in the past 15 years may allow some previously investigated alloys to be studied in greater detail and allow other promising alloys to be developed. Such improved alloys are needed for a cost-effective topping cycle.

8.3 OTHER APPLICATIONS

These following recommendations for future work cover areas that are not addressed in this report but are suggested by the trends observed:

1. Perform a comparative study between thermoelectrics for ocean thermal gradient power conversion and ammonia Rankine cycle power conversion.
2. Perform a scoping study of a thermoelectric application in a total heat system of about 100-kW(e) output with an end use of space heating and cooling.
3. Determine the market needs and economics of small standby power sources in the range of 1 kW(e) to 10 kW(e) and compare the competitiveness of solar and thermoelectric systems using cascaded/segmented TEG techniques.

REFERENCES

1. Yim, W.M., E.V. Fitzke, and R.D. Rosi, "Thermoelectric Properties of Bi_2Te_3-Sb_2Te_3-$SbSe_3$ Pseudo-Ternary Alloys in the Temperature Range 77 to 300°K," Journal of Materials Science, 1966, p. 52-65.
2. "Line Focus Solar Central Power Systems," (Strawman power tower concept, p.46) DOE RFP No. Et-78-R-03-2073, July 31, 1978.
3. Russell, J.L., Jr., et al, "Preliminary System Analysis of a Fixed Mirror Solar Power Central Station," General Atomic Company Report GA-A13974, EPRI Report ER-434, June 1977.
4. Eggers, G.H., et al, "Solar Collector Field Subsystem Program on the Fixed Mirror Solar Concentrator," Final Report for the Period March 28, 1976 through September 30, 1976, General Atomic Company Report GA-A14209, December 31, 1976.
5. Addendum No. 1 to DOE RFP No. EM-78-R-03-1882, "Solar Production of Process Steam Ranging in Temperature from 300°F to 550°F," April 15, 1978.
6. Hampl Interim Report, 3M Company, Contract E(11-1)-233.
7. Pisharody, R.K., and L.P. Garvey, "Modified Silicon-Germanium Alloys with Improved Performance," Proceedings of the 13th Intersociety Energy Conversion Engineering Conference, August 20 to 25, 1978, San Diego, p. 1963.
8. Haiser, B., T. Christenbury, F. Russo, J. McGrew, "Thermoelectric Generator Design Manual," National Aeronautics and Space Administration Report NASA-CR-109637, Teledyne Systems Corporation Report INDO-7089-1, February 20, 1070.
9. Barnett, F.M., J.J. Clawson, and K.C. Vyas, "Medium Btu Gas Fits Refiners Needs," Hydrocarbon Processing, June 1978, p.131.
10. Goldsmid, H.J., and A.W. Penn, "Boundary Scattering of Phonons in Solid Solutions," Journal of Applied Physics, 1968, p.253

GENERAL ATOMIC COMPANY
P. O. BOX 81608
SAN DIEGO, CALIFORNIA 92138

APPENDIX I-C

SYSTEM ANALYSIS AND COSTS PROJECTIONS FOR SOLAR THERMOELECTRIC DEVICES

SYNCAL CORPORATION
430 Persian Drive
Sunnyvale, California 94086

SYSTEM ANALYSIS AND COSTS PROJECTIONS

FOR SOLAR THERMOELECTRIC DEVICES

15 September 1978

Prepared For
Solar Energy Research Institute
Golden, Colorado

Prepared By
Syncal Corporation
Sunnyvale, California

TABLE OF CONTENTS

SYSTEM ANALYSIS AND COSTS PROJECTIONS FOR SOLAR THERMOELECTRIC DEVICES

I. INTRODUCTION

This report summarizes the work performed on a study to assess the economic advisability of using thermoelectric energy conversion in the obtainment of large scale electrical power from solar radiation impinging on the Earth. Although the study summarized by this report has been, of necessity, limited in scope and time, it has considered most areas of importance in the performance of a meaningful economic assessment of solar thermoelectric energy conversion for large scale power. The report gives a brief historical description of the use of incident solar heat in the thermoelectric conversion to electricity. It provides a description of the current state-of-the-art of thermoelectric technology in general and goes into some detail in areas of this technology that appear to be applicable to solar thermoelectrics. The reliability aspects of state-of-the-art thermoelectric generator technology is briefly considered for the technologies considered most appropriate for Solar Thermoelectric Generators (STGs). In connection with this, some consideration is given to the effect of reliability on thermoelectric generator costs. Based on the survey of state-of-the-art thermoelectric generator technology, two separate technologies have been considered for economic analysis in terms of the cost of electricity as a function of the quantity of electricity produced. These two technologies represent a low temperature technology and a high temperature technology and they have been utilized in the development of detailed thermoelectric generator designs that use incident solar heat for the obtainmnet of electricity. The STG cost projections primarily concern themselves with costs associated with the thermoelectric generator portion of the STG and do not in detail consider the costs of associated hardware, such as hot and cold side heat exchangers required in the obtainment of input heat and the rejection of waste heat from the STG.

The cost projections for the thermoelectric generators do, however, include the costs of materials, fabrication and equipment needed in the manufacture of the generators. Finally, the effect of advances in thermoelectric energy material and generator technology are considered from the standpoint of the effect of such advances on the cost of electricity produced by STGs.

II. HISTORICAL BACKGROUND

Although the history of thermoelectric energy conversion has a background that dates from 1821 when Seebeck observed that materials subjected to a temperature gradient produce a voltage, practical utilization of thermoelectricity is relatively recent. The first 50 years or so after the discovery of the Seebeck effect were primarily devoted to the formulation of the theory of thermoelectricity, based partly on experimental and partly on theoretical considerations. The former consideration included the additional discovery of the so-called Peltier effect that actually forms the cornerstone of thermoelectric energy conversion. The latter considerations resulted in the prediction of an additional thermoelectric effect, the so-called Thomson effect that was subsequently confirmed by experiment. Aside from the basic work performed during this time, there was practically no utilization of thermoelectricity in applications of any type. It was towards the end of the nineteenth century that thermoelectricity started to be used in thermometry in the form of metallic thermocouples. Very little effort was devoted to the obtainment of electrical power by means of thermoelectricity until after the end of the nineteenth century. This was due to two primary reasons. First, the detailed theory of thermoelectric power conversion was not developed until 1910 when Altenkirch established that materials possessing high values of Seebeck coefficient and electrical conductivity and low values of thermal conductivity are those best suited for the practical utilization of thermoelectricity. Even though Altenkirch showed this to be the case on the basis of theoretical considerations,

the reduction of the theory to practice did not occur because materials possessing such characteristics were not generally known at that time. In fact, it was much later that practical thermoelectric devices were actively fabricated and became utilized in practical applications. It was the advent of the transistor and the associated development of semiconductors that finally enabled the discovery of materials that enabled the fabrication of thermoelectric devices with conversion efficiencies of interest in specialized applications. For this reason, the practical utilization of thermoelectricity did not start until the early 1950's. Since that time, however, the field has made rapid progress and now a variety of materials exist that enable the obtainment of practical amounts of electricity from a variety of sources of heat. Over the past several decades, thermoelectric power conversion devices have become utilized in numerous applications, such as those for powering spacecraft, implantable biomedical devices and various communications related terrestrial uses.

Although thermoelectric devices are being used in conjunction with a wide spectrum of heat sources, except for theoretical and rather limited experimental efforts, such heat sources have generally not included the direct incident heat of the sun, either in terrestrial or space applications. The primary reason for this is that the incident solar flux at the distance of the Earth from the sun is quite low and when coupled with the fairly low conversion efficiency of most thermoelectric devices, it has been assumed that the cost of the electricity thus obtained is high as compared to other forms of energy conversion. Although this has been generally true in the past, it may not be true if one reconsiders the use of solar thermoelectric energy conversion in view of the present state-of-the-art technologies and projects the levels of power thus obtained to extremely high values; it is especially this last consideration that has not been emphasized in the past and forms the basic reason for the study described in this report.

The use of solar thermoelectric power generation goes back to at least 1922 when Coblentz described a solar thermoelectric generator. This generator, of course, did not possess especially attractive performance because of the unavailability of good thermoelectric materials at that time. Not much work on solar thermoelectric generators was performed after that until the advent of semiconductors. In the early 1950's, Maria Telkes devoted considerable effort to a reassessment of the use of STGs. Inasmuch as most of the state-of-the-art thermoelectric materials had not been developed at that time, Telkes concluded in 1953 that conversion efficiencies of only of the order of three percent are possible. Such low values of conversion efficiency did not justify the exploitation of this form of energy conversion and as a consequence the use of STGs remained dormant until the 1960's. By that time, many new thermoelectric materials and associated technologies had been developed that warranted a new look at the field. Inasmuch as most of the new considerations of STGs restricted themselves to limited levels of power in specialized applications, it was generally still concluded that STGs are not especially suitable when compared to other ways of obtaining electrical power, even in specialized applications. It was towards the end of the 1960's and 1970's that specialized fabrication techniques were developed for thermoelectric devices for the large scale manufacture of such devices. Most of these devices, however, were intended for use with sources of heat other than incident solar radiation. In fact, except for a few studies performed during this time and related studies pertaining to the use of solar thermoelectric power generation in near-sun missions in space, relatively little attention has been paid to the practical large scale utilization of STGs for the obtainment of very large amounts of electrical power. In fact, it is the present study that probably represents the most comprehensive consideration of this form of energy conversion within the recent past. As already mentioned, the difference between this study and those performed in the past is the present day availability of a considerably broader spectrum of state-of-the-art thermo-

electric materials and associated technologies and the fact that the present study addresses itself to the production of very large amounts of electrical power.

Past studies of the use of solar thermoelectric power generation have in some cases addressed themselves to the economics of this form of energy conversion. Usually, however, in all cases it has been assumed that fairly small quantities of electrical power are to be generated. Namely, most such studies have been aimed at determining the cost of specific STGs in a fairly low power output range. For example, Katz described the details of construction of an STG and estimated the cost of a 125 watt generator in terms of the electricity produced by the generator. He estimated that the cost per kilowatt-hour of electricity produced by the generator is of the order of seven to ten cents. Although these cost figures appear to be quite low, it must be remembered that the cost represents the value of the dollar in 1961. Based on todays costs, the corresponding cost figures would very likely be of the order of two times greater. It is believed that at such costs, solar thermoelectric energy conversion would not be competitive with more conventional forms of obtaining electrical power. It is for this reason that the present study is especially interesting. It gives a more realistic basis for the advisability of large scale use of solar thermoelectric energy conversion.

III. STATE-OF-THE-ART OF THERMOELECTRIC ENERGY CONVERSION

Presently, the most widely used thermoelectric power generation materials are bismuth telluride, lead telluride, the selenides and silicon-germanium alloys. Each material has its own range of useful operating temperatures and the figure-of-merit of each differs considerably. Bismuth telluride is used in thermoelectric cooling as well as in power generation. In power generation its useful range of operating temperatures covers from room temperature to about 250 to 300°C. Lead telluride is commonly used in power generators at temperatures between room temperature and some 600°C. The selenides are commonly used between 150

and 850°C; a phase transformation in the p-type material at 150°C renders its use at lower temperatures impractical. The useful range of operating temperatures of silicon-germanium alloys extends from room temperature to about 1000°C. The relative values and temperature dependencies of the figures-of-merit of the four materials are shown in Figure 1. It is noted from Figure 1 that bismuth telluride possesses the highest figure-of-merit of any of the four materials. The selenides, lead telluride and silicon-germanium alloys have lower values of figure-of-merit. As stated, the extent of the range of useful operating temperatures is, however, different for the different materials. Because the conversion efficiency of a thermocouple can be approximated by $\eta=(1/4)\not{Z}\Delta T$, it is apparent that the extent of the useful range of operating temperatures is as important to the performance of a thermocouple as is the figure-of-merit of its thermoelectric material. It is thus found that the performance available from power generators using the four thermoelectric materials is not unduly different. In fact, it is generally found that generators that use the selenides and silicon-germanium alloys are capable of somewhat greater performance than those that use either bismuth telluride or lead telluride. Lead telluride, in turn, affords somewhat better performance than bismuth telluride. It should be recognized, however, that the higher performance available with the higher temperature materials can be realized only at relatively high thermopile hot side operating temperatures; the higher performance is therefore obtained at the expense of potentially more serious material problems as well as higher heat losses associated with a device.

The four commonly used thermoelectric materials not only differ in their ranges of useful operating temperatures and their figures-of-merit, but also in many other characteristics that are important to the construction and operation of practical thermoelectric power generators. Bismuth telluride and lead telluride are susceptible to poisoning by oxygen and by many other materials. Power generators that use bismuth telluride and lead telluride must therefore be evacuated and sealed

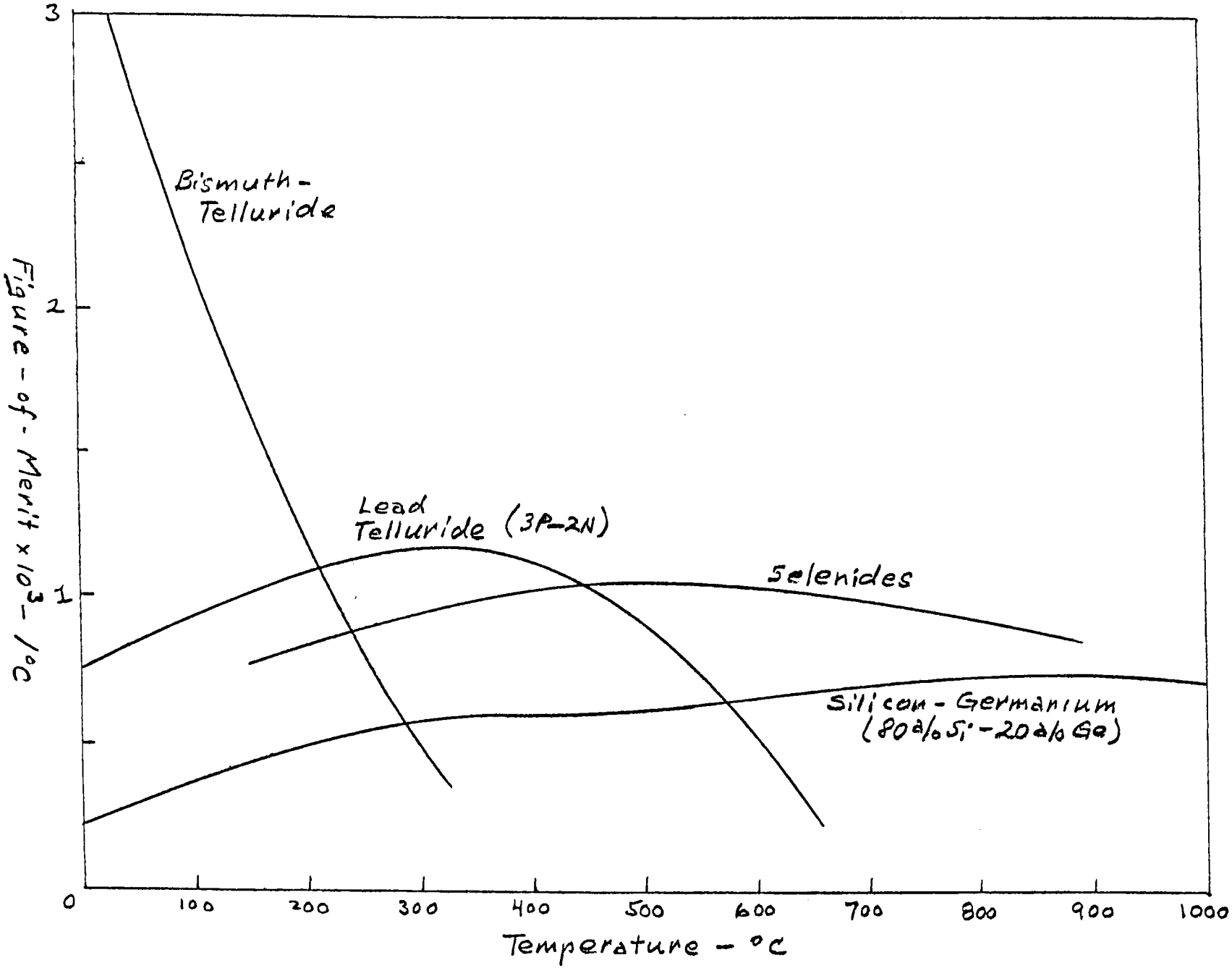
Bismuth-
Telluride
Lead
Telluride (3P–2N)
Selenides
Silicon - Germanium
(80 a/o Si - 20 a/o Ge)
Figure - of - Merit x 10³ - /°C
Temperature - °C
0
1
2
3
100
200
300
400
500
600
700
800
900
1000

Figure 1

if it is intended to operate them at temperatures higher than about 200°C and great care must be taken in the selection of contact and other materials used inside the generators. In addition to being sealed, thermoelectric generators that use tellurides and operate at high temperatures are generally back-filled with an inert gas in order to minimize sublimation of the thermoelectric material. Silicon-germanium alloys, on the other hand, are quite insensitive to their operating environment. Oxygen has no effect on the properties of silicon-germanium alloys and generators using this material therefore do not have to be sealed. Operation under a positive inert atmosphere is also not necessary because silicon-germanium generators are generally not designed for operation at temperatures at which sublimation presents a problem. The selenides are extremely susceptible to oxygen poisoning and therefore must always be operated either under vacuum or an inert atmosphere. The density of silicon-germanium alloys is of the order of 3.0 to 3.5 gms/cc. The densities of the two tellurides are about 2.5 times higher. The selenides also have a higher density. Silicon-germanium alloys and the selenides possess a linear thermal expansion coefficient of the order of 4 to 5 x 10^{-6}/°C; the corresponding values for lead and bismuth telluride are about 18 x 10^{-6}/°C. Silicon-germanium alloys and the selenides possess a tensile strength of some 3 to 5,000 psi. The tensile strength of lead telluride and bismuth telluride is less than 2,000 psi. Similarly, the compressive strength of silicon-germanium alloys and the selenides is considerably higher than that of the two tellurides.

The choice of contact electrodes and/or contacting methods for the four thermoelectric materials is quite different. It is obvious that the highest performance contacts between thermoelements and their end-electrodes are those that make use of metallurgical bonding. It has been found, however, that metallurgical bonding is generally possible only for relatively restricted operating conditions. The reaction that forms the basis of the metallurgical bond continues during thermocouple operation and bond life is therefore dependent on operating temperatures.

In metallurgically bonded systems, therefore, the design hot side operating temperature is usually determined by the intended life of the generator. Considerations such as relative linear thermal expansion and chemical compatibility also enter the selection of contact electrode materials for the various thermoelectric materials. On this basis it has been found that tungsten and silicon as well as certain silicon alloys are excellent electrode materials for silicon-germanium alloy thermoelements, although the useful life of a tungsten/silicon-germanium bond becomes very short, less than a few thousand hours, at temperatures of 600°C and higher. Silicon and silicon alloy electrode systems as well as electrode systems in which graphite is used as a diffusion barrier between the silicon-germanium alloy thermoelements and tungsten have a much higher temperature capability for most normal operating times. The former-type electrode systems possess useful operating lives in excess of ten years at a silicon-germanium thermocouple hot junction temperature of 1000°C.

The selenides are commonly either not metallurgically contacted at the ends of the thermoelements at all or are only contacted at the cold end. Selenide thermocouples are therefore essentially pressure loaded to contact electrodes. Although in some applications this form of contacting may be adequate, such as in the case of a centrally located radioisotope heat source, the pressure contacts do result in decreased device reliability and in the case of solar thermoelectric devices, in extraneous heat losses associated with the spring loading mechanism; obviously in solar thermoelectric applications the individual thermocouples of a generator are not pressure loaded against the heat source and therefore the hot and cold sides of the generator structure must be interconnected by components other than the thermoelectric material.

The common contacting material used in metallurgically bonded lead telluride thermocouples is iron. Iron has a linear thermal expansion coefficient that very closely matches that of lead telluride. At elevated temperatures and under conditions of long-term operation some iron, however, diffuses into the lead

telluride and in the case of the n-type material, results in a deterioration of its thermoelectric properties. As a consequence, it is common to use a nickel diffusion barrier between n-type lead telluride and iron in a metallurgically bonded lead telluride thermocouple. Even with this electrode system, however, it is found that thermocouple hot side contacts do not exhibit very long life at temperatures in excess of some 530°C. A method used to solve the problem of bond deterioration at the hot sides of lead telluride thermocouples utilizes the concept of mechanical contacts rather than metallurgical ones; another method restricts the operation of metallurgically bonded lead telluride thermocouples to hot side operating temperatures of some 500°C or less. Occasional use is made of both methods to enhance the reliability of a lead telluride generator, although at a somewhat penalized level of generator performance. Electrical and thermal losses across mechanical interfaces in lead telluride systems are usually minimized by using a spring at the cold side of each thermoelement; the spring affords sufficient pressure to enable intimate contact between the lead telluride thermoelements and contact electrodes. Mechanically contacted lead telluride thermocouples sometimes use refractory metal electrodes because interaction between refractory metals and lead telluride is nearly non-existent at practically all temperatures used in the operation of lead telluride generators. The significant difference between the linear thermal expansion characteristics of lead telluride and most refractory metals is of little consequence at a mechanical interface.

The most common form of contacting of bismuth telluride thermocouples makes use of a solder that is capable of operation at the maximum permissible operating temperatures of bismuth telluride. The form of the contact between the solder and bismuth telluride thermoelements is primarily mechanical because the formation of the contact is not dependent on a reaction between bismuth telluride and the contacting material. In the case of bismuth telluride thermocouples, occasional use is also made of pressure loaded mechanical interfaces, much as in

the case of lead telluride devices. Spot welded contacts are sometimes also used, as are sputtered or plated contacts.

Considering the various so-called state-of-the-art thermoelectric materials and their associated technologies for solar thermoelectric applications, it is necessary to consider the applicability of each to such applications. It must be noted that each material and its associated technology is more applicable in use with certain types of heat sources than others. Inasmuch as the present study pertains to STGs in air operation, it is necessary to consider the ability of the various materials to operate in an air environment. It is recognized, of course, that it may be possible to fabricate STGs in which the material is hermetically sealed under an inert gas atmosphere or in vacuum. If it is possible, however, to eliminate the need for such sealing, considerable cost savings may be projected for obvious reasons. Of the four so-called state-of-the-art thermoelectric materials, all of them, except the selenides, are capable of some air operation. In the case of bismuth telluride and lead telluride, the maximum temperature of air operation is limited to about 200°C. At higher temperatures both materials are susceptible to poisoning by oxygen with a resultant degradation of thermoelectric properties. It is only the alloys of silicon and germanium that are capable of operating in air at all temperatures at which such alloys are used in practical power conversion applications. Therefore, it may be stated that the selenides and lead telluride should be hermetically sealed under an inert gas atmosphere or be sealed under vacuum if they are to be used in STGs intended for terrestrial use. Bismuth telluride and silicon-germanium alloys can be used in an air environment, although this applies to bismuth telluride only up to temperatures of the order of 200°C. It is partly for this reason that the present study has eliminated lead telluride and the selenides from any detailed consideration from use in practical STGs. Another reason for not considering these materials and their associated technologies is the inability of either material to be reliably metallurgically contacted at the hot sides. The hot side construction

of both makes use of a pressure contact that is normally maintained by means of a spring and piston arrangement at the cold end of each thermoelement. In addition to fabrication complexity and its associated costs, this type of construction is inherently not as reliable as one that makes use of metallurgical bonding of the contacts. Bismuth telluride and silicon-germanium alloy devices can both make use of metallurgically bonded thermoelements. It is thus those two materials and their associated technologies that have been considered in some detail for use in STGs in the present study. It must be emphasized, however, that each possesses its own useful range of operating temperatures. It will be recalled from above that bismuth telluride devices can only operate between ambient room temperature to about 250°C. Silicon-germanium alloys are capable of operation up to 1000°C. Of these two materials, silicon-germanium alloys are generally capable of producing higher values of conversion efficiency. In an STG application this means that the total amount of collector area is reduced for STGs using silicon-germanium alloys. Even though the figure-of-merit of bismuth telluride is considerably higher than that of silicon-germanium alloys, the greater useful operating temperature range enables the obtainment of higher values of conversion efficiency with the latter material. On the other hand, because in an STG heat losses form an integral part of generator design and have an obvious impact on its final performance, both materials will be subjected to a subsequent more detailed consideration; heat losses, of course, decrease significantly with decreasing operationg temperatures.

A characteristic of thermoelectric power conversion is that the voltage produced and conversion efficiency of a thermoelectric generator are theoretically independent of the ratio of the length to cross-sectional area of each thermoelement. This means that if it is desired to minimize the amount of thermoelectric material used in a generator, it is theoretically possible to minimize the size of the thermoelements to as small as manufacturing techniques permit. Although this phenomenon is true in theory, in practice it is found that such miniaturization is not only limited

by manufacturing techniques, but is also limited by the fact that the contacts between thermoelements and their end electrodes generally possess finite values of electrical resistance. This contact resistance in itself is obviously independent of thermoelement length and depends inversely on the cross-sectional area of the thermoelement. The effect of the contact resistance on generator performance, however, is not dependent on thermoelement area, but rather depends on its length. The reason for this is that the generator resistance has a dependence on both thermoelement area and length in such a way that the area dependence of generator resistance and contact resistance are the same and therefore variations in it affect both resistances identically; the ratio of the two resistances is therefore independent of thermoelement area. Inasmuch as thermoelement length only affects generator resistance, it does affect the ratio of the two resistances and therefore the performance available from the generator. This performance dependence on thermoelement length and contact resistance may be written as

$$P = P_o \frac{\ell(\rho/\rho_c)}{\ell(\rho/\rho_c)+2}$$

where P is the power output of the generator with contact resistance, P_o is the power output of the generator without contact resistance, ℓ is the length of the thermoelements, ρ is the electrical resistivity of the thermoelectric material and ρ_c is the effective electrical resistivity of the contacts. The reason that contact resistivity is called an effective resistivity is that it does not possess a length dependence and therefore is not a true resistivity. Contact resistivity, ρ_c, is defined as

$$\rho_c = AR_c$$

where A is the cross-sectional area of each thermoelement and R_c is the contact resistance of each thermoelement contact. The above relationships clearly

indicate the dependence of generator performance on contact resistance and thermoelement length and also show that performance is independent of thermoelement area. The relationships are illustrated in Figure 2.

In addition to the miniaturization of individual thermoelements within a thermoelectric generator being limited by finite values of contact resistance and manufacturing convenience, an additional limitation is the thermal insulation that generally surrounds the thermoelements. Inasmuch as most thermal insulations are pressed from fibers or powders, a limit exists as to how small such insulations can be made in practice. In the case of extremely small thermoelements, this means that the relative area of thermal insulation to that of the thermoelements is generally greater than it is in the case of large thermoelements. This means that thermal losses associated with the insulation are also greater. The consequence of this phenomenon is that the amount of solar heat collected by a collector must be greater, with a consequent increase in collector size.

Although it is not possible to give precise limits as to the degree of miniaturization possible with different thermoelectric materials, based on a combination of the factors that limit miniaturization it may be stated that in the case of bismuth telluride, the smallest practical thermoelements have a size of the order of 0.030 inch on the side. Considerably smaller bismuth telluride thermoelements have been made, but the yield of making very small thermoelements rapidly decreases below approximately 0.030 inch. In the case of silicon-germanium alloy thermoelements, considerably smaller dimensions are possible. In fact, thermoelements having side widths in the range of 0.001 to 0.002 inch and lengths of about 0.010 inch have been made reproducibly. Electrical contact resistivity values for both thermoelectric technologies also vary over a considerable range, primarily depending on the type of contact used. Typically, such contact resistivity values are approximately ten to 100 times smaller than the bulk resistivity of the thermoelectric material.

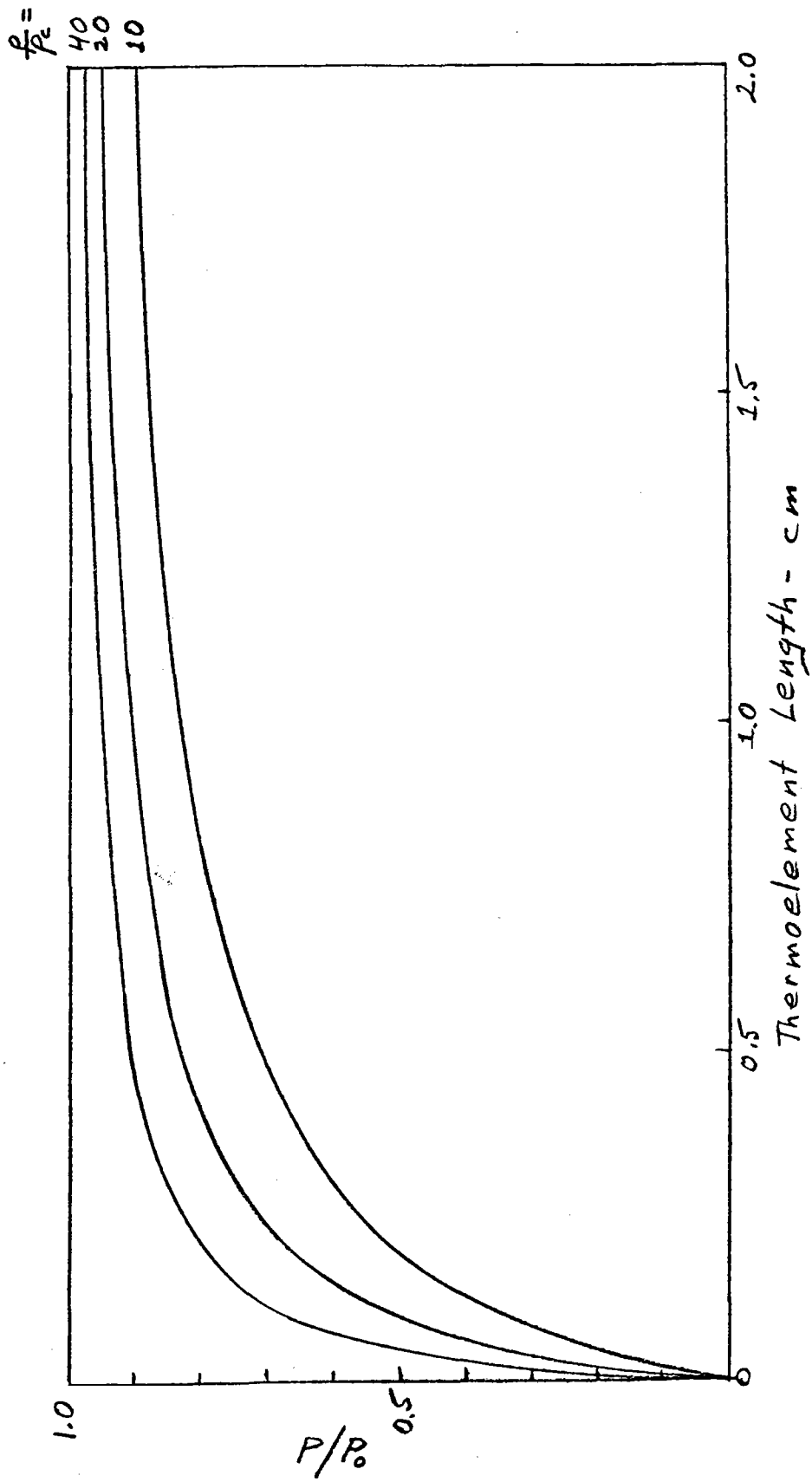

Figure 2

In addition to the four generally used thermoelectric materials that have been discussed above, a large variety of other materials exists, but these materials are not especially widely used because their performance characteristics are somewhat lower than those of the materials discussed. Although these other materials have not been subjected to detailed consideration in the present study, mention of them is made because many of these materials are considerably less exotic than the better known thermoelectric materials and as such the availability and cost of their constituents may be such that in extremely wide-spread use, they may be more economical than the better known materials. Mention might be made of various silicides, such as iron silicide, cobalt silicide, manganese silicide and chrome silicide, as falling into this category. Although not treated in detail in the present study, it is suggested that future studies on the subject may well look into the use of some of these materials in solar thermoelectric applications. For purposes of illustration, Figure 3 shows plots of figures-of-merit of some of these materials as a function of temperature.

As mentioned above, the present study addresses itself primarily to the use of bismuth telluride and silicon-germanium alloys in the conversion of solar heat to electricity. For sake of completeness, typical thermoelectric properties of these materials as a function of temperature are given in the appendix. It is noted that the thermoelectric properties of the silicon-germanium alloy are time dependent. This is due to an adjustment in the solid solubility of dopant within the material and reflects the varying dopant solubility as a function of temperature. Although the thermoelectric properties of the silicon-germanium alloy therefore change with time, this change is completely predictable and asymptotically approaches equilibrium values after long operating times.

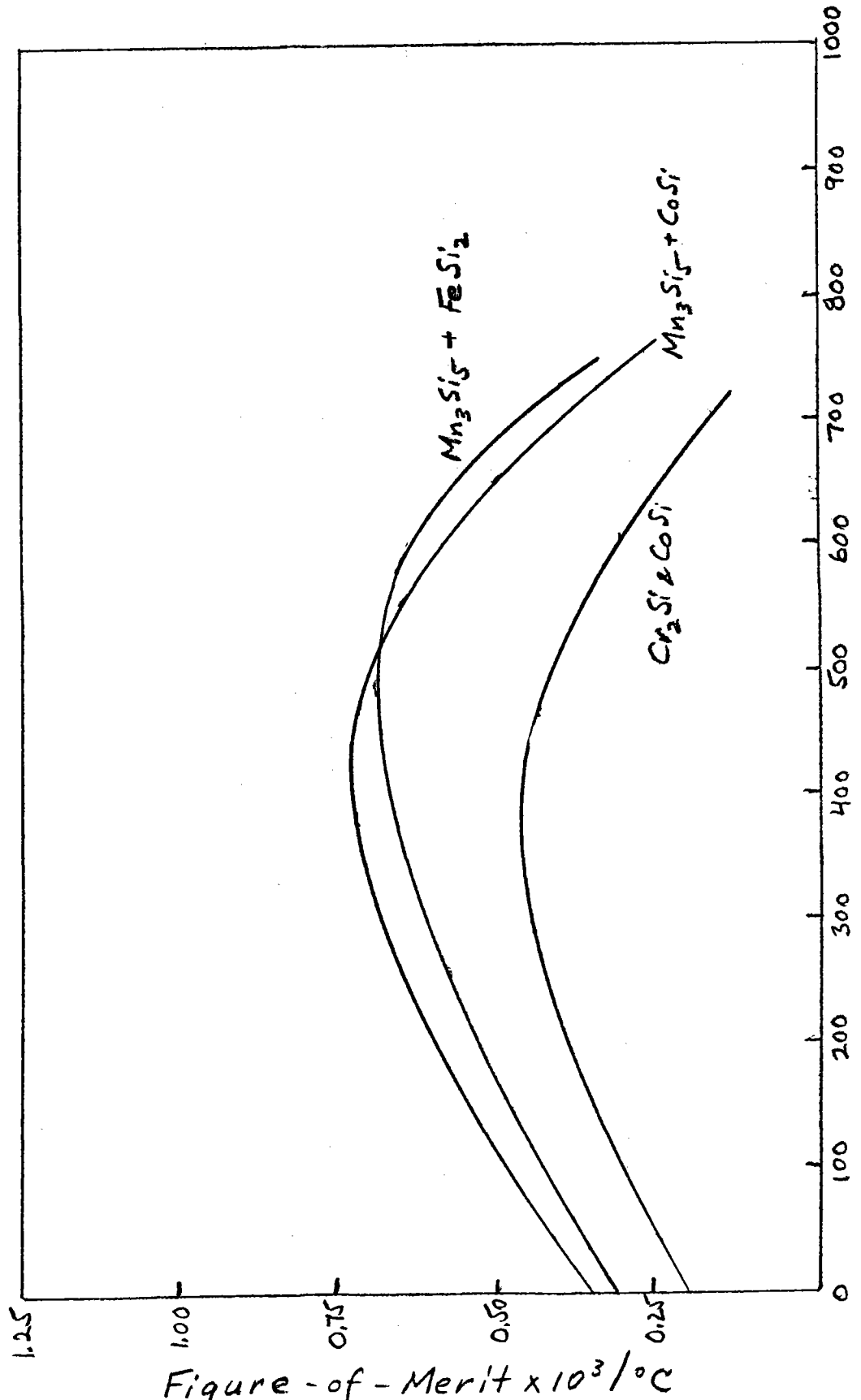
$Mn_3Si_5 + FeSi_2$
$Mn_3Si_5 + CoSi$
$Cr_2Si_2 \& CoSi$
Temperature - °C
0
100
200
300
400
500
600
700
800
900
1000
1.25
1.00
0.75
0.50
0.25
Figure - of - Merit x 10^3/°C

Figure 3

IV. STG DESIGN CONCEPTS

A variety of different design concepts exist for STGs. Although each of these design concepts differs from the others, they all have three basic features in common. Namely, they all possess a hot side heat exchanger that intercepts incident solar heat and transfers it to the rest of the device. They all have a thermopile that converts a portion of the heat transferred through the device to electricity. Finally, they all possess a cold side heat exchanger that rejects the waste heat from the device. In each of the three areas common to each thermoelectric generaor, it is possible to use a variety of different design approaches. For example, the hot side heat exchanger may consist of one of various different types of solar concentrators that intercept incident solar radiation at its very low values of flux and concentrate the flux to values required of any given thermoelectric generator. Usually the concentration ratio has to be fairly considerable because incident solar radiation on the surface of the Earth is quite low, being of the order of 0.05 to 0.10 watts/cm^2; the precise flux level generally depends on atmospheric conditions and the precise location on Earth, as well as on the time of day that the incident flux is determined. It should be noted that immediately outside the atmosphere, incident solar flux impinging upon the Earth is approximately 0.14 watts/cm^2. Considerable attenuation of flux therefore occurs in the passage of solar radiation through the atmosphere. Mention might be made of various different types of concentrators either used or contemplated for use in connection with STGs. Possibly the simplest type of concentration is obtained by means of a flat-plate collector that absorbs incident solar heat and transversely conducts it to the thermoelectric material. Although this type of concentration is not optimum, it has been used in experimental devices. Other types of concentrators make use of parabolic and conical mirrored surfaces that reflect and concentrate incident solar radiation to any desired flux level. Additionally, mention may be made of forms of concentration that make use of either Fresnel lens or Cassegrain reflectors. The precise

choice of concentrator in terrestrial solar applications in the end must be determined by its effect on the economics of this type of energy conversion and it is not a priori obvious which is the most advantageous type of concentrator. Inasmuch as the precise choice of concentrator is beyond the scope of the present study, it is suggested that a future detailed study be allocated for it. In the present study it is simply assumed that an appropriate form of concentration does exist for the obtainment of solar flux levels necessary for the operation of the various STGs considered in the study.

Just as it is possible to utilize a variety of different types of solar concentrators in the design of an STG, it is obviously possible to make use of a variety of thermoelectric materials and their associated technologies in the fabrication of the generator itself. Some of the better known thermoelectric materials and their associated technologies were discussed in the preceding section. It will be recalled that based on the discussions of the preceding section, it was concluded that bismuth telluride is probably the most obvious choice of material and technology for use in low temperature STGs. The most obvious choice of a high temperature material for use in such generators is the one based on silicon-germanium alloys. For this reason, subsequent discussions on solar thermoelectric designs address themselves to these materials and their associated technologies.

Just as varous possibilities exist for the hot side heat exchanger design and the choice of a thermoelectric material, a variety of possibilities also exist in the design of the cold side heat exchanger of an STG. Mention might be made of direct rejection of heat into the environment by means of a simple radiator which rejects heat by the combined effects of radiation and natural convection. It is also possible to use this design concept in connection with the forced convection of heat by means of a blower type system that forces air across the surface of the cold side heat exchanger. Additionally, it is possible to make use of various cooling fluids that circulate across the cold side heat exchanger and transport heat

away from the thermoelectric generator. Heat can also be rejected from the cold side heat exchanger by simple conduction if the cold side heat exchanger of an STG is placed in intimate contact with a massive heat sink, such as the ground on which the generator is located. Just as in the case of solar contrators and the hot side heat exchanger, the present study has not addressed itself in detail to the selection of a concept for the design of a cold side heat exchanger. It is suggested that detailed design considerations of a cold side heat exchanger be addressed in a subsequent study that culminates in a prototype STG design.

The overall configuration of an STG can assume various forms. The simplest such form is of a flat-plate type in which the hot and cold side heat exchangers consist of two parallel plates with appropriate absorptivity and emissivity coatings and in which a portion of the space between the two plates is occupied by the thermoelectric material in such a way that it is in intimate contact with each of the plates. Generally, the volume occupied by the thermoelectric material forms a small portion of the volume between the plates because of the necessity to obtain considerable concentration of the incident solar radiation. The volume between the two plates not occupied by the thermoelectric material is taken up by thermal insulation that minimizes the direct transfer of heat between the two plates. The thermoelectric material between the plates is generally distributed either in terms of single thermocouples or clusters of thermocouples in a uniform manner across the whole surface area of each plate. Distributing of the thermoelectric material in such a manner is more advantageous than locating all of it at the center of the two plates because of heat transfer considerations. This design concept is schematically illustrated in Figure 4.

Other STG design concepts make use of concentrators and may also assume various forms. For example, it is possible to use a single large concentrator which intensifies incident solar radiation and heats the hot side of a compact thermoelectric generator of a planar configuration that consists of multiple thermocouples.

Cross-Section of Flat-Plate STG Cell

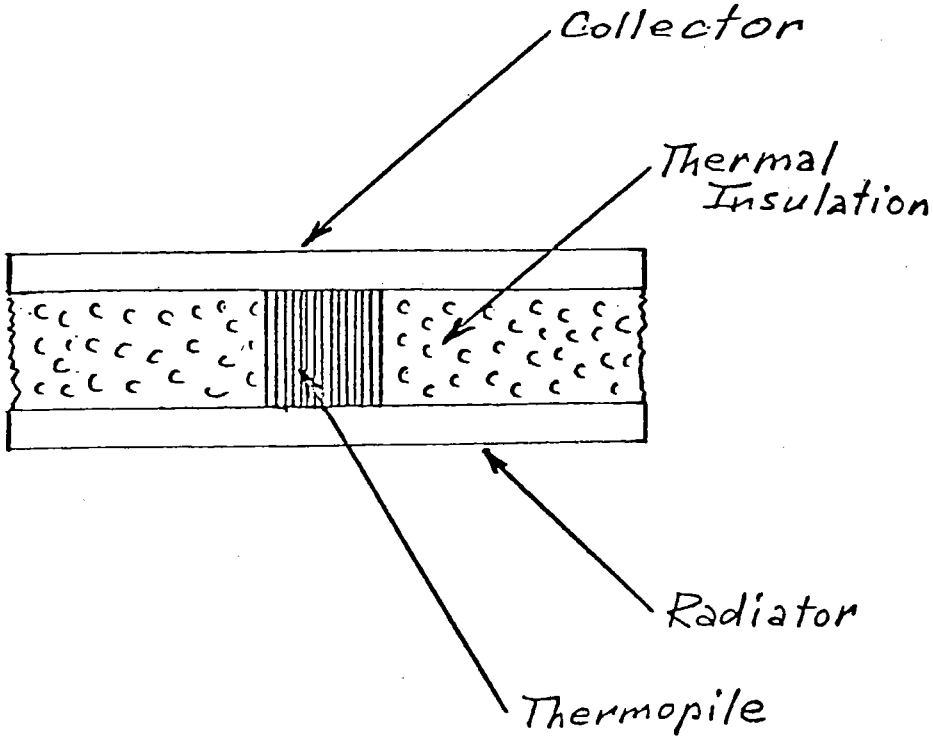

Figure 4

At its cold side, the thermoelectric generator is cooled by means of a cold side heat exchanger of any of the types discussed above. Such a solar thermoelectric generator is illustrated in Figure 5. For purposes of illustration, the generator depicted in Figure 5 makes use of a cold side heat exchanger that rejects heat by combined radiation and convection.

The flat-plate and the compact solar thermoelectric generator designs may be combined into a design that utilizes certain features of each. Namely, rather than using a single concentrator, it is possible to make use of a generator in which the thermoelectric material is distributed uniformly across the generator and heat collection is accomplished by means of multiple miniature concentrators. In this design concept, each concentrator with its associated thermoelectric material, either in the form of a single thermocouple or multiple thermocouples, forms a basic building block of the overall generator. This design concept is schematically illustrated in Figure 6. Again it should be noted that the type of cold side heat exchanger shown in the figure is only used for purposes of illustration and actual use may be made of any type of cold side heat exchanger discussed above. Moreover, this is also true of the concentrator; any type of concentrator may be used.

Finally, other types of STG design concepts are obviously also possible. For example, the thermoelectric material may be placed in a cylindrical configuration in which concentrated heat is transported to the material by means of a heat pipe and is rejected by any type of mechanism discussed above in connection with cold side heat exchangers. A typical design concept for a cylindrical STG is illustrated in Figure 7. Again, the choice of hot and cold side heat exchangers in the form of a conical concentrator and radiation fins has been used strictly for purposes of illustration.

Considering the various STG design concepts discussed in the preceding paragraphs, it may be analytically shown that the most advantageous concepts

Compact STG Concept

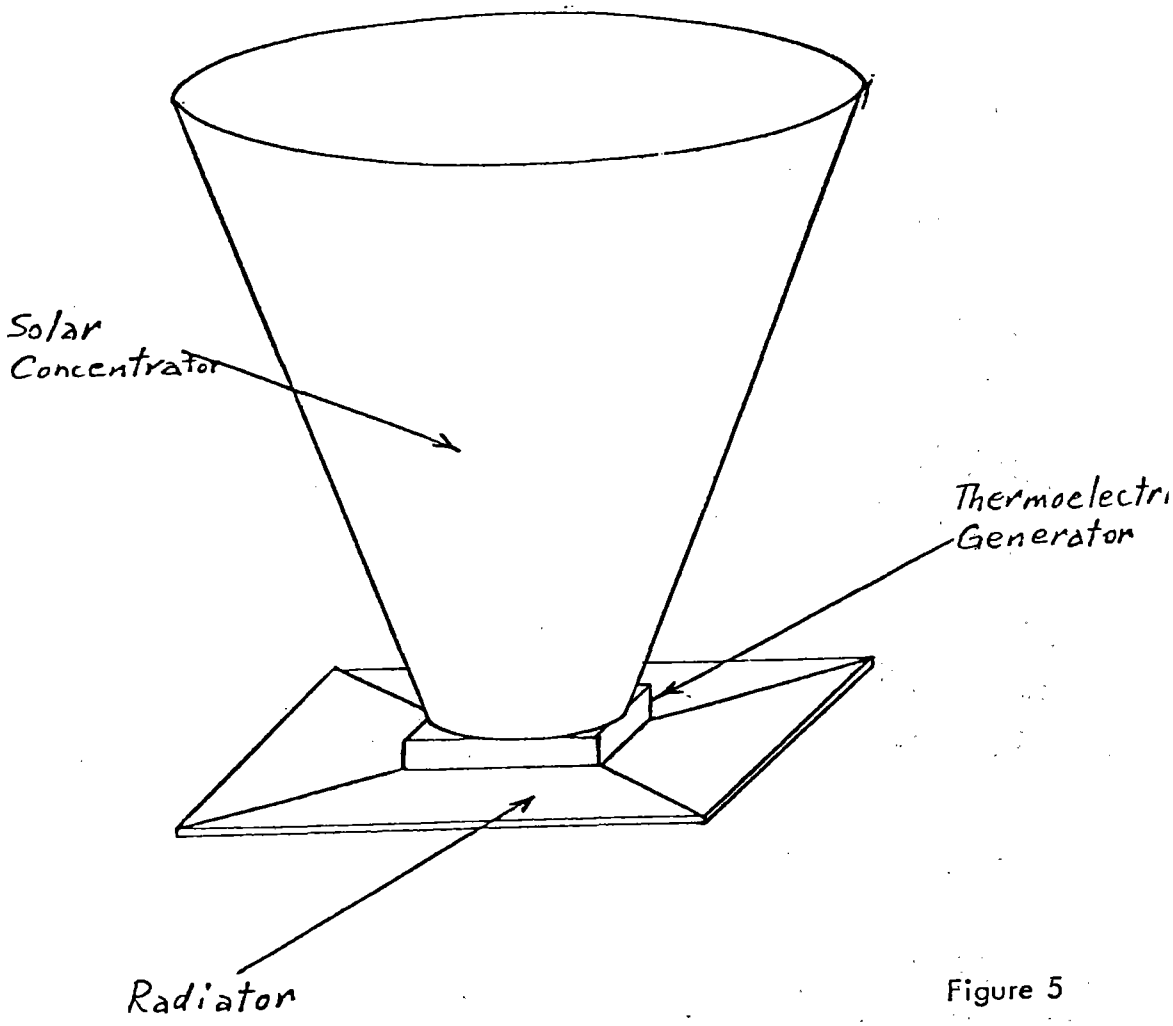

Figure 5

Distributed STG with Concentrators

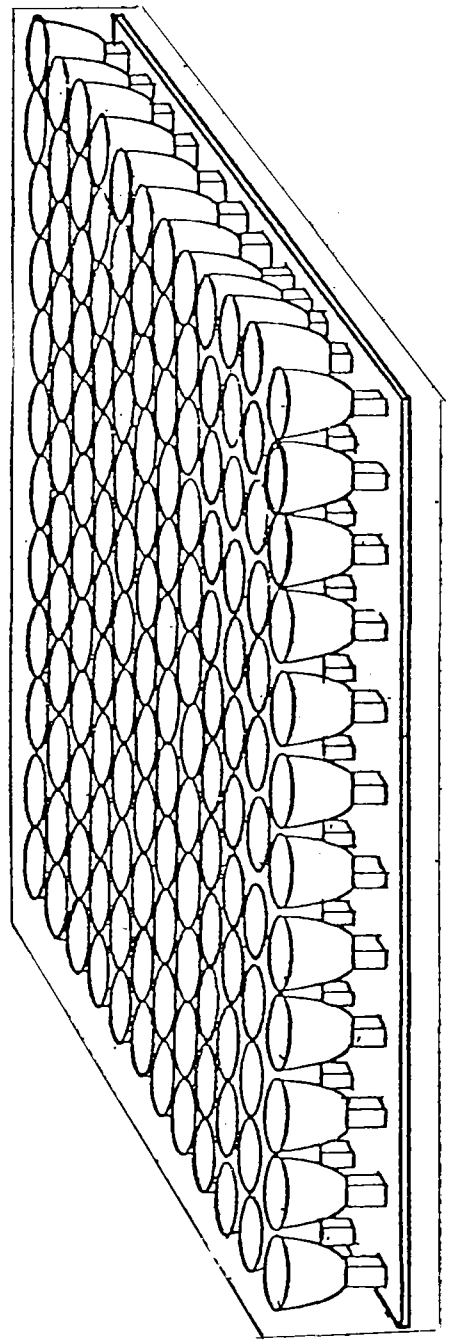

Figure 6

Cylindrical STG Design

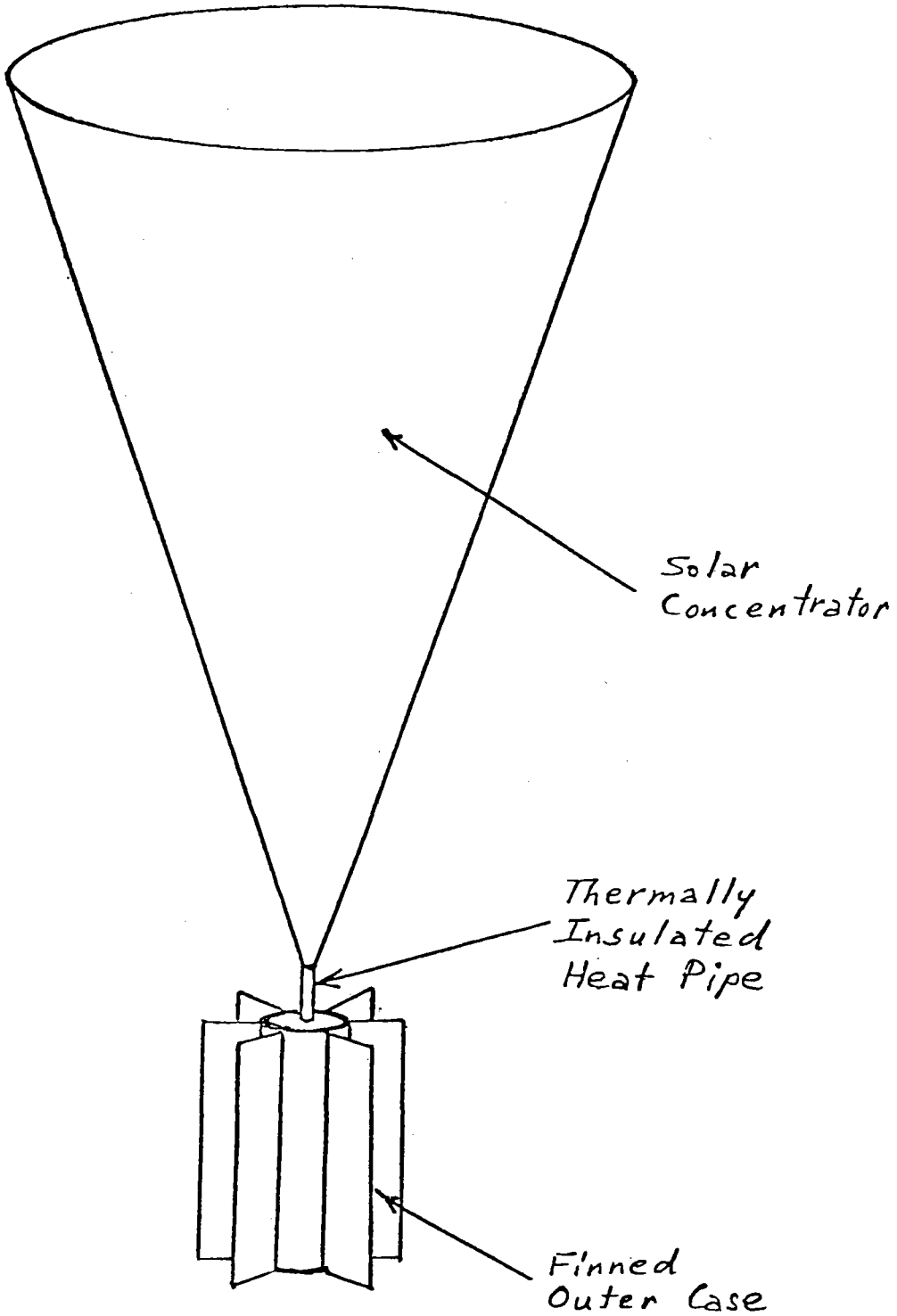

Figure 7

are based on the use of concentrators rather than a flat-plate type solar collector. The primary reason for this is that the concentrator in a properly designed STG itself remains relatively cool as compared to the hot side of the generator. Heat losses from the hot side of the generator, therefore, take place primarily from an area that is equivalent to the area occupied by the thermoelectric material and not by the area represented by the collector area. In the case of a flat-plate solar collector, this is not true. An STG making use of a concentrator, therefore, is subject to considerably lower heat losses from its hot side than is a flat-plate type generator and for this reason the generator performs more efficiently and enables the reduction of concentrator and cold side heat exchanger areas. Attendant cost savings may, therefore, be projected.

Detailed thermoelectric generator designs were developed on the present program for use with any of the forms of heat reception and heat rejection discussed above. For simplicity, these thermoelectric generator designs are based on the formulation of a basic building block in the form of a parallelepipedal thermoelectric module. Any number of such modules may be used in a final system design. These modules make use of bismuth telluride and silicon-germanium alloy thermoelements and are designed to operate at any temperatures within the range of temperatures at which each of the two thermoelectric materials can be operated. The module designs have been evolved by means of previously developed mathematical models and are characterized by compactness; each module design makes use of thermoelements of sizes consistent with accepted manufacturing techniques, while minimizing the amount of thermoelectric material used within them. It should be noted that the bismuth telluride thermoelectric module must be hermetically sealed and operated either under an inert atmosphere or in vacuum, if it is desired to operate the module at a hot side temperature higher than about 200°C. This is not the case with the thermoelectric module utilizing silicon-germanium alloys. Each of the module designs was subjected to detailed parametric performance analyses

as a function of hot and cold side operating temperatures; obviously the performance of each module design depends on temperatures. Moreover, for simplicity, the performance characteristics determined for the thermoelectric module design that uses silicon-germanium alloys has been formulated for an operating time of one year; it will be recalled that the thermoelectric properties of silicon-germanium alloys are not only temperature dependent, but also time dependent as well (see Appendix). The selection of the thermoelectric properties that correspond to one year of operating time is considered to be realistic from the standpoint that relatively little property change occurs after an operating time of one year. It must be noted that even though all of the performance characteristics for each type module have been determined for a specific module configuration and dimensions, it is possible to assume the use of any number of modules in a practical solar thermoelectric application. Any quantity of available electricity may therefore be projected on the basis of these module designs. As concerns the output voltage of each module under various operating conditions, it is noted that, just as power output, the voltage depends on the detailed operating temperatures. Inasmuch as it is envisioned that large quantities of these modules would be used in a practical application, an appropriate series-parallel connection of the individual modules will enable the obtainment of practically any desired value of direct output voltage. Questions of precise power and voltage requirements must be, of necessity, left to a subsequent study that considers the detailed design of a prototype STG.
It should be mentioned also that just as a single generator can make use of any number of basic thermoelectric modules, so can an overall power conversion system make use of any number of individual thermoelectric generators, with the final numbers of each depending on the detailed requirements of a given application. Finally, the basing of a thermoelectric generator design on a building block type thermoelectric module conveniently enables the development of detailed manufacturing costs for each module as a function of the quantity of modules. This enables

the estimating of costs associated with the thermoelectric conversion of incident solar radiation to electricity. Without the design of a generator for a specific application, this is the most meaningful way of generating cost data.

Although a variety of detailed design concepts exist for bismuth telluride thermoelectric modules, the one selected for cost projections in the present study is one that probably possesses the greatest simplicity and therefore the lowest overall cost. This module concept assumes individual n- and p-type bismuth telluride thermoelements of a cubic configuration with 0.030 inch sides. As previously mentioned, this size represents essentially the smallest bismuth telluride thermoelement that can be very conveniently manufactured and represents an optimum as regards thermoelement miniaturization and associated manufacturing costs. It is assumed that the thermoelements are solder-connected to two metallized alumina plates, with gaps of the order of 0.010 inch separating the individual thermoelements. The thermoelements are placed in a 24 x 24 array between the alumina plates such that one thermoelectric module consists of 287 thermocouples; two thermoelements are eliminated from two adjacent corners of the module because it is at these places within the module that output leads are connected. The lateral cross-sectional area of each module is therefore approximately one square inch. If it is assumed that the two alumina plates have thicknesses of 0.01 inch, the module will be about 0.05 inch thick. The fabrication sequence of the module involves the metallizing of each of the two alumina plates on one surface with nickel in such a way that the desired circuit pattern of individual thermoelement electrical connections is reflected by the pattern. The thermoelements are prepared by the mechanical slicing of the thermoelectric material from ingots to the desired dimensions. Two opposite ends of each thermoelement are then plated in preparation for soldering to the alumina plates. Solder is then place on top of the location of each thermoelement on the bottom plate. The plate is heated to a temperature adequate to melt the solder and individual thermoelements are located in their appropriate places

on the plate. More solder is placed on top of each thermoelement and the assembly is again heated to a temperature adequate for melting the solder. Finally, the top plate is carefully placed on top of the thermoelements. Solder connections are effected as the assembly cools to temperatures at which the solder hardens. The output lead wires are then soldered in the two corners of the module with omitted thermoelements and the connections are made to the metallized alumina plate intended to serve as the cold side of the module. It should be noted that a variety of bismuth telluride, tin and lead based solders may be used for this purpose. If it is desired to operate the module at temperatures as high as 250°C, it is necessary that the solder be either lead rich or pure lead. It must also be noted that the use of high temperature solders in the final assembly of the module necessitates the performance of the operation under an argon atmosphere in order that the oxidation of the thermoelectric material be prevented. As mentioned, many other module assembly techniques exist, but it is felt that this method is basically the simplest and least expensive in the manufacture of large quantities of modules. It should be noted that the largest-scale manufacturing of bismuth telluride thermoelectric modules at present involves the manufacturing of cooling modules. Although most thermoelectric cooling modules use a relatively low temperature solder, much of which is bismuth, the manufacturing technique is essentially similar to the one described above. Based on the experience of various thermoelectric cooling device manufacturerers, it may be concluded that the process here assumed is, in fact, the least expensive of any manufacturing process. The details of the module using bismuth telluride are summarized in Table I for easy reference.

The bismuth telluride module described in the preceding paragraph was subjected to detailed electrical performance and thermal performance calculations as a function of its hot and cold side operating temperatures. These calculations used the thermoelectric property data given for bismuth telluride in the Appendix and assumed a contact resistance of ten percent for each thermoelent. It is noted

Table I

Thermoelectric Module Characteristics

	Bismuth Telluride	Silicon-Germanium
Number of Thermocouples	287	1250
Thermoelement Cross-Section - inch	0.030 x 0.030	0.010 x 0.010
Thermoelement Length - inch	0.030	0.100
Inter-thermoelement Separation - inch	0.010	0.001
Module Cross-Section - inch	0.970 x 0.970	0.551 x 0.551
Module Height - inch	0.050	0.125
Maximum Temperature - ^{o}C	200	1000

that contact resistance values generally cover a broad range and somewhat depend on the type of contact used. Based on experience with the types of thermoelectric modules described above, it is felt that the assumed value of contact resistance is quite realistic and representative of solder-type contacts. The electrical power produced by the module as a function of its hot side operating temperature at various values of cold side temperature are shown in Figure 8. As may be expected, it is noted in Figure 8 that the electrical power produced by the module is a strong function of its operating temperatures, particularly of the temperature difference across the module. Moreover, it is noted that the power produced per unit temperature difference across the module tends to be higher at lower operating temperatures than it is at the higher operating temperatures. This is due to the fact that bismuth telluride has a figure-of-merit that is highest at lower temperatures and decreases with increasing temperature. The thermal performance of the module is depicted in Figure 9 in terms of the heat input required of the module at the various operating temperatures. Again it is noted that the required heat input is a strong function of operating temperatures and increases nearly linearly with the temperature difference across the module. It should be noted that the heat input values of Figure 9 not only account for the heat passing through the thermoelements, but also take into account the direct heat transfer between the hot and cold side alumina plates in between individual thermoelements. It is assumed that the volume not occupied by thermoelements is empty except for air and the heat loss portion of the calculation assumes that heat is transferred between the plates by means of radiation, conduction and natural convection through air. Inasmuch as the amount of heat bypassing the thermoelements is relatively small, no attempt has been made to introduce a thermal insulation into the space between the thermoelements. This has been done in a general attempt at cost savings. It must be emphasized, however, that insulation could be easily introduced if it were felt to be important. The value of heat input to the thermoelectric module is important in the design of

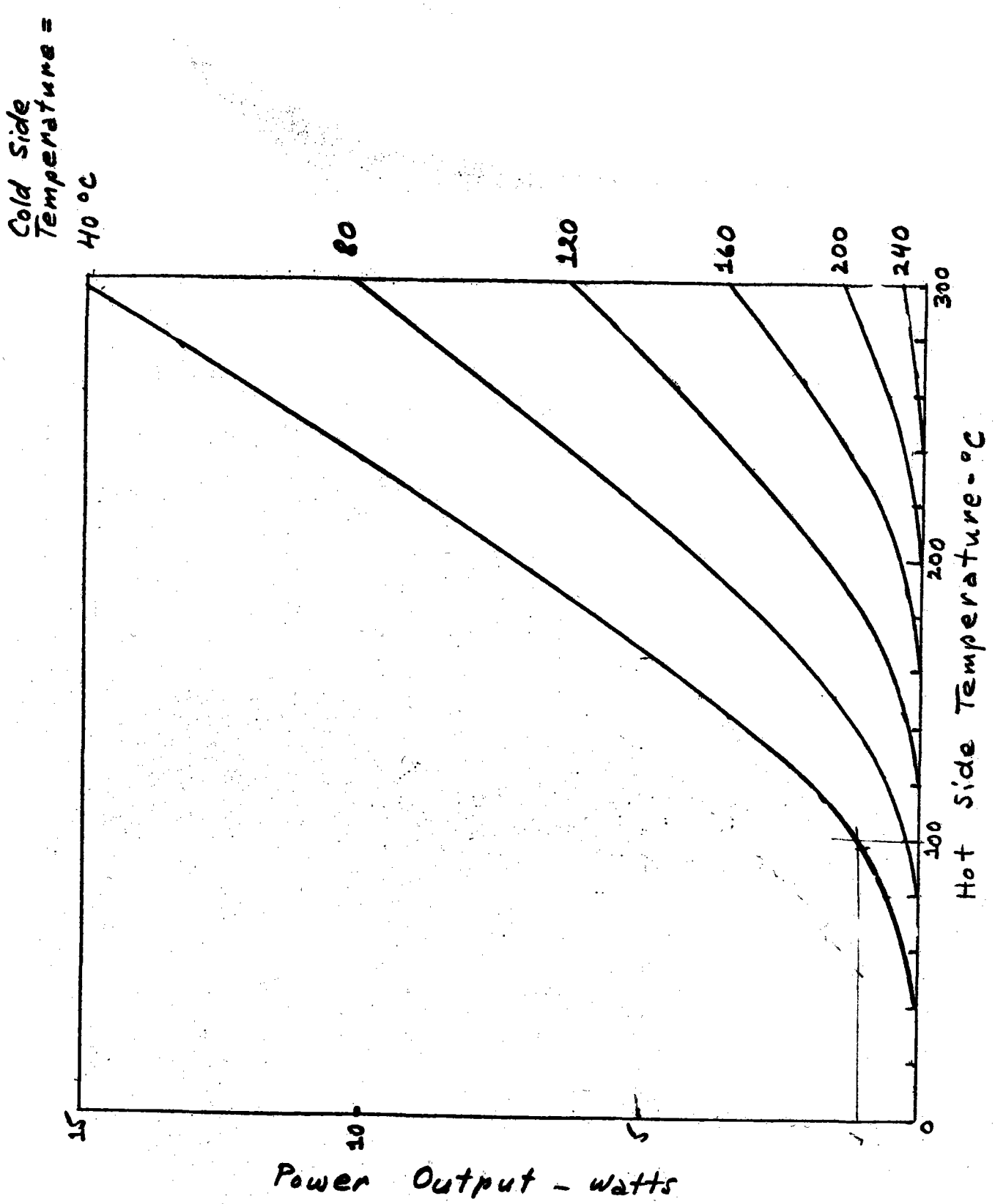
Cold Side Temperature = 40 °C
80
120
160
200
240
300
200
100
0
Hot Side Temperature - °C
15
10
5
0
Power Output - watts

Figure 8

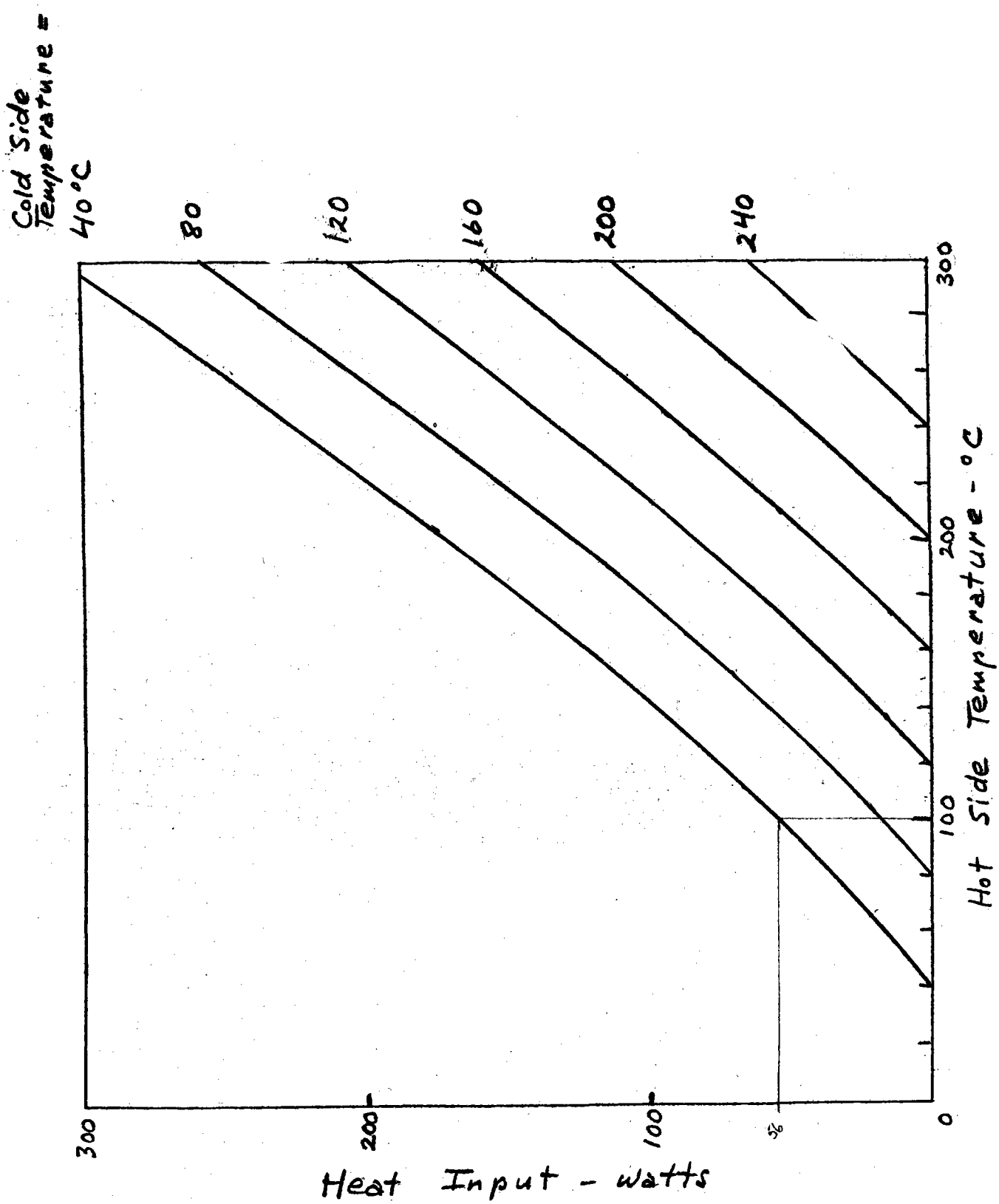
Cold Side Temperature = 40°C
80
120
160
200
240
300
200
100
0
Hot Side Temperature - °C
300
200
100
Heat Input - watts

Figure 9

the concentrator or collector used in conjunction with the module. In fact, it is this value of heat that largely determines the size of the concentrator. Here it is, of course, recognized that an additional amount of heat must be allocated to the input to account for the heat lost directly from the hot side of the thermoelectric generator. Inasmuch as the total surface area of the hot side of the thermoelectric generator is generally considerably smaller than the concentrator, the amount of direct heat loss forms usually only a small portion of the total heat impinging on the generator. This is especially true at the lower operating temperatures typical of bismuth telluride thermoelectric generators. In fact, it may be assumed that the amount of heat lost from the hot face of a generator through radiation and natural convection is of the order of 10 percent or less of the total heat entering the collector or concentrator. In the case of a flat-plate type collector, heat losses will be, of course, substantially greater and may be as high as 50 percent.

Just as in the case of bismuth telluride thermoelectric modules, a variety of design concepts exist for thermoelectric modules using silicon-germanium alloys. Thermoelectric module design concepts exist in which individual thermoelements are of fairly substantial size, with each thermocouple bonded through an electrical insulator to a common cold side and having individual heat collector plates for each thermocouple at the hot side. This is the so-called Air-Vac design concept and has been used in various radioisotope thermoelectric generators, such as those operating on the Voyager spacecraft. Another design concept utilizes miniature silicon-germanium alloy thermocouples that are bonded within a silicon dioxide matrix. This design concept enables the fabrication of extremely small thermocouples without any danger of mechanical breakage of the thermocouples as would occur if miniature thermocouples were not supported on all sides, such as in the Air-Vac type approach. Another silicon-germanium alloy module design concept utilizes the shrink-fitting of silicon-germanium alloy thermocouples between two concentric cylinders. This concept enables the fabrication of extremely compact generators that produce large quantities of power output if the heat entering the device is transported either by a liquid metal loop or a heat pipe placed at the

center of the device. This concept, however, is not especially amenable to a miniaturization of the individual thermocouples because the contact resistance in a pressure loaded device is generally much higher than it is in a metallurgically bonded device.

A review of the various thermoelectric module design concepts that utilize silicon-germanium alloys has resulted in the selection of the concept that enables the greatest degree of miniaturization for the purposes of the present study. This design concept is the one in which individual silicon-germanium alloy thermoelements are bonded into a silicon dioxide matrix such that the whole lateral surface area of each thermoelement is totally supported by the matrix and a metallurgical bond exists across the whole surface of each thermoelement. The electrical interconnections between various thermoelements and thermocouples within the module are made by means of miniature contacts at the two opposite faces of the module in such a way that the individual thermocouples are placed in a series circuitry; the freedom exists, of course, to also build redundancy into the module by using a series-parallel type circuitry. The cold side contacts interconnecting the individual thermoelements are effected by the metallization of the whole cold face of the module and then photoetching the desired circuit pattern. Tungsten is commonly used as the material for making cold side contacts. Inasmuch as tungsten reacts with silicon and germanium at temperatures in excess of some 600 to 700°C, it cannot be used as the hot side contact if the module is intended to operate at temperatures in excess of those. For this purpose, use is made of silicon contacts that are metallurigically bonded to each thermoelement. Such contacts are capable of long term reliable operation at temperatures well in excess of 1000°C. Finally, the contacts at the hot and cold faces of the module are covered with a layer of silicon dioxide such that the whole electrical circuitry of the module, including all thermoelements are totally encased in silicon dioxide. Output lead wires are connected at the cold side to the two ends of the circuit by means of metallurgical

bonding. Based on extensive experience with thermoelectric modules of this type, it has been found that a construction of this type is extremely rugged and the total enclosure of the circuit within silicon dioxide prevents any inadvertant shorting within the module as a result of contaminants or other extraneous materials that may come in contact with the module. It must be emphasized that individual thermoelements in this module design concept may be of extremely small size and therefore it is this concept that enables full miniaturization and the use of minimum quantities of thermoelectric material. Moreover, because all contacts are metallurgically bonded to individual thermoelements, contact resistance in this design concept also tends to be minimized.

Based on considerations related to module performance, manufacturing convenience and module miniaturization, a thermoelectric module design based on the silicon-germanium alloy module concept discussed above was selected for detailed cost analyses on the present study. This module design utilizes 1250 individual silicon-germanium alloy thermocouples in a 50 x 50 matrix. Each thermoelement within the module has side widths of 0.010 inch and lingths of 0.100 inch. Each thermoelement is separated from adjacent thermoelements by a layer of silicon dioxide of a thickness of 0.001 inch. The overall module dimensions are approximately 0.55 x 0.55 inch in cross section and 0.125 inch height. It should be noted that the height of the module is considerably greater than the 0.100 height of each thermoelement. The reason for this is that it is assumed that two metal support plates are bonded to the two opposite faces of each module to give the module rigidity. Each plate is assumed to possess essentially the same cross sectional area as the module and to have a thickness of about 0.010 inch. These plates are electrically separated from the circuitry of the module by means of silicon dioxide layers on the two opposite faces of each module. The plates are made of either molybdenum or tungsten because both of these materials closely match the thermal expansion coefficient of silicon dioxide. Inasmuch as the module will be subjected

to high temperature operation in air, the refractory metal plates are chrome plated to eliminate oxidation of the underlying metal. The module design just described represents the basic building block for an STG that makes use of silicon-germanium alloys. Obviously, any number of these modules may be electrically interconnected to yield a system of any desired size. The modules may be bonded to a common heat sink of whatever type desired and may be heated with any type of concentrator that provides adequate heat for each module. Details of the module are shown in Table

The silicon-germanium alloy module described above was subjected to detailed electrical performance and thermal performance calculations as a function of its hot and cold side operating temperatures. These calculations used the thermoelectric property data given in the Appendix for silicon-germanium alloys after one year of operation. The calculations also assumed a contact resistance of five percent for each thermoelement. It is believed that this assumed value for contact resistance is quite high for the metallurgical contacts assumed for the thermoelements, but for the sake of conservatism in the final results, this value has been selected. The electrical power produced by the module as a function of its hot side operating temperature at various values of cold side operating temperature are shown in Figure 10. It is noted in Figure 10 that the electrical power produced by the module is greatly dependent on the temperature difference between its hot and cold sides and in general increases with increasing average temperatures. This phenomenon reflects the temperature dependence of the figure-of-merit of silicon-germanium alloys; unlike that of bismuth telluride, the figure-of-merit of silicon-germanium alloys increases as a function of temperature and attains a maximum at temperatures of the order of 700 to 900°C. The thermal performance of the module is shown in Figure 11 in terms of the heat input required of the module at various operating temperatures. It is noted in Figure 11 that heat input also depends greatly on the operating temperatures of the module and increases nearly proportionately with the temperature difference across the module. It should be

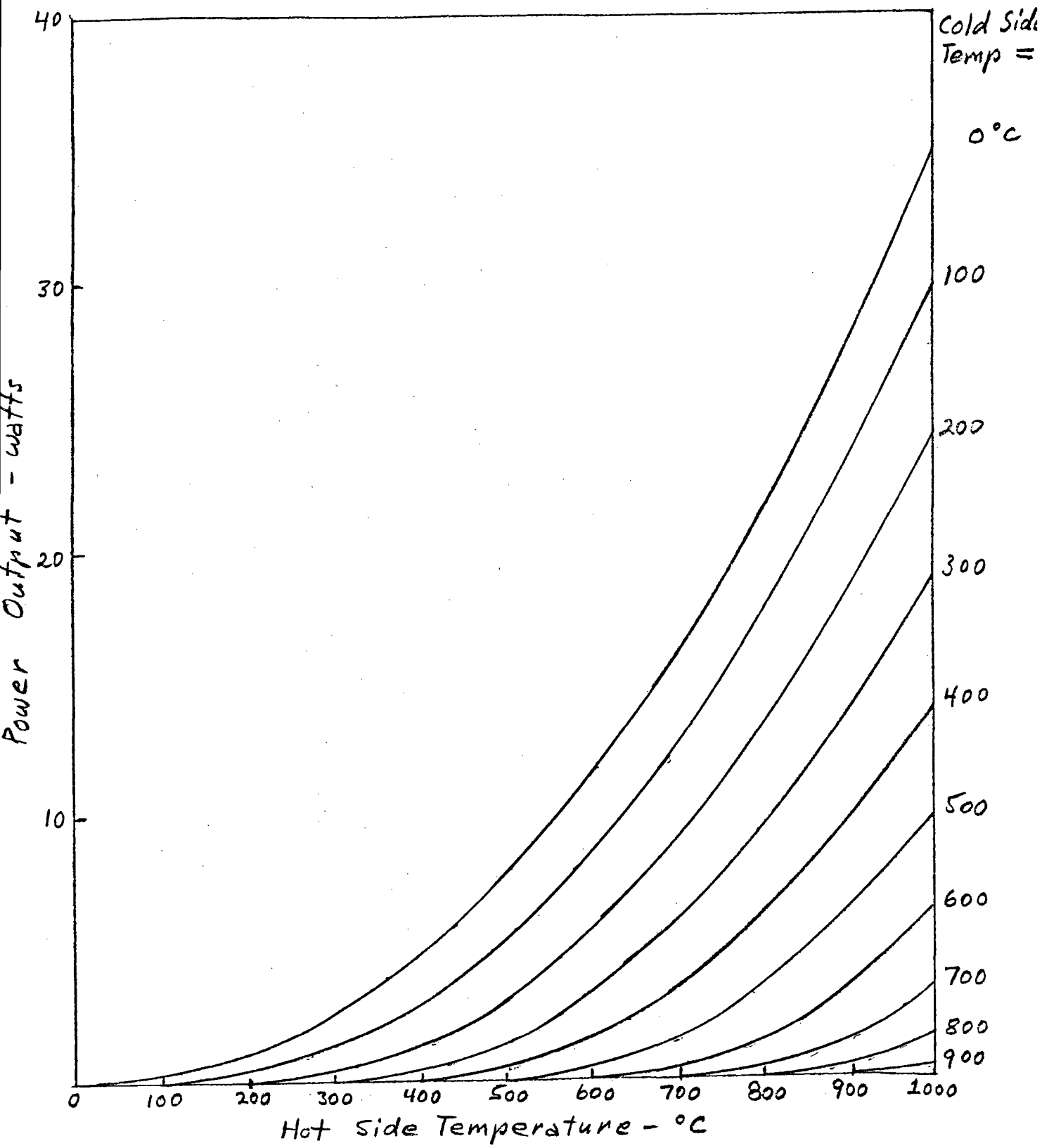
40
30
20
10
Power Output - watts
0
100
200
300
400
500
600
700
800
900
1000
Hot Side Temperature - °C
Cold Side Temp =
0°C
100
200
300
400
500
600
700
800
900

Figure 10

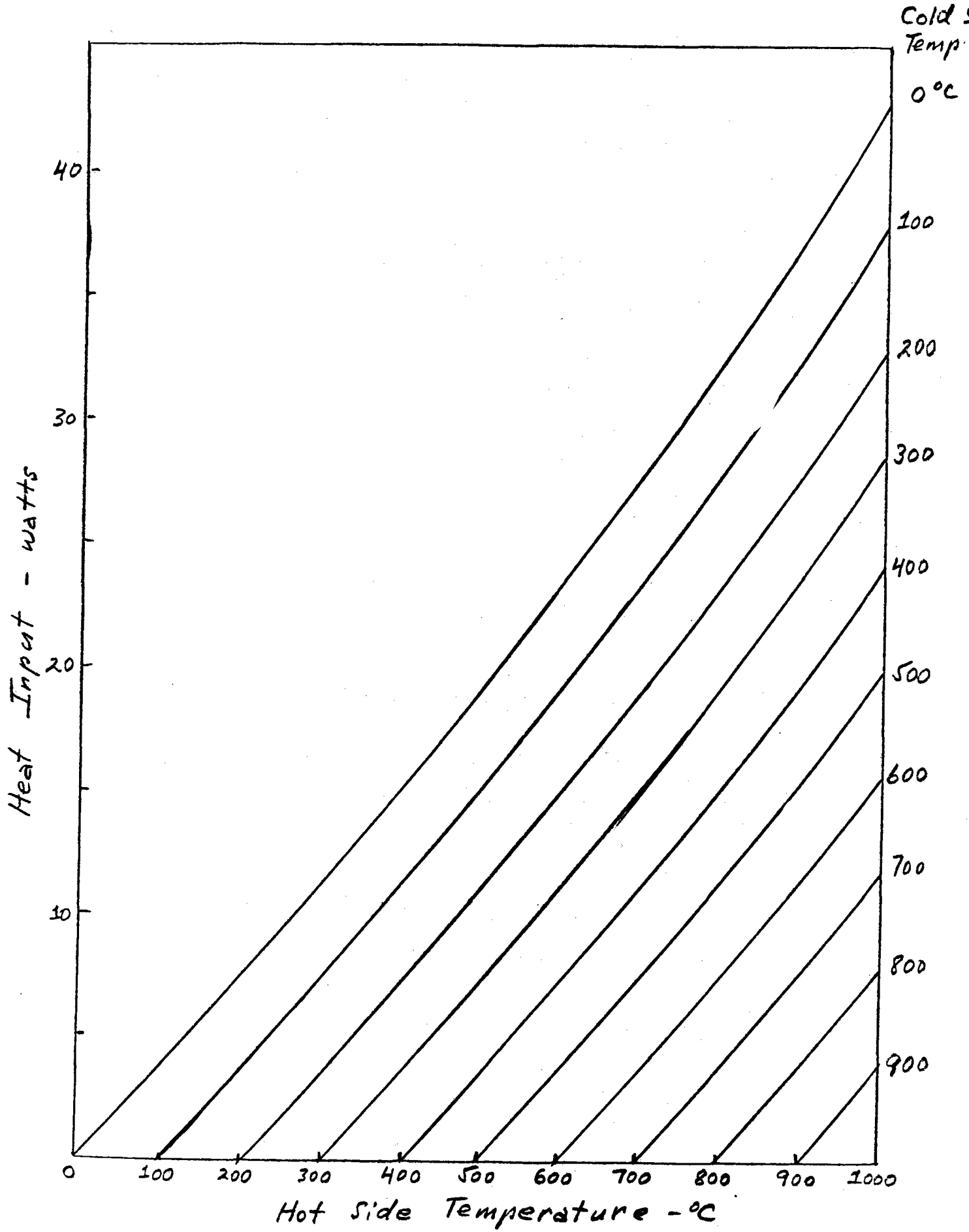
Cold S
Temp
0 °C
100
200
300
400
500
600
700
800
900
40
30
20
10
0
100
200
300
400
500
600
700
800
900
1000
Heat Input - watts
Hot Side Temperature - °C

Figure 11

noted that the heat input values shown in Figure 11 not only take into account the heat passing through the thermoelements, but also include that portion of the heat bypassing the thermoelements through the silicon dioxide layers in between the thermoelements. As in the case of the bismuth telluride module described above, the heat input values of Figure 11 represent the amount of heat that is necessary for module operation at the various temperatures shown. This means that the collector or concentrator must be capable of providing this quantity of heat and because the heat values do not show the quantity of heat rejected from the hot face of the module, such values represent minimum values. In practice, therefore, slightly greater quantities of heat than those shown in Figure 11 are necessary for module operation. The amount of heat lost from the hot face of the thermoelectric module is obviously temperature dependent. It may be assumed that at the highest indicated operating temperatures this amount is of the order of 30 percent. At lower operating temperatures, it is considerably less. If instead of a concentrator, use is made of a flat-plate type collector, heat losses are substantially greater, especially at the highest operating temperatures, and may, in fact, attain values in excess of 50 percent.

V. RELIABILITY CONSIDERATIONS

As with any device, it is also with STGs that the reliability of the device in the end has a great effect on the overall cost of electricity produced by it. No matter how attractive the performance of an STG and no matter how inexpensively it can be manufactured, it is of crucial importance that the device be capable of reliable long term operation in order for it to be practicable. As a part of the present study, a cursory look was taken at this aspect of the two types of STGs discussed in the preceding section. As will be recalled, an STG is characterized by three main components: the collector or concentrator, the thermoelectric generator and the cold side heat exchanger. Inasmuch as the present study has not

addressed itself in detail to either the collectors or concentrators or the cold side heat exchangers attention on the question of reliability has been concentrated in the area of the thermoelectric generator.

Considering the two separate thermoelectric materials and their technologies, as discussed in the preceding section, it may be stated in general that whereas relatively little quantitative reliability information exists on bismuth telluride, considerable amounts of information are available on silicon-germanium alloys. The reason for this discrepancy in data between the two materials and their associated technologies is based on the fact that bismuth telluride has not received any noticable attention from various U. S. Government users; the converse is true of silicon-germanium alloys. It is primarily the various U. S. Government users that typically finance extensive reliability studies on various thermoelectric materials and their technologies because most Government applications, such as those in space, require extreme values of reliability. Inasmuch as bismuth telluride is primarily being used in terrestrial and commercial applications, it has not received the attention accorded other thermoelectric materials, including silicon-germanium alloys. The lone exception to this is a U. S. Navy study conducted within the past several years as a part of a half-watt RTG program. In this instance, however, use was made of various bismuth telluride modules and module technologies which are not commonly used in wide spread commercial applications. In fact, the modules and the technologies used on that program represented fairly experimental and/or exotic technologies that quite probably are not applicable to large-scale mass production, a requirement of STGs intended for the generation of large quantities of electricity. As such, the results of the study are not especially applicable in the present case. This is even more the case because none of the thermoelectric modules evaluated on the U. S. Navy program possessed constructional and contacting techniques described in the preceding section for the bismuth telluride module design assumed on the present study.

A search of the literature and other available information did not yield any basic information on the time and temperature behavior of the solder/bismuth telluride type bond. In fact, no reliability information at all appears to be available in the literature regarding this type of system. This is also true of all other types of bismuth telluride technology, even though the Russian literature contains a fair amount of information on the basics of bismuth telluride as a thermoelectric material. In fact, the only study of consequence regarding the reliability and degradation associated with bismuth telluride devices appears to be the aforementioned study performed by the U. S. Navy. As already stated, however, that particular study is of little help in assessing the reliability of the thermoelectric module technology associated on the present study. Based on various forms of data available at Syncal Corporation regarding modules of that type, an estimate has been made about the failure rate of individual thermoelements and/or bonds in modules of the type in question. Namely, it is estimated that a failure rate of about 10^{-7} per hour approximately represents such devices in long term operation at 200°C. This failure rate, however, is based on limited data and therefore cannot be considered to be absolutely accurate. Nevertheless, for present pruposes it is adequate and enables the approximate determination of the reliability of the module design discussed in the preceding section. Unfortunately, the data on which this failure rate is based are not adequate to enable the projection of the failure rate as a function of temperature. Inasmuch as 200°C may be close to the maximum temperature that bismuth telluride devices should be operated in a solar thermoelectric application, even this may not be a severe shortcoming; it will be recalled that in high temperatures operation, such devices must be protected from an oxygen atmosphere by hermetic sealing. Because this undoubtedly results in significantly higher device costs, it is considered that hermetic sealing is undesirable and therefore device hot side operating temperatures should be limited to less than 200°C.

Making the conservative assumption that each thermoelement within the thermoelectric module has three possible methods of failing, namely the breakage of the thermoelement itself and the opening of either the hot or the cold side bond between the thermoelement and the metallized alumina plate, it is seen that there are basically 861 components within the module subject to failure. Inasmuch as all of the components within the module are connected electrically in series, the failure of any one component will result in the failure of the module. If it is assumed that the failure rate of each such component is represented by the failure rate given above, it is seen that the average time to failure of the thermoelectric module is about 11,600 hours or slightly more than one year. It is believed that this result is very conservative because, for example, it is unrealistic to assume that the cold side contact operationg at a very low temperature is subject to the same failure rate as the hot side contact operating at a much higher temperature. In fact, if it is assumed that the failure rate of each thermoelement, including its contacts, is of the order given above, then it is seen that the average time to failure of the thermoelectric module is nearly 35,000 hours or almost four years. These considerations pertain to a module that is connected electrically in series. Considerably longer average time to failure can be achieved if the circuitry is changed to a series-parallel type circuitry. In fact, if this is done, as it can be easily, the average time to failure for the module can be extended well beyond ten years. Lifetimes of this order may be considered completely adequate for a thermoelectric system intended for use in solar thermoelectric applications. Even considerably shorter lifetimes may be adequate. It is felt, however, that a minimum practicable lifetime should be at least of the order of a few years or more.

Although considerably more reliablility information exists on silicon-germanium alloy thermoelectric generators than does on bismuth telluride devices, most of this information pertains to the so-called Air-Vac type thermocouples because it is these that have been and are being used in space applications. Never-

theless, a bulk of data also exists on the modules of the type discussed in the preceding section. Moreover, some of the Air-Vac type reliability data can be directly applied to the latter type modules because the hot and cold side bond systems are essentially identical. Independently of that, continuous life tests on RTGs and other types of thermoelectric generators at temperatures approaching 1000°C with modules of the type in question have been recorded for times in excess of 30,000 hours. On the basis of these tests at Syncal Corporation and also in various government centers, it is estimated that the failure rate per thermoelement in a module of the type described is of the order of 5×10^{-9} per hour in operation at temperatures in the range of 900 to 1000°C at the hot side. The lifetimes of the tungsten bond at the cold side of the module and the silicon bond at the hot side of the module have been independently determined on the basis of kinetic tests and are shown in Figure 12 as a function of temperature. It is noted in Figure 12 that the cold side bond using tungsten has a projected lifetime of the order of ten years when operating at 600°C. At lower temperatures its lifetime is considerably longer. The silicon bond is projected to possess a lifetime in excess of ten years in operation at 1000°C. Again, at lower temperatures the lifetime is considerably further extended. Inasmuch as in a solar thermoelectric application, it is envisioned that the thermoelectric generator would certainly operate at a cold side temperature lower than 600°C and a hot side temperature lower than 1000°C, it may be concluded that the lifetime of the device for operating times of the order of ten to 20 years is not bond limited. Moreover, applying the failure rate given above to the module of the design described in the preceding section shows that the average time to failure of an electrically series connected module is of the order of 80,000 hours or in excess of nine years when operating at a hot side temperature of 1000°C. Lifetime is considerably enhanced if the hot side operating temperature is decreased to operating temperatures lower than 1000°C.

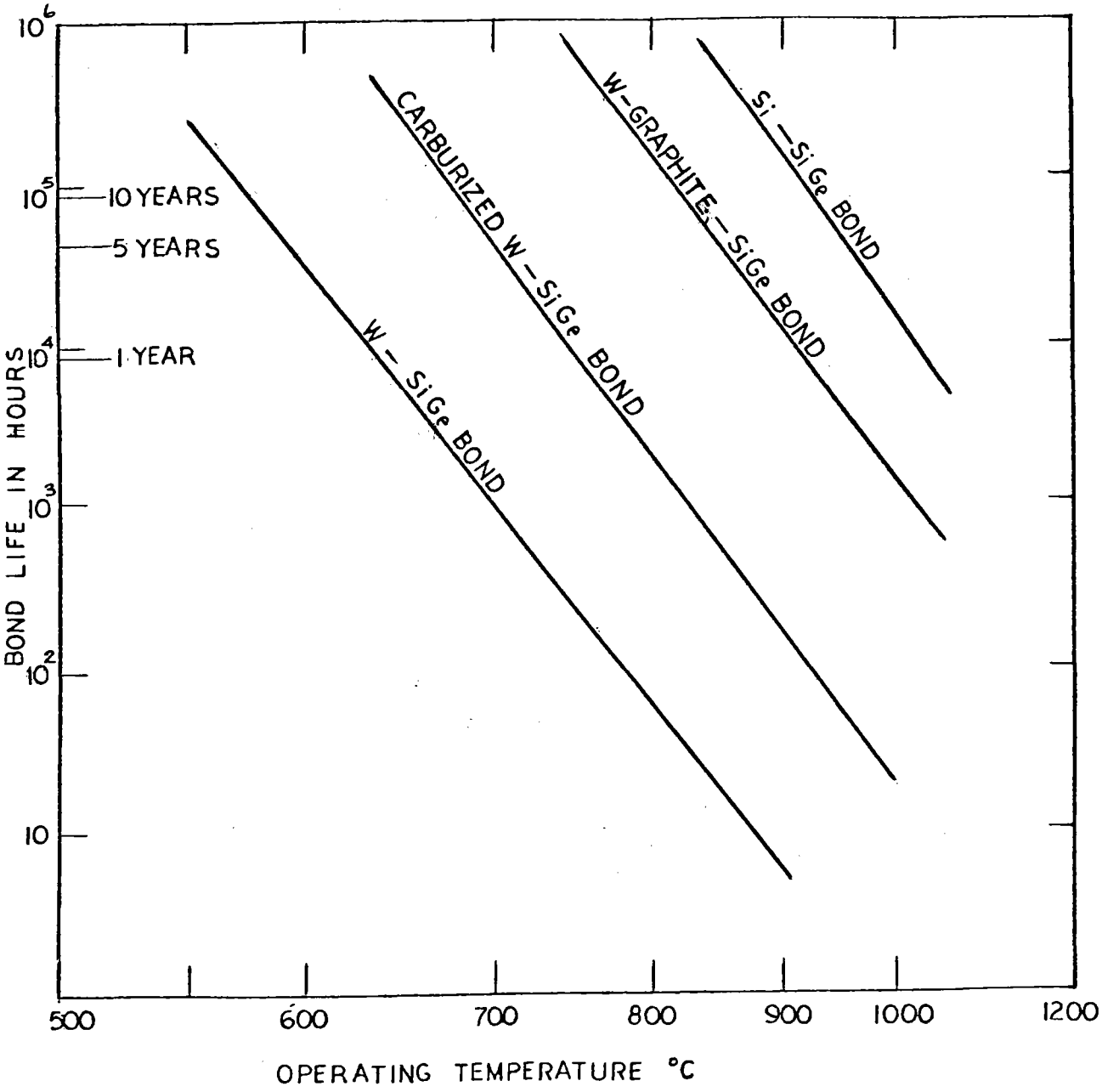

FIGURE 12 BOND LIFE FOR SiGe ALLOY BONDED TO VARIOUS CONTACTING MATERIAI

From the foregoing it is seen that a reliability treatment of the bismuth telluride and the silicon-germanium alloy thermoelectric modules selected on the present study shows probable operating lifetimes of the order of several years or longer. Reliable long term operation of a thermoelectric module in a solar thermoelectric application is, of course, of crucial importance in the final assessments of costs associated with this type of energy conversion. The cost of a solar thermoelectric energy conversion system is essentially equal to its initial cost in terms of fabrication and installation costs. The longer the system operates without failure, obviously the lower is the per unit cost of electricity produced by it. This assumes that maintenance costs are negligible compared to the initial costs of the system. In a properly designed solar thermoelectric system, this should be the case. Whenever a thermoelectric module does fail, no attempt should be made to repair the module because generally repair costs are higher than the cost of replacing the module with a new one. As already stated, the lifetime of each thermoelectric module within a practical power conversion system should be at least several years. As seen above, this should be the case with both types of modules selected for cost analyses on the present study.

VI. SOLAR THERMOELECTRIC GENERATOR COST EVALUATION

The assessment of the practicability of using solar thermoelectric power conversion to obtain electricity depends on the costs of electricity thus produced and how these costs compare to the cost of electricity produced by other methods. The cost of electricity produced by solar thermoelectric power conversion depends on the fabrication costs of the required devices, their installation costs, maintenance costs and the expected lifetime of each device. This section of the report addresses itself to these costs and derives anticipated costs associated with solar thermoelectric energy conversion used to produce electrical power. The costs derived here are

of necessity approximate and not totally complete because, as already stated above, they do not consider the costs associated with the total system. Namely, the cost associated with collectors and/or concentrators and cold side heat exchangers are not being considered. The present costs estimates pertain primarily to those associated with the thermoelectric modules used in practical power conversion systems. Furthermore, the estimated costs are partly based on actual expense in the manufacture of relatively small quantities of thermoelectric modules of the type previously discussed and are partly based on projections of these costs to extremely large quantity production. Even though the costs thus derived are considered to be realistic, it must be emphasized that they are only projected costs and thereby represent best estimates.

Assuming the availability of appropriate manufacturing equipment, the cost associated with the manufacture of both bismuth telluride and silicon-germanium alloy thermoelectric modules consist of material and labor costs; the cost associated with the necessary manufacturing equipment will be considered separately below. In order to obtain the total cost, it will be necessary to also consider overhead and related administrative costs. As concerns material costs, the amount of material used in thermoelectric modules of each type, as previously discussed, is extremely small. Except for the thermoelectric material itself, other material costs within the modules are practically negligible, being of the order of a small fraction of a dollar in each case. Even the cost of the thermoelectric material is quite low. In the case of the bismuth telluride module, the quantity of thermoelectric material per module is approximately 0.01 cm^3. The amount of thermoelectric material in the silicon-germanium alloy module is somewhat greater, being of the order of 0.4 cm^3. Assuming a cost of approximately one dollar per gram for the thermoelectric material, it is found that the bismuth telluride cost per module is approximately seven to ten cents and the silicon-germanium alloy cost is only slightly in excess of one dollar. Even though these material cost figures do not include material

losses as a result of less than perfect yield, it is generally found that any reject material can be reworked into useable material at a fraction of its original cost. It may thus be concluded that the cost of material within the modules of each type is of the order of a dollar or so.

In order to assess the labor costs associated with the manufacture of each type thermoelectric module, it is necessary to consider the detailed manufacturing steps and to assign an estimated number of labor hours to each step as a function of quantity of modules manufactured. This has been done for both the bismuth telluride and the silicon-germanium alloy modules. The detailed manufacturing steps for the former type module are given in Table II and for the latter type module in Table III. Based on actual experience in the manufacture of each type module for relatively small quantities of such modules and based on projections to considerably greater quantities of modules, it has been possible to estimate the total number of labor hours associated with the manufacture of each type module as a function of the total number of modules manufactured. The results of these labor hour projections for both types of modules are shown in Figure 13 in terms of labor hours per module as a function of total number of modules manufactured. It is noted in Figure 13 that in small quantities, the silicon-germanium alloy module require a greater amount of labor per module than does the bismuth telluride module. In very large quantities, however, it is projected that the amount of labor required to produce a silicon-germanium alloy type module is actually less than the amount required in the production of bismuth telluride modules. The reason for this phenomenon is that the silicon-germanium alloy modules not only possess a greater number of manufacturing steps than do the bismuth telluride modules, but many of these steps involve high temperature furnace runs that involve some labor. In small quantities, therefore, silicon-germanium alloy modules require the expenditure of considerably greater labor than do bismuth telluride modules. As concerns large quantity production, all of the processes used in the silicon-germanium alloy module

Table II

SILICON-GERMANIUM ALLOY THERMOPILE FABRICATION STEPS

1. Slice n- and p-type silicon-germanium alloy material to a thickness slightly greater than the final thermoelement side width (see Drawing 1, Figure 12).
2. Lap slices to a thickness equal to the final thermoelement side width.
3. Oxidize the slices in air to obtain an oxide coating in preparation for sedimentation.
4. Sediment SiO_2 powder on one face of each slice, with the SiO_2 thickness being much less than the slice thickness (see Drawing 2).
5. Sinter the SiO_2 coating on each slice in an air furnace at an appropriate temperature (see Drawing 3).
6. Stack the slices with sintered SiO_2 coatings in such a way that n- and p-type slices alternate (see Drawing 4).
7. Bond the stack of silicon-germanium slices with SiO_2 coatings in an air furnace at an appropriate temperature.
8. Slice the stack in a direction perpendicular to individual slices to a thickness slightly greater than the final thermoelement width, resulting in so-called "composite" slices which consist of alternating SiO_2 and silicon-germanium alloy strips (see Drawing 5).
9. Lap the composite slices to a thickness equal to the final desired thermoelement width.
10. Repeat Step 3 to prepare the composite slices for sedimentation.
11. Sediment SiO_2 on one face of each slice, with the SiO_2 thickness being much less than the thickness of each slice (see Drawing 6).
12. Sinter the coated composite slices in an air furnace at an appropriate temperature (see Drawing 7).
13. Stack the composite slices with sintered coatings in such a way that n- and p-type thermoelements within adjacent slices alternate (see Drawing 8).
14. Bond the stack in an air furnace at an appropriate temperature.
15. Saw the stack of slices in a direction perpendicular to the individual thermoelements into thermopiles with each thermopile being slightly longer than its final design length.
16. Lap the individual thermopiles to the final design length.
17. Seal molybdenum output contacts with SiO_2 in vacuum to the appropriate sides of the thermopiles such that one side of each contact is even with the intended cold side of the thermopile.
18. Bond silicon contacts to the hot side of each thermopile such that each contact interconnects an appropriate number of n- and p-type thermoelements, with the appropriate number depending on the intended redundancy of the final circuit.
19. Bond SiO_2 and chromium coated tungsten slabs over the silicon contacts on the hot face of the thermopile in a vacuum furnace at an appropriate temperature.
20. Prepare photomasks of the desired circuit pattern for the cold end of each thermopile, with the circuit terminating at the two molybdenum output leads.
21. Metallize tungsten over the entire face of the cold side of the thermopile.
22. Photo-etch the desired circuit pattern on the tungsten coating by using the photomask prepared in Step 20.
23. Bond SiO_2 and chromium coated tungsten slabs onto the cold end of the thermopile thereby completely covering the tungsten contact pads.

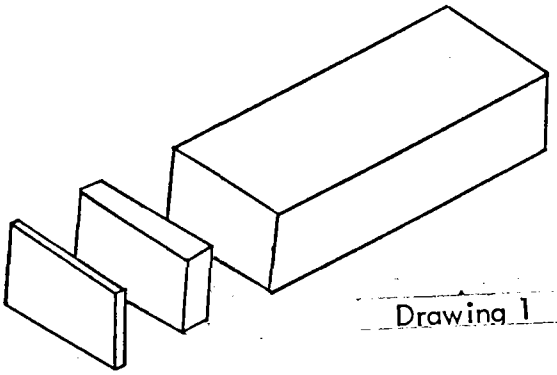

Drawing 1

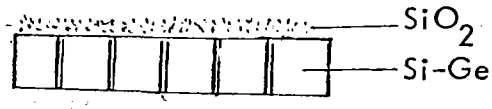

Drawing 6

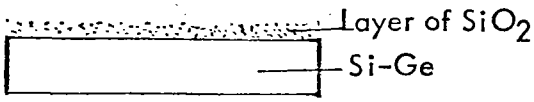

Drawing 2

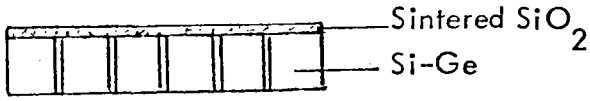

Drawing 7

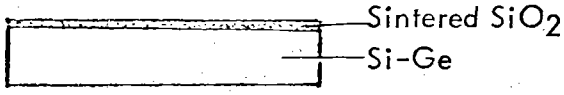

Drawing 3

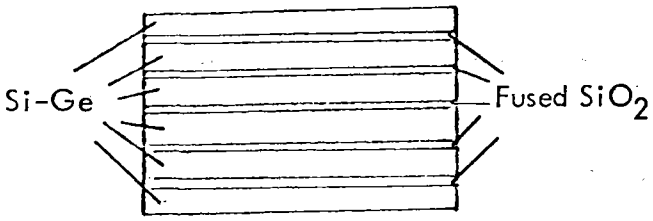

Drawing 4

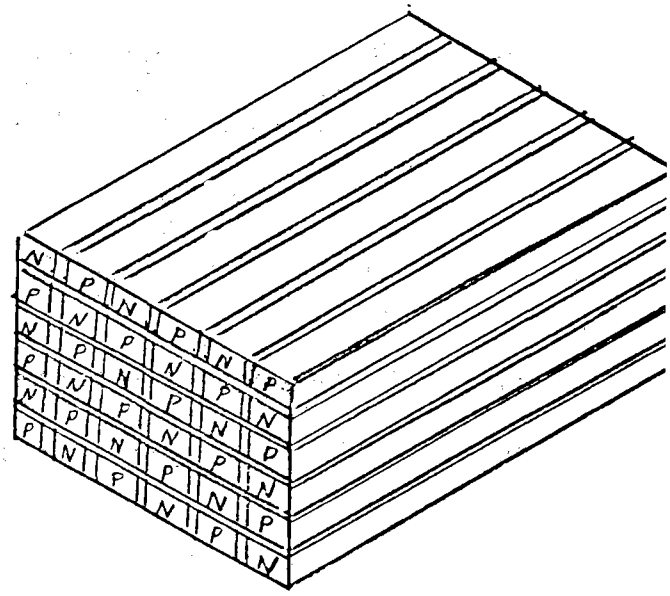

Drawing 8

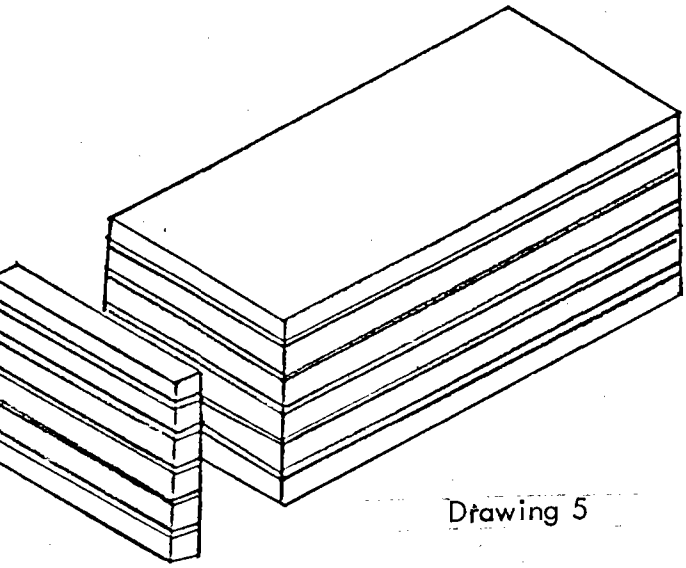

Drawing 5

Figure 12

Table III

BISMUTH TELLURIDE THERMOPILE FABRICATION STEPS

1. Slice n- and p-type bismuth telluride material into thermoelements of desired dimensions.

2. Prepare alumina plates by metallizing nickel on one face of each in such a way that appropriate circuit pattern results on each plate.

3. Pre-tin hot and cold faces of each thermoelement with solder of appropriate composition.

4. Repeat Step 3 for each alumina plate.

5. Place appropriate solder "blank" on each tinned nickel strap on the cold side alumina plate of each module and heat plate until solder melts.

6. Place n- and p-type bismuth telluride thermoelements in an alternating pattern on the molten solder on the alumina plate (use 0.010 inch diameter crossed wires to locate thermoelements).

7. Place solder "blank" on top of each thermoelement and wait until it melts.

8. Place hot side alumina plate on tope of thermoelements and apply slight pressure.

9. Cool module and remove locating wires.

10. Solder electrical output leads to module.

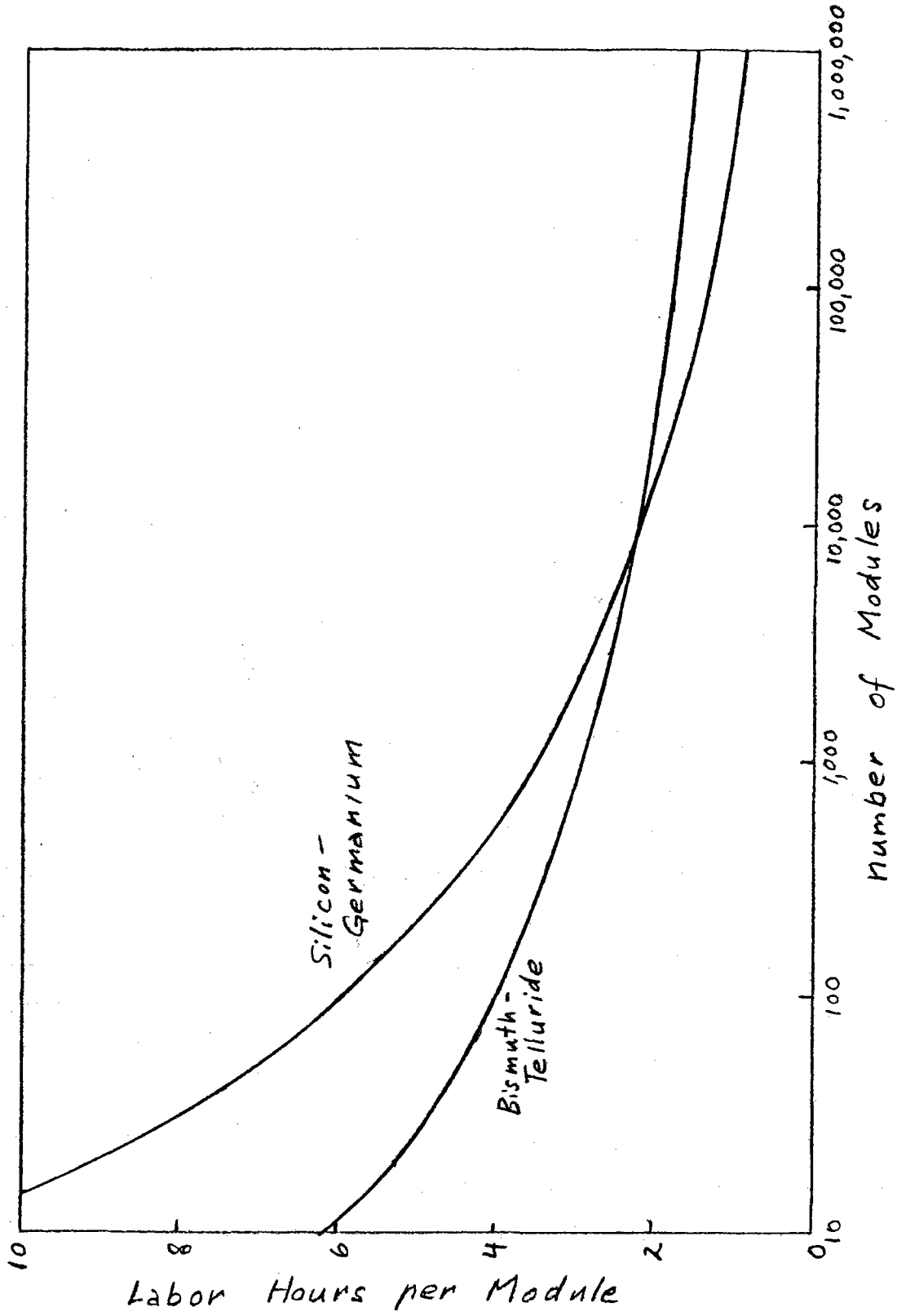
Silicon - Germanium
Bismuth - Telluride
Labor Hours per Module
10
8
6
4
2
0
10
100
1,000
10,000
100,000
1,000,000
Number of Modules

Figure 13

manufacture are amenable to mass production techniques, utilizing techniques already being used in the semiconductor industry. Even though the manufacture of bismuth telluride modules lends itself to some automation and thereby decreased amount of labor hours as a function of the quantity of modules produced, there is a limit as to the degree of automation and therefore to the labor hours expended in the manufacture of each module. It should be noted that the labor hours depicted in Figure 13 represents the total time involved in all of the manufacturing steps outlined for the two types of modules in Tables I and II and therefore represents the total amount of labor required in the manufacture of these modules.

The bulk of the labor used in manufacture of both bismuth telluride and silicon-germanium alloy modules is of the type categorized in the semiconductor industry as "assembler". Some labor of personnel of greater skill is, of course, also needed, as is of a technical and supervisory nature. Estimating that approximately 90 percent of the labor is of the assembler type and the remaining ten percent of a more skilled type, it is possible to determine an approximate labor rate appropriate to the manufacture of both types of modules. Although labor rates themselves vary for each labor category, for the purposes of the present study it is assumed $4.00 per hour and $8.00 per hour may be representative of the assembler and more skilled type labor categories. This yields an effective rate of $4.40 per hour for the projected manufacture of both types of modules. Utilizing this effective labor rate, it is obviously possible to convert the required labor hours per module shown in Figure 13 to a corresponding dollar expenditure for labor. The addition of a fixed material cost per module, finally enables the determination of the total cost required in the manufacture of the two types of modules. Although administrative and overhead costs vary from manufacturing plant to manufacturing plant, for the purposes of the present cost estimate, it is assumed that a labor overhead rate of 80 percent and an administrative rate of 15 percent are representative of manufacturing plants. Applying the overhead rate to the labor rate expended

in the manufacture of each module and then applying the administrative rate to the combined material, labor and labor overhead rates enables the final determination of the total cost in the manufacture of the two types of modules as a function of the total number of modules manufactured. These costs per module for each type of module are shown in Figure 14.

It is now possible to combine the results shown in Figure 14 with those shown in Figures 8 and 10 for the performance of each type module as a function of its operating temperatures in order to arrive at a figure for the cost of electricity produced by the modules as a function of the total amount of electricity produced by them. This combination is straightforward and is shown in Figures 15 and 16 for the bismuth telluride and silicon-germanium alloy modules, respectively. It is noted in Figures 15 and 16 that the cost of unit electricity is a decreasing function of the total amount of electricity produced and is also inversely proportional to the temperature difference employed across each type of thermoelectric module. A comparison of the results shown in Figures 15 and 16 shows that the unit cost of electricity is lower for silicon-germanium alloy modules, especially large values of power produced and relatively large temperature differences of module operation, as compared to bismuth telluride modules. At small quantities of power produced and for comparable temperature differences of module operation, the unit cost of electricity is somewhat lower for bismuth telluride modules. In both cases, however, large quantity costs associated with power production are quite low and should be comparable or lower than many other forms of power production. Whether they are depends, of course, on the ultimate cost of the associated components not included in the cost figures of Figure 15 and 16. These associated components represent solar collectors or concentrators and the appropriate cold side heat exchangers.

In assessing the economic advisability of using thermoelectric energy conversion to obtain practical quantities of electrical power from incident solar

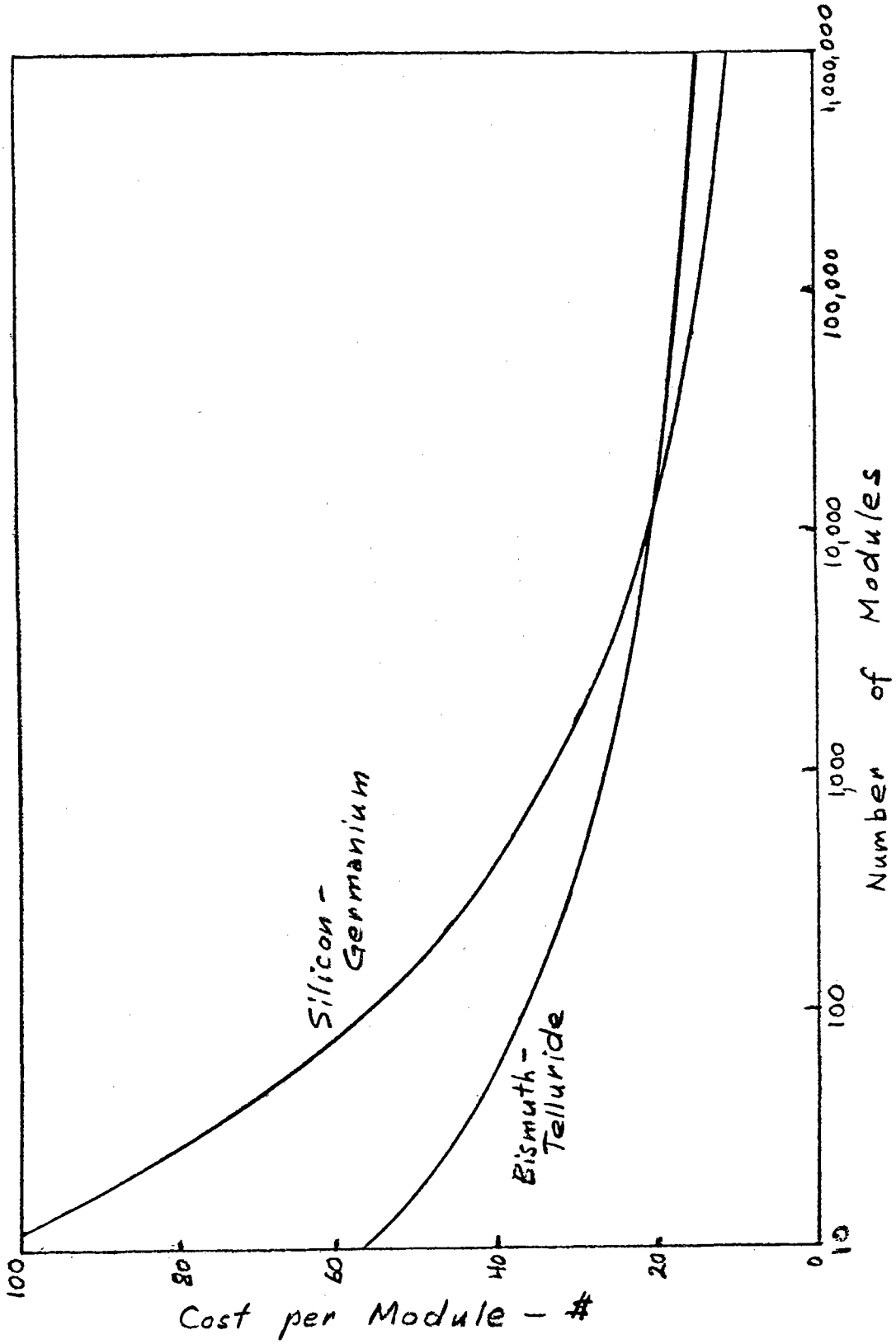
Silicon - Germanium
Bismuth - Telluride
Cost per Module - #
100
80
60
40
20
0
10
100
1,000
10,000
100,000
1,000,000
Number of Modules

Figure 14

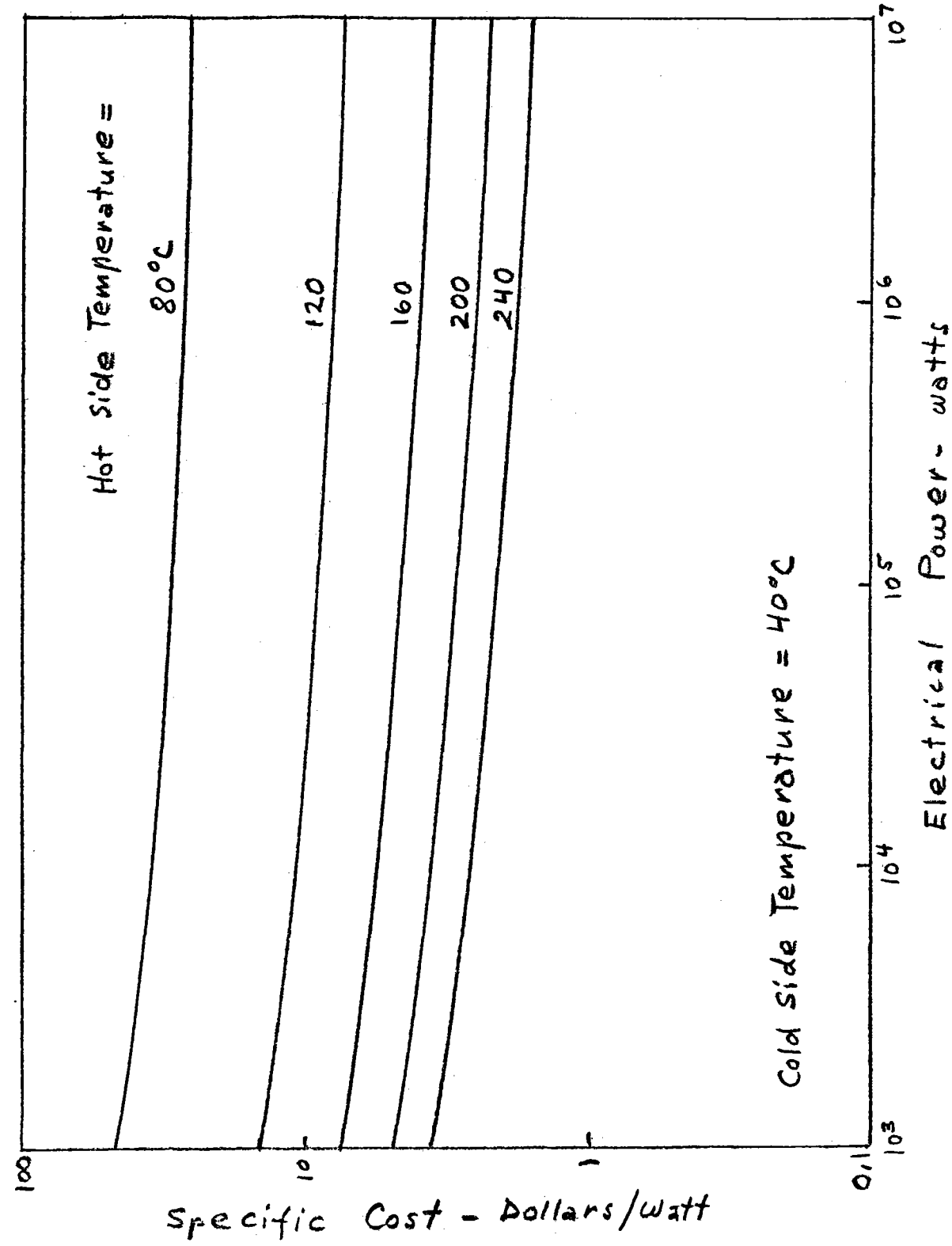
Hot Side Temperature =
80°C
120
160
200
240
Cold Side Temperature = 40°C
Electrical Power - watts
10^7
10^6
10^5
10^4
10^3
100
10
1
0.1
Specific Cost - Dollars/watt

Figure 15

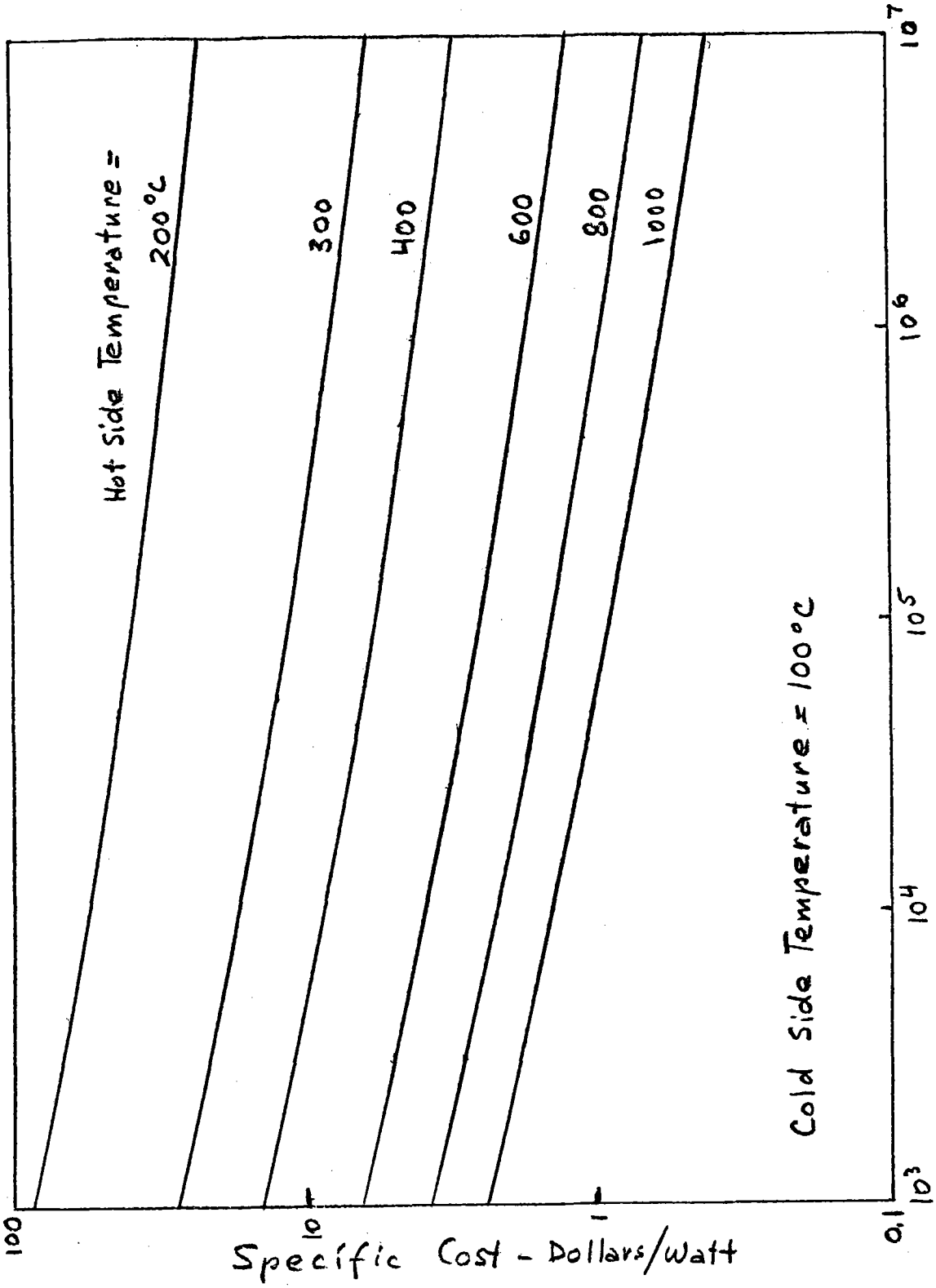
Hot Side Temperature =
200°C
300
400
600
800
1000
Cold Side Temperature = 100°C
Electrical Power - watts
10^7
10^6
10^5
10^4
10^3
100
10
1
0.1
Specific Cost - Dollars/watt

Figure 16

radiation, it is necessary to also consider equipment costs associated with the manufacture of thermoelectric modules and apply the overall cost of such equipment on a depreciated basis to module costs. In order to do that, it is necessary to estimate the module production volume on each piece of equipment. In considering the types of equipment necessary in the manufacture of the two different types of thermoelectric modules, a general comment may be made that equipment needs relative to the manufacture of bismuth telluride modules are considerably less than are those associated with the manufacture of silicon-germanium alloy modules. A listing of necessary equipment to completely manufacture each type of module is shown in Table IV in terms of the equipment and the approximate cost of the equipment. Wherever no cost figure appears for certain types of equipment, it is implied that that particular piece of equipment is not needed in the manufacture of the type of module shown. As already stated, it is noted in Table IV that the manufacture of bismuth telluride modules requires considerably less equipment than does the manufacture of silicon-germanium alloy type modules. The equipment list shown in Table IV pertains to equipment adequate for the average manufacture of about 100 modules of each type per typical one-shift work day. In order to convert equipment cost to the additional cost of the production of electricity, it may be assumed that the equipment is totally depreciated over a reasonable and yet realistic time period. This depreciation cost, plus estimated equipment maintenance cost on a per module basis should be added to the per module cost of each type module shown in Figure 14, except that such depreciation and maintenance is assumed to be already contained in the overhead figure previously used in the computation of per module cost. Equipment maintenance can be considered to typically result in some ten to 20 percent increase in the total equipment cost over a five year period. It is this same five year period that may be considered as the typical life of the equipment and for this reason equipment depreciation should be conducted over that time period.

Table IV

*Requirements for Equipment Module Manufacture

	Bismuth Telluride	Silicon-Germanium
Orbital Ball Mill	$ 6,000	$ 6,000
Hot Press (Vacuum & Controlled)	18,000	18,000
Wafering Saw	8,000	8,000
Lapping Machine	5,000	5,000
Sedimentation Equipment	-----	1,500
Air Furnace	-----	1,500
Continuous Air Furnace	-----	4,500
Metallizing Equipment	3,200	-----
Controlled Atmosphere Furnace	-----	4,200
Controlled Atmosphere Glove Box	1,000	-----
Vacuum Furnace	-----	5,700
Sputtering Equipment	-----	27,000
Photomasking Equipment	-----	5,000
Microscope	1,500	1,500
Diamond Saw	2,200	2,200

* Does not include disposable lab equipment such as quartz ampoules, beakers, etc.

Finally, a comparison of the costs of producing electricity by means of thermoelectric energy conversion from incident solar radiation with the cost associated with other types of electrical power generation are only possible if the cost data generated in this section of the study are combined with the reliability figures given in the preceding section in order to arrive at overall energy costs in terms of kilowatt hours. It is somewhat difficult to do this because of the limited amount of available reliability data on the two types of thermoelectric modules considered in the present study. It will be recalled, however, that expected lifetimes of these modules over all of the operating temperature conditions assumed in the present study for each type of module are of the order of a few years or more. Such expected operating lifetimes can be combined with the cost data given in this section to arrive at representative values or overall energy costs. When this is done, it is concluded that energy costs associated with this type of energy conversion of the order of a few cents per kilowatt hour are possible. Again, it is recognized that this energy cost does not consider the total system cost as regards solar collectors or concentrators and cold side heat exchangers. If it is assumed that these costs double the costs herein included, it may still be concluded that solar energy can be converted to electricity by means of thermoelectric energy conversion for relatively few cents per kilowatt hour. These cost figures, of course, assume relatively large scale conversion. If small amounts of energy are converted, the costs assumed with such conversion are significantly higher.

VII. IMPACT OF TECHNOLOGY ADVANCES ON COSTS

The present study has addressed itself to the use of two of the most applicable state-of-the-art thermoelectric materials to the conversion of incident solar radiation to electricity. Both of these materials are fairly complex from the standpoint of preparation and constituent materials. Even though the cost of each

forms only a small portion of the total projected cost of electricity produced by them, it is conceivable that in extremely large quantities, some of the constituents may be of sufficiently exotic nature as to result in supply problems and consequently escalating costs. For example, one such material may be germanium. The present study has not addressed itself to this and it has been assumed that the materials are basically of unlimited supply. Inasmuch as this may not be the case, it is good to consider possible advances in thermoelectric technology and what impact such advances may have on the costs associated with the conversion of incident solar radiation into electricity. Programs are currently under way to either improve the conversion efficiency of existing thermoelectric materials or to develop new and more efficient materials than those presently available. If these programs are successful, it is quite conceivable that the cost figures given in the preceding section may be reduced by as much as 50 percent. Even though this may be the case, a question of material constituent availability may still be a potential problem because in each case, the improved thermoelectric materials presently being developed all contain fairly exotic constituents. Even though such materials may be ideal for limited applications in space and elsewhere, they may not be especially suitable for extremely large scale use in connection with solar thermoelectric energy conversion. Nevertheless, potential costs savings of up to 50 percent are conceivable. Among the materials being presently investigated as resulting in improved conversion efficiencies are silicon-germanium alloys with small additions of III-V compounds and various alloys of rare earth selenides and sulfides. In all cases, these materials are capable of operation at least up to 1000°C.

Even though improved thermoelectric materials potentially enable significant cost savings, most of these materials are being developed for fairly high temperature applications. Even though high temperatures may be suitable for solar thermoelectric energy conversion, as exemplified by the use of silicon-germanium alloys, inherently it is at the lower temperatures that solar thermoelectric energy

conversion may be more suitable. For this reason, efforts should be undertaken to develop thermoelectric materials with improved performance characteristics at temperatures in the range of ambient to about 500°C. No such efforts are being expended today because practically all of the impetus to develop new thermoelectric materials is the direct or indirect result of the space program; because of its nature, the space program requires the use of high temperature materials. It is considered that this area of research and development is very fertile and with relatively modest expenditures quite likely would result in materials considerably more attractive than those presently available for terrestrial solar thermoelectric energy conversion. Another area of research and development that may be directly applicable to such energy conversion is one of low cost materials. Practically all present day thermoelectric materials possess relatively high cost and utilize constituents of possibly limited supply. No effort has been expended in the United States on the development of low cost materials of unlimited supply. And yet, such efforts in other countries, most notably in the Soviet Union, have resulted in thermoelectric materials with performance characteristics only slightly less than those of the best state-of-the-art thermoelectric materials but at considerably lower costs and unquestioned large scale supply. In many instances, the technology associated in the incorporation of such materials into practical devices is also considerably simplified over those associated with the better known materials. Additional cost savings are therefore possible. Mention might be made in this context of various silicides and alloys thereof. Examples of such materials are iron silicide, cobalt silicide, chrome silicide and various refractory metal silicides (see Figure 3).

Thermoelectric Properties of Bismuth Telluride

Temperature °C	N-Type			P-Type		
	Electrical Resistivity mΩ-cm	Seebeck Coefficient μv/°C	Thermal Conductivity w/°C-cm	Electrical Resistivity mΩ-cm	Seebeck Coefficient μv/°C	Thermal Conductivity w/°C-cm
40	0.91	188	0.0133	0.74	164	0.0133
60	0.99	193	0.0139	0.84	169	0.0139
80	1.07	197	0.0144	0.94	173	0.0144
100	1.16	198	0.0150	1.03	177	0.0150
120	1.24	199	0.0156	1.13	182	0.0156
140	1.29	198	0.0162	1.23	185	0.0162
160	1.34	194	0.0167	1.33	187	0.0167
180	1.36	188	0.0173	1.43	187	0.0173
200	1.37	179	0.0178	1.52	184	0.0178
220	1.37	168	0.0184	1.62	178	0.0184
240	1.37	155	0.0190	1.72	170	0.0190
260	1.37	142	0.0197	1.82	164	0.0197
280	1.37	128	0.0203	1.92	156	0.0203
300	1.37	112	0.0209	2.02	149	0.0209

Seebeck Coefficient of n- and p-type 78 a/o Si - 22 a/o Ge Alloy

$\mu v/^{\circ}C$

Temp. °C	N-Type					P-Type				
	Initial	1500 Hours	1 Year	5 Years	12 Years	Initial	1500 Hours	1 Year	5 Years	12 Years
0	93	93	93	93	93	115	115	115	115	115
50	111	111	111	111	111	128	128	128	128	128
100	130	130	130	130	130	141	141	141	141	141
150	147	147	148	149	150	152	152	152	152	152
200	165	166	168	171	174	163	163	163	163	163
250	183	185	193	204	210	173	173	173	173	173
300	199	210	229	247	259	182	182	182	182	182
350	216	247	268	293	307	192	192	192	192	192
400	232	280	297	320	332	201	201	201	201	201
450	246	297	314	328	338	210	210	210	210	210
500	258	304	318	328	338	217	218	219	219	221
550	269	306	316	324	333	226	227	228	230	232
600	276	303	311	317	325	235	237	241	243	246
650	279	297	304	309	316	243	250	256	260	266
700	278	290	296	300	306	252	265	281	296	309
750	276	282	286	290	294	260	287	317	347	357
800	273	274	276	279	281	268	306	334	345	351
850	268	268	268	268	268	277	311	330	338	343
900	266	265	264	263	262	285	312	325	332	336
950	265	264	263	262	261	294	310	320	327	331

Electrical Resistivity of n- and p-type 78 a/o Si - 22 a/o Ge Alloy

mΩ - cm

Temp. °C	N-Type					P-Type				
	Initial	1500 Hours	1 Year	5 Years	12 Years	Initial	1500 Hours	1 Year	5 Years	12 Years
0	0.80	0.80	0.80	0.80	0.80	0.88	0.88	0.88	0.88	0.88
50	0.85	0.85	0.85	0.85	0.85	0.92	0.92	0.92	0.92	0.92
100	0.92	0.92	0.92	0.92	0.92	0.99	0.99	0.99	0.99	0.99
150	1.01	1.01	1.03	1.04	1.04	1.05	1.05	1.05	1.05	1.05
200	1.11	1.13	1.18	1.23	1.29	1.13	1.13	1.13	1.13	1.13
250	1.23	1.30	1.44	1.63	1.79	1.22	1.22	1.22	1.22	1.22
300	1.37	1.64	1.93	2.40	2.66	1.31	1.31	1.31	1.31	1.31
350	1.55	2.33	2.82	3.55	3.96	1.40	1.40	1.40	1.40	1.40
400	1.75	3.01	3.56	4.30	4.67	1.51	1.51	1.51	1.51	1.51
450	2.00	3.43	3.93	4.48	4.80	1.62	1.62	1.62	1.62	1.62
500	2.22	3.57	3.99	4.41	4.69	1.71	1.73	1.74	1.76	1.78
550	2.41	3.48	3.85	4.21	4.46	1.83	1.88	1.89	1.91	1.95
600	2.53	3.30	3.60	3.93	4.15	1.95	2.02	2.08	2.11	2.18
650	2.53	3.04	3.30	3.60	3.80	2.07	2.22	2.34	2.44	2.35
700	2.45	2.75	2.98	3.23	3.40	2.18	2.46	2.84	3.29	3.65
750	2.32	2.48	2.62	2.82	2.96	2.30	2.92	4.17	5.60	6.12
800	2.18	2.24	2.29	2.37	2.48	2.42	3.60	4.85	5.42	5.72
850	2.04	2.03	2.03	2.02	2.03	2.55	3.71	4.54	4.98	5.20
900	1.97	1.92	1.91	1.89	1.87	2.68	3.59	4.17	4.57	4.75
950	1.92	1.89	1.88	1.83	1.80	2.81	3.42	3.86	4.22	4.34
1000	1.89	1.87	1.84	1.80	1.76	2.94	3.29	3.60	3.91	4.01

Thermal Conductivity of n- and p-type 78 a/o Si - 22 a/o Ge Alloy

mw/°C-cm

Temp. °C	N-Type					P-Type				
	Initial	1500 Hours	1 Year	5 Years	12 Years	Initial	1500 Hours	1 Year	5 Years	12 Years
0	51.6	51.6	51.6	51.6	51.6	58.5	58.5	58.5	58.5	58.5
50	50.3	50.3	50.3	50.3	50.3	57.3	57.3	57.3	57.3	57.3
100	49.2	49.2	49.2	49.2	49.2	56.2	56.2	56.2	56.2	56.2
150	48.0	48.0	48.0	48.0	48.0	55.1	55.1	55.1	55.1	55.1
200	46.9	46.9	46.9	46.9	46.9	54.0	54.0	54.0	54.0	54.0
250	45.9	45.9	45.9	45.9	45.9	53.0	53.0	53.0	53.0	53.0
300	44.9	44.9	44.9	44.9	44.9	52.0	52.0	52.0	52.0	52.0
350	44.0	44.0	44.0	44.0	44.0	51.0	51.0	51.0	51.0	51.0
400	43.2	43.2	43.2	43.2	43.2	50.1	50.1	50.1	50.1	50.1
450	42.5	42.5	42.5	42.5	42.5	49.2	49.2	49.2	49.2	49.2
500	41.9	41.9	41.9	41.9	41.9	48.3	48.3	48.3	48.3	48.3
550	41.5	41.5	41.5	41.5	41.5	47.7	47.6	47.5	47.5	47.5
600	41.2	41.2	41.1	41.1	41.1	47.2	47.1	47.0	46.9	46.8
650	41.1	41.0	40.9	40.8	40.8	46.8	46.6	46.3	46.2	46.1
700	41.0	40.8	40.7	41.6	40.6	46.6	46.2	45.7	45.6	45.6
750	41.0	40.8	40.6	41.5	40.4	46.7	46.1	45.4	45.1	45.1
800	41.3	40.9	40.6	41.4	40.3	47.0	46.2	45.2	44.8	44.7
850	42.1	41.3	40.8	40.5	40.4	47.9	46.5	45.3	44.9	44.7
900	43.7	42.3	41.2	40.8	40.6	49.4	47.2	45.9	45.3	45.0
950	46.2	43.7	42.0	41.4	41.1	51.8	48.7	47.1	46.3	46.0
1000	49.9	45.5	43.1	42.3	42.0	55.5	51.1	49.0	48.1	47.6

Document Control Page	1. SERI Report No. TR-35-078	2. NTIS Accession No.	3. Recipient's Accession No.

4. Title and Subtitle
Conversion System Overview Assessment
Volume I: Solar Thermoelectrics
Volume II: Solar-Wind Hybrid Systems
Volume III: Solar Thermal/Coal or Biomass Derived Fuels

5. Publication Date: August 1979

6.

7. Author(s) T. S. Jayadev, J. Henderson, J. Finegold, C. Bingham, R.S. Copeland, D. Benson

8. Performing Organization Rept. No.

9. Performing Organization Name and Address

Solar Energy Research Institute
1536 Cole Boulevard
Golden, Colorado 80401

10. Project/Task/Work Unit No. Task # 3503

11. Contract (C) or Grant (G) No.
(C)
(G)

12. Sponsoring Organization Name and Address

13. Type of Report & Period Covered: Technical Report

14.

15. Supplementary Notes

16. Abstract (Limit: 200 words)

This report, in three Volumes, covers three distinct areas of solar energy research: solar thermoelectrics, solar-wind hybrid systems, and synthetic fuels derived with solar thermal energy. Volume I presents the assessment of thermoelectrics for solar energy conversion. There is significant potential for solar thermoelectrics in solar technologies where collector costs are low; e.g., Ocean Thermal Energy Conversion (OTEC) and solar ponds. Thermoelectrics also may have potential in other renewable energy source applications such as geothermal energy and waste heat utilization. Reports of two studies by manufacturers assessing the cost of thermoelectric generators in large scale production are included in the appendix and several new concepts of solar thermoelectric systems are presented. Volume II discusses solar-wind hybrid systems. There are large areas in the United States where solar and wind resources are comparable in magnitude, and there are diurnal and seasonal complementarities which offer the potential for cost-effective hybrid systems. Volume III deals with the conversion of synthetic fuels with solar thermal heat by a combination of solar energy with coal or biomass. A preliminary assessment calculating the cost of fuel produced as a function of the cost of coal and biomass shows that within the projected ranges of coal, biomass, and solar thermal costs, there are conditions when solar synthetic fuels will become cost-competitive.

17. Document Analysis

a. Descriptors Solar Energy ; Hybrid systems ; Wind Power ; Thermoelectric Conversion ; Ocean Thermal Energy Conversion ; Wind Energy Conversion Systems ; Thermoelectric Generators ; Solar Ponds ; Synthetic Fuels ; Refuse Derived Fuels ; Load Management ;

b. Identifiers/Open-Ended Terms Gasification

c. UC Categories
Volume I: 59b, 62, 62e, 64 Volume III: 62e
Volume II: 59b, 60, 62

18. Availability Statement

NTIS, US Dept. of Commerce
5285 Port Royal Rd.
Springfield, VA 22161

19. No. of Pages Vol. I-214 Vol. II-41 Vol. III-35

20. Price Vol. I-$9.25 Vol. II-$4.50 Vol. III-$4.50

Form No. 3200-13 (6-79)

☆ U.S. GOVERNMENT PRINTING OFFICE 1979 - 681-436/80 Reg. 8